Statistical Thermodynamics of Block Copolymer Adsorption

Promotor:	dr. G.J. Fleer, hoogleraar in de fysische en kolloïdchemie
Co-promotor:	dr. J.M.H.M. Scheutjens, universitair hoofddocent bij de Vakgroep Fysische en Kolloïdchemie

Olaf A. Evers

Statistical Thermodynamics of Block Copolymer Adsorption

Proefschrift
ter verkrijging van de graad van
doctor in de landbouw- en milieuwetenschappen,
op gezag van de rector magnificus,
dr. H.C. van der Plas,
in het openbaar te verdedigen
op vrijdag 23 februari 1990
des namiddags te vier uur in de aula
van de Landbouwuniversiteit te Wageningen

ISN: 268194

Stellingen

I

Van een theorie voor de beschrijving van de adsorptie van di-blokcopolymeren mag verwacht worden dat zij de individuele geadsorbeerde polymeermolekulen in twee afzonderlijke delen weet te onderscheiden en niet slechts de geadsorbeerde laag als geheel zoals dat in de theorie van Munch en Gast het geval is.

M.R. Munch en A.P. Gast, Macromolecules 21, 1366 (1988).

II

Het door Hopkins en Howard experimenteel waargenomen maximum in de geadsorbeerde hoeveelheid van styreen/methyl-methacrylaat blokcopolymeren als funktie van de fraktie adsorberende segmenten kan door de in dit proefschrift beschreven theorie goed verklaard worden.

A. Hopkins en G.J. Howard, J.Polym.Sci. A-2 9, 841 (1971).

Dit proefschrift, hoofdstuk 2.

III

Patel et al. vinden voor de interaktie van geadsorbeerde diblokcopolymeren geen "master curve" bij variatie van de lengte van het adsorberende blok doordat zij in de door hen gebruikte schalingstheorie de relatie tussen laagdikte en geadsorbeerde hoeveelheid niet meester worden.

S. Patel, M. Tirrell en G. Hadziioannou, Colloids Surfaces 31, 157 (1988).

Dit proefschrift, hoofdstuk 3.

IV

De kwaliteit van een korte wetenschappelijke voordracht is omgekeerd evenredig met het aantal formules en symbolen dat de toehoorder te verwerken krijgt.

V

De wettelijk voorgeschreven Algemene Periodieke Keuring van motorvoertuigen (APK) dient door een onafhankelijk keuringsinstituut of -bedrijf te worden verricht.

VI

Het computerbesturingssysteem UNIX verdient geen plus-punt voor het gebruik van een min-teken als symbool om een optie aan een kommando toe te voegen.

Proefschrift Olaf A. Evers
Statistical Thermodynamics of Block Copolymer Adsorption
Wageningen, 23 februari 1990

Contents

Introduction

The behaviour of polymers at solid/liquid interfaces and the effect of adsorbed polymer on the stability of colloidal suspensions have been the subject of many theoretical and experimental studies over the last decades.

Especially, the theoretical model of Scheutjens and Fleer[1-3] for adsorption of homopolymers at solid/liquid interfaces has proven to be a very succesful tool for a better understanding of polymer adsorption. This self-consistent mean field theory gives a detailed picture of the equilibrium state of the interfacial region without making *a priori* assumptions about the conformations of the adsorbed molecules. Quantitative predictions on, for example, the adsorbed amount, the layer thickness, or the free energy of interaction between two adsorbed polymer layers can be made. The flexibility of this theory is another reason for its succes. Over the last ten years much work has been done to extend the theory of Scheutjens and Fleer to more complicated systems like polymer liquids[4], adsorption of ring polymers[5], adsorption of polyelectrolytes[6-9], terminally attached chains[10], and association colloids.[11,12]

The theory as formulated originally[1-3] applies only to the case that a monomeric solvent is present. In this study a more general derivation of the Scheutjens-Fleer theory is given, so that it can be applied to adsorption of block copolymers from a multicomponent mixture of arbitrary composition, including the case that the system contains only chain molecules. One situation of great practical interest is adsorption of block copolymers from solution. Adsorbed block copolymers are found to have their weakly or non-adsorbing block protruding far into the solution. These non-adsorbing blocks form a steric barier so that, for instance, colloidal particles covered with block copolymers will repel each other. Block copolymers can

therefore be found as additives in many industrial products like paints, inks, lubricants, coatings, blends, etc.

POLYMERS

Flexible, linear polymer molecules are long chains of connected repeating units (monomers or segments). The number of monomer units in a polymer molecule can be very high, upto 100,000. This makes the dimensions of a linear polymer chain rather peculiar. For example, a stretched polymer chain containing 5000 monomer units is approximately 1 μ long and has a diameter of the order of 0.2 nm. This would correspond to a cable having a diameter of 1 cm and a length of 50 m! If there are no external forces and if the internal forces between the segments are weak its average configuration due to thermal motion will not be linear, but will be that of a more or less spherical random coil.

Polymers which contain only one type of monomer unit are called homopolymers. Copolymers differ from homopolymers in that they have two or more different types of monomer units. The order of these units determines the type of copolymer. One may distinguish the following types of copolymers.

Alternating copolymers: The different monomer types succeed each other. Each bond within the copolymer connects two monomers of different type.

Statistical copolymers: The sequence of the monomer units is statistically determined during the proces of polymerisation.

Block copolymers: The monomer units are grouped in sequential blocks, each block containing only monomer units of the same type. For instance, a PVP-PS diblock copolymer contains two blocks: one part of the chain consists of vinyl-pyridine units and the other part of styrene units.

Copolymers with a given sequence: The sequence of the monomer units is predetermined. Examples of this type are proteins, DNA, and RNA. These copolymers thank their biological properties partially to their specific three-dimensional configuration (e.g., helix, double helix, β-sheet,

etc.) which is a result of their particular monomer sequence and the strong internal forces.

We can also distinguish between flexible and non-flexible or rigid copolymers. For example, DNA is a relatively rigid molecule because of its double helix configuration. In this thesis we will only deal with flexible linear block copolymers.

In most practical system the polymers are dissolved in a solution. Therefore, some remarks on the solubility of polymers is in order. In general, the solubility of long polymer chains is low: many polymers do not dissolve in a solvent in which the monomer is quite soluble. First we consider the solubility of homopolymers. If a homopolymer chain is hardly soluble in a particular solvent, the solvent is said to be of a poor or bad quality. The quality of a solvent is determined by the net interaction between monomer units and solvent. When the solvent quality becomes very poor, e.g., because of a decreasing temperature, the polymer becomes insoluble. When a homopolymer becomes insoluble the solvent and the polymer form separated phases. The temperature at which this happens is called the Θ-temperature and the solvent at that temperature is called a Θ-solvent for that particular type of polymer.

For block copolymers the situation is more complex. The solvent may be good for certain blocks but very poor for others. Since the blocks are chemically connected this can result in (soluble) aggregated structures like (spherical) micelles or (lamellar) membranes by local phase separation. This happens when the polymer concentration exceeds the critical micelle or critical membrane concentration (cmc). In these aggregated structures the insoluble blocks are shielded from the solvent by the soluble blocks.

ADSORPTION OF POLYMERS

If there is no attraction between the surface and the monomer units chain molecules will try to avoid the interfacial region because they have less spatial freedom in the vicinity of a surface than in the bulk solution. When molecules accumulate at a surface they are said to

adsorb. If there are attractive forces between the surface and the segments present, even when these forces are rather weak, polymer molecules will adsorb strongly because of the large number of attachement points per polymer molecule.

During adsorption the average configuration of a polymer chain will change drastically. Flexible, linear polymers adsorb from solution on a solid surface to give a conformation with trains, loops, and tails (see figure 1a). The sequences of segments which are in contact with the surface are called trains. The trains are interconnected by loops, and the chain ends are either adsorbed or form dangling tails. For a homopolymer the distribution of segments over trains, loops, and tails depends on the solvent quality, the polymer concentration, the chain length, and on the surface affinity of the segments.

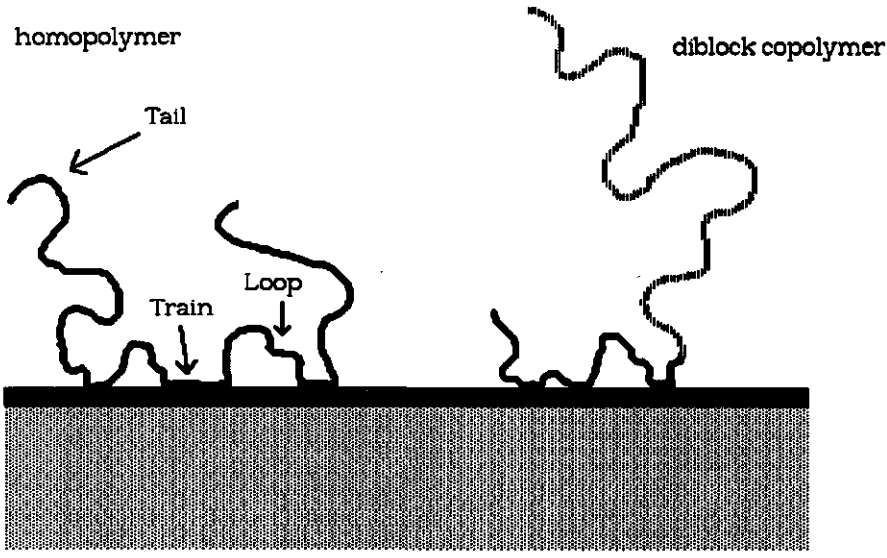

Figure 1. *Distribution of segments over trains, loops, and tails of an adsorbed homopolymer (a) and a diblock copolymer (b) .*

There have been many attemps to describe the average configuration of adsorbed homopolymers. The theoretical studies on adsorption of homopolymers can be roughly divided into four groups:

single chain theories, (self-consistent) mean field theories, scaling theories, and Monte-Carlo simulations.

The earliest theories[13-19] on polymer adsorption are based on single chain statistics and hence limited to isolated chains on a surface. Crowding affects and surface saturation are not accounted for. Mean field theories explicitly consider these effects.

The mean field theories account for the interaction between polymer segments and solvent molecules through a mean field approximation. Some theories[20,21] use specific assumptions on the segment density profile near the surface. A more general theory has been given by Roe[22] who did not make a priori assumptions about the density profile. However, by his averaging procedures the inversion symmetry for chain conformations is not properly accounted for and chain end effects are neglected. DiMarzio and Rubin[23] introduced a matrix method to calculate the probability of each conformation that an isolated chain adsorbed at one surface or between two plates can adopt on a lattice. Their method is elegant and does not suffer from additional assumptions. However, in its original form it is restricted to isolated chains since they did not account for polymer-solvent interactions. Scheutjens and Fleer.[1-3] combined the concepts of this matrix method with the Flory-Huggins mean field lattice theory[24] for polymer solutions, and developed a self-consistent mean field theory. In this theory the interactions and the conformations of the molecules are interrelated in a self-consistent way: the distribution of the molecules over the various conformations depends on the local potentials which the segments of the molecules experience as a result of all the chains in this particular distribution. The method of Scheutjens and Fleer does, in general, not lead to analytical solutions but produces a set of implicit matrix equations that can be solved by numerical methods. More recently, a continuum analogue of the Scheutjens-Fleer theory has been presented by Ploehn et al.[25,26] introducing a continuous self-consistent field in a Schrödinger-like diffusion equation, as an extension of earlier work of Edwards[27] and De Gennes[28]. Analytical solutions for the volume fraction profile are found by performing an eigenfunction expansion and taking only the

dominating eigenfunctions into account. This limits the accuracy compared to the theory of Scheutjens and Fleer.

Scaling theories[29-33] divide the adsorption layer into regimes. For each regime the density profile is obtained using scaling arguments (power laws). In some cases the profile is preassumed, e.g., in the outer (so called distal) regime the profile is assumed to be exponential. It has been shown[34,35] that scaling methods are adequate for weakly overlapping, highly swollen, long flexible chains in good solvents where mean field theories are less adequate. Hence, it applies to polymer solutions that are relatively dilute. However, in adsorption situations scaling theories are not very useful since the densities in the adsorption layer are usually so high that mean field theories are more appropriate, except in the periphery for which scaling theories assume an exponential decay.

Because homopolymers consist of one type of monomer only, the average distribution of a segment over the trains, loops, and tails as a function of the segment ranking number in the chain is symmetric. For adsorbed block copolymers, for which both chain ends are not equivalent, we can expect a different distribution of segments over trains, loops, and tails that can also be asymmetric. Since different types of segments have different surface affinities, the conformation of an adsorbed block copolymer molecule depends highly on its sequential composition. The simplest block copolymer, i.e., a diblock copolymer, is found to have a much more extended conformation than the corresponding homopolymer.[36-46] Such an extended layer can be explained by assuming that an average conformation in which the block having the lowest surface affinity forms one dangling tail which is anchored to the surface by its connection to the adsorbing block, see figure (1b). Therefore, adsorbed block copolymers are often described as anchored tails.[36,40-45]

Recently, a few theories[40-42,47,48] have been developed which apply scaling rules[29,30] or a mean field approximation[33] for terminally attached chains to the case of block copolymer adsorption. In all these theories the shape of the density profile of the adsorbed block copolymer layer is pre-assigned. The adsorbing block is assumed to

form a compact layer covering the surface. The non-adsorbing block is seen as a "brush" having a certain thickness and a density which, in the limit of high coverage, is independent of the distance to the surface. The number of adsorbed chains or, in other words, anchoring points for the non-adsorbing blocks and the thickness of the "brush" is either found by scaling arguments[40-42] or by incompressibility conditions combined with minimization of the free energy.[47,48] Since these theories are based on a predefined shape of the density profile their validity is limited to selective solvents, and to a small range of chain compositions.

As mentioned before, depending on the solvent quality for the different segment types block copolymers can form soluble aggregates like micelles. For adsorption of surfactants it has been found experimentally[49-52] that, when the cmc has been reached, most the additivelly added surfactant associated into micelles and thus the adsorbed amount hardly increases. This effect of micellization on the adsorption of block copolymers has been included in some of the earlier mentioned theories.[47,48] In the self-consistent field theory presented in this thesis the effect of micellization is not considered. Therefore the model is applied to block copolymers that do not self-aasociate. However, such an extension of the Scheutjens-Fleer theory can be made. By introducing a spherical lattice in this theory and applying small system thermodynamics, Van Lent[53,54] accounted for micellization and studied its effect on adsorption.

INTERACTON BETWEEN LAYERS OF ADSORBED POLYMERS

Polymers are widely used to modify the surface of colloidal particles in order to stabilize or flocculate them.[55-58] Because of Van der Waals interactions colloidal particles will experience an attractive force towards one another. This attraction may be overcome by electrostatic repulsion if the particles are charged, or by steric repulsion if the particles carry adsorbed polymer layers. Steric

repulsion occurs when adsorbed polymer on two or more particles overlap in solvents better than a Θ-solvent. Enhancement of the attraction is possible when the solvent quality becomes very poor or by bridging attraction (if the adsorbed polymers form bridges, see figure 2, left). For bridging it is required that the surface coverage with polymer is below saturation. In order to prevent bridging of homopolymers, the surface coverage has to be sufficiently high (see figure 2, right).

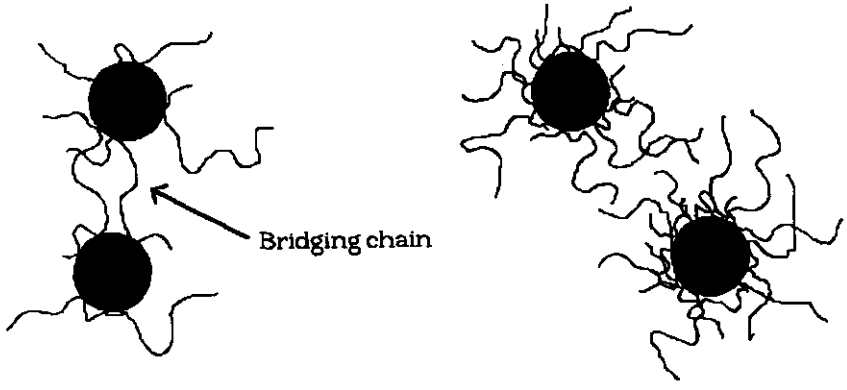

Figure 2. *Bridging and non-bridging polymers*

Diblock copolymers are better stabilizers than homopolymers because, like terminally attached chains, they are less likely to form bridges because of the strong steric repulsion of the non-adsorbing blocks. This has been verified experimentally by measuring directly the interaction force between two mica sheets with adsorbed block copolymers as a function of their separation,[59,60] using a surface force apparatus developed by Israelachvili.[61] Several authors[36,41-43] have reported results on the interaction between adsorbed diblock copolymer layers, measured with such an apparatus. In good solvents strong repulsive forces are found, showing an onset of interaction at very large surface separation, which strongly depends on the chain composition.[40,43] Only in solvents much worse than a Θ-solvent for the non-adsorbing block attractive long range forces have been

observed.[40-43] From these results it can be concluded that bridging does not occur for these diblock copolymers.

Using scaling laws for terminally attached chains Patel et al.[42] have derived an expression for the interaction force between block copolymer layers. For a range of diblock copolymers, all having a long adsorbing block of the same length, the force-distance curves could be scaled and merged into one master curve. However, their theory does not apply to smaller lengths of the adsorbing block. Also the effect of surface affinity and solvent quality cannot be adequately studied with this model, because it is based upon the assumption of terminal anchoring.

OUTLINE OF THIS STUDY

This thesis contains three chapters which can be read more or less independently.

In chapter 1 the general formulation of the self-consistent field theory is presented. Equations for the segment potential profiles, the segment density distributions and the free energy are derived from the partition function, using the method of Lagrange multipliers. Some numerical results on the structure of the adsorption layer of di- and triblock copolymers are shown. The results for diblock copolymers are compared with those for terminally attached chains.

In chapter 2 a brief review of the theory is given in a less mathematical and more physical manner. A number of results on the adsorbed amount and the hydrodynamic layer thickness of adsorbed di- and triblock copolymers are presented. It is shown how these parameters depend on the chain composition, surface affinity, and solvent quality. Special attention is given to the effect of the block length on the adsorbed amount. For diblock copolymers a relatively simple relation is found between the adsorbed amount (as compared to a corresponding homopolymer) and the block length ratio of both blocks.

In chapter 3 the theory is applied to interaction between layers of adsorbed block copolymers. The concept of full equilibrium and restricted equilibrium for multicomponent systems is worked out, and equations for the surface excess free energy in both cases are derived. In full equilibrium all molecules in the mixture can leave freely the gap between the plates when these are brought closer together. Hence, full equilibrium refers to the case where the chemical potential of every molecule type remains constant with varying plate distance. Restricted equilibrium conditions are relevant when some (or all) types of molecules except the solvent are unable to leave the gap when the plate distance is decreased. A number of results on the interaction between adsorbed layers of di- and triblock copolymers are given. We examine especially the effect of the chain composition on the interaction. It will be shown that under good solvency conditions it is possible to scale the interaction curves at various bock lengths on to one master curve. The results will be discussed in relation to the direct force-distance measurements between adsorbed diblock copolymer layers obtained with the surface force apparatus.

REFERENCES

(1) J.M.H.M. Scheutjens, and G.J. Fleer, J.Phys.Chem. 83, 1619 (1979).

(2) J.M.H.M. Scheutjens, and G.J. Fleer, J.Phys.Chem. 84, 178 (1980).

(3) J.M.H.M. Scheutjens, and G.J. Fleer, Macromolecules 18, 1882 (1985).

(4) D.N. Theodorou, Macromolecules 21, 1391 (1988); ibid. 21, 1400 (1988)

(5) B. van Lent, J.M.H.M. Scheutjens, and T. Cosgrove, Macromolecules 20, 366 (1987)

(6) H.A. van der Schee, and J. Lyklema, J.Phys.Chem. 88, 6661 (1984).

(7) O.A. Evers, G.J. Fleer, J.M.H.M. Scheutjens, and J. Lyklema, J.Colloid Interface Sci. 111, 446 (1986).

(8) M. Böhmer, O.A. Evers, and J.M.H.M. Scheutjens,

Macromolecules, submitted.

(10) T. Cosgrove, T. Heath, B. van Lent, F. Leermakers, and J.M.H.M. Scheutjens, Macromolecules 20, 1692 (1987).

(11) F.A.M. Leermakers, and J.M.H.M. Scheutjens, J.Chem.Phys. 89, 3264 (1988).

(12) F.A.M. Leermakers, and J.M.H.M. Scheutjens, J.Chem.Phys. 89, 6912 (1988).

(13) R. Simha, H.L. Frisch, and F.R. Eirich, J.Phys.Chem. 57, 584 (1953)

(14) H.L. Frisch and R. Simha, J.Chem.Phys. 24, 652 (1956); ibid. 27, 702 (1957).

(15) E.A. DiMarzio, J.Chem.Phys. 42, 2101 (1965)

(16) C.A.J. Hoeve, E.A. DiMarzio, and P. Peyser, J.Chem.Phys. 42, 2558 (1965).

(17) C.A.J. Hoeve, J.Chem.Phys. 43, 3007, (1965).

(18) E.A. DiMarzio, and F.L. McCrackin, J.Chem.Phys. 43, 539 (1965)

(19) A. Silberberg, J.Chem.Phys. 46, 1105 (1967)

(20) A. Silberberg, J.Chem.Phys. 48, 2835 (1968)

(21) C.A.J. Hoeve, J.Polymer Sci. C 30, 361 (1970); ibid. 34, 1 (1971)

(22) R.J. Roe, J.Chem.Phys. 60, 4192 (1974)

(23) E.A. DiMarzio, and R.J. Rubin, J.Chem.Phys. 55, 4318 (1971)

(24) P.J. Flory, "The principals of Polymer Chemistry", Cornell Univeristy Press, Ithaca, NY (1953)

(25) H.J. Ploehn, W.B. Russel, B. William, and C.K. Hall, Macromolecules 21, 1075 (1988)

(26) H.J. Ploehn, W.B. Russel, and B. William, Macromolecules 22, 266 (1989)

(27) Edwards, Proc. Phys. Soc. 85, 613 (1965), J.Phys. A 2, 145 (1969)

(28) De Gennes, Rep. Prog. Phys. 32, 187 (1969)

(29) S.J. Alexander, J.Phys (Paris) 38, 983 (1977).

(30) P.G. de Gennes, Macromolecules 13, 1069 (1980)

(31) P.G. de Gennes, Macromolecules 14, 1637 (1981)

(32) P.G. de Gennes, "Scaling Concepts in Polymer Physics", Cornell University Press, Ithaca N.Y. (1979)

(33) A.P. Gast and L.J. Leibler, J.Phys.Chem. 89, 3997 (1986).

(34) D.W. Schaefer, Polymer 25, 387 (1984)

(35) G.J. Fleer, J.M.H.M. Scheutjens, and M.A. Cohen Stuart, Colloids and Surfaces 31, 1 (1988)

(36) H.J. Taunton, C. Toprakcioglu, and J. Klein, Macromolecules 21, 3333 (1988).

(37) A. Hopkins, and G.J. Howard, J.Polymer Sci. A-2 9, 841 (1971).

(38) J.A. Baker, and J.C. Berg, Langmuir 4, 1055 (1988).

(39) J.V. Dawkins, and G. Taylor, Faraday Trans. I 76, 1263 (1980).

(40) S.S. Patel, PhD thesis, University of Minnesota (1988).

(41) G. Hadziioannou, S. Patel, S. Granick, and M. Tirrell, J.Amer.Chem.Soc. 108, 2869 (1986)

(42) S. Patel, M. Tirrell, and G. Hadziioannou, Colloid Surfaces 31, 157 (1988).

(43) J. Marra, and M.L. Hair, Colloids Surfaces 34, 215 (1989).

(44) M.A. Ansarifar, and P.F. Luckham, Polymer 29, 329 (1988)

(45) M.A. Ansarifar, and P.F. Luckham, Polymer Communications 29, 177 (1988)

(46) J.F. Tassin, R.L. Siemens, W.T. Tang, G. Hadziioannou, J.D. Swalen, and A. Smith, J.Phys.Chem. submitted (1988).

(47) M.R. Munch, and A.P. Gast, Macromolecules 21, 1366 (1988).

(48) C. Marques, J.F. Joanny, and L. Leibler, Macromolecules 21, 1051 (1988)

(49) K.G. Mathai, and R.H. Ottewil, Trans.Faraday Soc. 62, 750, ibid. 759 (1966)

(50) J.M. Corkhill, J.F. Goodman, and J.R. Tate, Trans.Faraday Soc. 62, 979 (1966)

(51) Th. van den Boomgaard, Th.F. Tadros, and J. Lyklema, J.Colloid Interface Sci. 116, 8 (1986)

(52) B. Kronberg, J. kuortti, and P. Stenius, Colloid Surfaces 18, 411 (1986)

(53) B. van Lent, PhD Thesis, Wageningen (1989).

(54) B. van Lent, and J.M.H.M. Scheutjens, Macromolecules 22, 1931 (1989)

(55) D.H. Napper, "Polymeric Stabilization of Colloidal Dispersions", Academic Press, London (1983).

(56) M. Cohen-Stuart, T. Cosgrove, and B. Vincent, Adv. Colloid Interface Sci. 24, 143 (1986).

(57) B. Vincent, Adv. Colloid Interface Sci. 4, 197 (1974)

(58) T.F. Tadros, in "The Effect of Polymers on Dispersion Properties", T.F. Tadros Ed., Academic Press, London (1982), 1.

(59) J.N. Israelachvili, and G.E. Adams, Nature (London) 262, 774 (1976); Trans.Faraday Soc. I 74, 975 (1978)

(60) K. Lodge, Adv. Colloid Interface Sci. 19, 27 (1983)

(61) J. Klein, J.Colloids Interface Sci. 111, 305 (1986)

CHAPTER 1

Structure of the adsorption layer of block copolymers

ABSTRACT

A generalization of the self-consistent field theory of Scheutjens and Fleer for adsorption of homopolymer from a binary solution towards a theory for adsorption of block copolymers from a multicomponent mixture is presented. No a priori assumptions about the conformations of the adsorbed molecules are made. Equations for the conformation probabilities, the segment density profiles, and the free energy are derived. Results on the segment density distribution in adsorbed layers of diblock and triblock copolymers are given. We find that diblock copolymers tend to adsorb with the adsorbing block rather flat on the surface and the less or non-adsorbing block in one dangling tail protruding far into the solution. We compare these predictions with those for terminally anchored chains and find overall agreement but also typical differences. The effect of the surface affinity and the solvent quality on the structure of adsorbed diblock copolymers is shown.

1.1 INTRODUCTION

Block copolymers play an important role as additives in many industrial products like inks, paints, lubricants, coatings, etc. In these systems block copolymers are used since they are very effective in stabilizing colloidal suspensions. This property finds its origin in the

way block copolymers adsorb. An adsorbed diblock copolymer has usually one block adsorbed on the surface in a rather flat conformation, whereas the other block, having a lower surface affinity, forms a dangling tail. This has important consequences for the interaction between two layers of adsorbed diblock copolymers, since formation of bridges in this situation is unlikely. Hence, block copolymers are better stabilizers than homopolymers. Because of their freely dangling blocks, adsorbed diblock copolymers are often interpreted and theoretically modeled as terminally anchored chains. For example, Hadziioannou et al.[1] applied the Alexander-de Gennes analysis[2,3] for anchored chains to adsorption of diblock copolymers.

In this article we present a self-consistent field theory for the adsorption of block copolymers of any block sequence without making a priori assumptions about the conformations of the adsorbed molecules. The theory is a generalization of the Scheutjens and Fleer theory[4-6] for the adsorption of homopolymers from a binary mixture. For binary mixtures containing a solvent monomer, the extension of the Scheutjens and Fleer theory to diblock copolymers is straightforward as has been shown by Leermakers et al.[7], who modeled the self-association of small surfactant molecules. Here we will extend the Scheutjens and Fleer theory to the case of adsorption of block copolymers from a multicomponent mixture of arbitrary composition, including the case that no monomeric solvent is present.

Scheutjens and Fleer use a lattice model to achieve a finite number of different conformations of adsorbed molecules. The distribution of molecules over the various possible conformations is found by minimization of the free energy, subject to the packing constraint that every lattice layer has to be filled with either a segment or a solvent monomer. The minimum of the free energy is obtained by differentiating the logarithm of the canonical partition function Q with respect to the number of polymer molecules in a given conformation. In order to satisfy the constraint of a filled lattice Scheutjens and Fleer

perform the differentiation of lnQ by adding a polymer chain of r segments long in a given conformation, and at the same time subtracting r solvent monomers. This method works only if a monomer solvent is present in the mixture. In this article the Lagrange multiplier method for obtaining a constrained extremum of a function is applied to the Scheutjens and Fleer formalism in such a way that no solvent monomers need be present in the mixture. Similar procedures have been used by other authors[8-13].

After the description of the theory, we present some typical results on the segment distribution in adsorbed layers of block copolymers. In a subsequent publication[14] we report more systematic results of the dependence of the adsorbed amount and the hydrodynamic layer thickness on the internal composition of block copolymers.

1.2 THEORY

1.2.1 Model

Consider a lattice between two parallel plates (figure 1.1). The lattice layers parallel to the surface are numbered from one surface to the other: z = 1,2,...,M, and have L lattice sites each. Every lattice site has Z neighboring sites, a fraction λ_0 of which is in the same layer and a fraction λ_1 in each of the adjacent layers. For example, in a hexagonal lattice (Z=12) $\lambda_0 = 6/12$ and $\lambda_1 = 3/12$. Each lattice site is assumed to be occupied by some segment. In this context, a solvent molecule (if present) contains usually one, but sometimes more segments. Segments in the layers adjacent to the surfaces are considered to be adsorbed.

A polymer molecule is represented by a chain of r_i connected segments numbered s = 1,2,...,r_i. We adopt the index i to denote to the type of molecule. For copolymers it is necessary to know the chemical nature of each segment s. The segment types are denoted by A,B,C,... For example, in the block copolymer AAABBBB segments s = 1,2,3 are of type A and s = 4,5,6,7 of type B. Solvent molecules and homopolymers are considered as special types of block copolymers. Therefore, we will use the general word molecule.

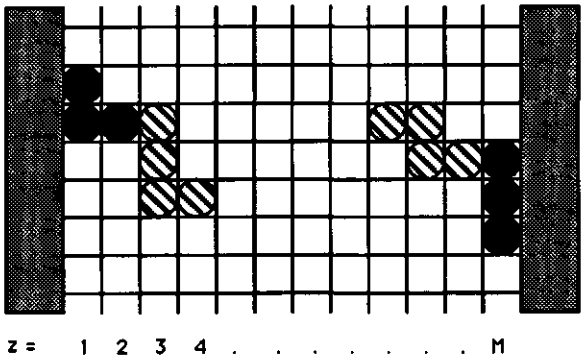

Figure 1.1. *Two chains AAABBBB in a lattice between two surfaces.*

In equilibrium, the molecules are distributed over the various possible conformations in the lattice in such a way that the free energy is at its minimum. We will adopt a mean field approximation within each lattice layer, i.e., density fluctuations within each layer are neglected and only the distance to either surface is relevant. Therefore, to characterize the energy of a molecule of type i in a certain conformation c, it is sufficient to specify the number $r_{Ai}^{c}(z)$ of segments of each segment type (A) that this conformation has in layer z. Thus, a conformation is uniquely defined by specifying the layer number of every segment s. The number of molecules i in conformation c is indicated as n_i^c. The conformation distribution of all molecules i between the two surfaces is denoted by $\{n_i^c\}$. The various

possible conformations are not equally probable: their frequency depends on the interaction energies, which are a function of the local concentrations of segments. Since we consider only density gradients perpendicular to the surfaces, we use average volume fractions in each lattice layer. The volume fractions are: $\phi_{Ai}(z)$ for segments A of molecules i in layer z, $\phi_i(z)$ for all segments belonging to molecules i, and $\phi_A(z)$ for all segments of type A, irrespective of the type of molecule. Obviously, $\phi_i(z) = \Sigma_A \phi_{Ai}(z)$ and $\phi_A(z) = \Sigma_i \phi_{Ai}(z)$. If molecules i have no segment of type A, then $\phi_{Ai}(z)$ is zero. The total number of molecules i between the two surfaces is denoted by n_i, with $n_i = \Sigma_c n_i^c$. Since all lattice sites are occupied, $\Sigma_i r_i n_i = ML$.

1.2.2 Partition Function

The grand canonical partition function Ξ of the system is given by a summation of canonical partition functions Q, weighted with their appropriate Boltzmann factors:

$$\Xi(\{\mu_i\},M,L,T) = \sum_{\text{all}\{n_i^c\}} Q(\{n_i^c\},M,L,T)\exp\left[\sum_i n_i\mu_i / kT\right] \qquad (1.1)$$

where μ_i is the chemical potential of molecules i. The summation on the right hand side of equation (1.1) is taken over all possible distributions of all molecules over the various conformations. Each set $\{n_i^c\}$ represents a single distribution which fills each lattice layer exactly.

First we derive an expression for the canonical partition function Q, which equals $\Omega \exp(-U/kT)$, where $\Omega(\{n_i^c\},M,L)$ is the degeneracy. Because of the mean field approximation, the total energy U is constant for a given concentration profile and, consequently, for a given set $\{n_i^c\}$. If we define $Q^* = \Pi_i Q_i^*$, where $Q_i^* = \Omega_i^* \exp(-U_i^*/kT)$ is the

canonical partition function of n_i molecules i in pure amorphous bulk state, we can write

$$\mathcal{Q} = \mathcal{Q}^*\left(\frac{\Omega}{\Omega^*}\right)\exp[-(U-U^*)/kT] \qquad (1.2)$$

where $\Omega^* = \Pi_i\Omega_i^*$ and $U^* = \Sigma_i U_i^*$.

The exponential in equation (1.2) contains the energy difference between the system and the reference state. The combinatory factor $\Omega_i^*(n_i)$ is the number of ways to arrange n_i molecules i over r_in_i lattice sites in a pure phase of liquid molecules i. An expression for Ω_i^* has been derived by Flory[15]:

$$\Omega_i^* = \frac{(r_in_i)!}{n_i!}\left(\frac{Z}{r_in_i}\right)^{(r_i-1)n_i} \qquad (1.3)$$

The factorial $(r_in_i)!$ accounts for the number of ways to place r_in_i distinguishable monomers over r_in_i lattice sites. A correction factor $Z/(r_in_i)$ comes in for each of the $(r_i-1)n_i$ monomers linked to a previous monomer. These monomers have only Z instead of r_in_i possible locations (if internal overlap of segments is allowed). Finally, a factor $n_i!$ corrects for the fact that the n_i molecules are mutually indistinguishable.

Scheutjens and Fleer[4] have derived an expression for Ω for the case of a binary mixture of a polymer and a solvent in a density gradient. It is easy to extend their equation so that it applies to a multicomponent mixture in a density gradient. The result is:

$$\Omega = (L!)^M \prod_{i,c}\left[\lambda^c(Z/L)^{r_i-1}\right]^{n_i^c}/n_i^c! \qquad (1.4)$$

where λ^c is a multiple product of r_i-1 bond weighting factors λ_0 and/or λ_1, see equation (1.5) below.

There is a close analogy between equations (1.3) and (1.4). The M factorials L! account for the number of ways of placing LM distinguishable monomers over the M distinguishable layers with L sites each, and replace the factorial $(r_i n_i)!$ in equation (1.3). The factor $\lambda^c(Z/L)^{r_i-1}$ corrects for the r_i-1 segments per chain i in conformation c that are linked to a previous one. This correction factor can be illustrated as follows.

As defined before, a conformation is characterized by specifying the layer number for each segment. For the first segment of a molecule in conformation c (which is to be placed in a specific layer) there are L possible locations. For the second segment there are $\lambda^c(2|1)Z$ possible locations, where $\lambda^c(2|1)$ is the fraction of nearest neighbors that segment 1 has in the layer where segment 2 is found. Clearly, $\lambda^c(2|1)$ is either λ_0 (if segments 1 and 2 are in the same layer) or λ_1 (if they are in adjacent layers). The number of arrangements within conformation c is then given by $L\lambda^c Z^{r_i-1}$ where λ^c is defined as

$$\lambda^c = \lambda^c(r_i|1) = \prod_{s=2}^{r_i} \lambda^c(s|s-1) \qquad (1.5)$$

For each of the n_i^c chains in conformation c the correction factor is the ratio between $L\lambda^c Z^{r_i-1}$ and L^{r_i}, which is the number of possibilities for r_i independent segments. Finally, the factorial $n_i^c!$ in equation (1.4) corrects for the fact that the n_i^c molecules i in conformation c are indistinguishable.

Equation (1.5) gives the multiple product of r_i-1 bond weighting factors for a complete chain. It is sometimes convenient to consider only part of a chain, from segment s' to s". Therefore we define $\lambda^c(s"|s')$ as

$$\lambda^c(s'' \mid s') = \prod_{s=s'+1}^{s''} \lambda^c(s \mid s-1) \qquad (1.6)$$

The logarithm of Ω/Ω^* can be approximated by applying Stirling's Formula, ln N! = N ln N - N . From equations (1.3) and (1.4) we find the relatively simple expression:

$$\ln \frac{\Omega}{\Omega^*} = \sum_{i,c} n_i^c \ln\left(\frac{L\lambda^c}{r_i n_i^c}\right) \qquad (1.7)$$

Substitution of equation (1.7) in equation (1.2) leads to the following expression for the logarithm of the canonical partition function $\mathcal{Q}$:

$$\ln \mathcal{Q} = \sum_{i,c} n_i^c \ln\left(\frac{L\lambda^c}{r_i n_i^c}\right) - (U - U^*)/kT + \ln \mathcal{Q}^* \qquad (1.8)$$

1.2.3 Equilibrium distribution

We will make the usual assumption of replacing the sum in the right hand side of equation (1.1) by its maximum term. The maximum term of the sum is determined by that set of conformations $\{n_i^c\}$ which satisfies the total differential

$$\sum_{i,c}\left[\left(\frac{\partial \ln \mathcal{Q}}{\partial n_i^c}\right)_{M,L,T} dn_i^c + \frac{\mu_i}{kT}\right] = 0 \qquad (1.9)$$

The variables n_i^c are subject to the constraints

$$L - \sum_{i,c} n_i^c r_i^c(z) = 0 \quad , \qquad \text{for } z = 1, 2, \ldots, M \qquad (1.10)$$

where $r_i^c(z)$ is the number of segments that a molecule i in conformation c has in layer z. Obviously, $\Sigma_z r_i^c(z) = r_i$. Physically, equation (1.10) means only that each lattice site in any layer z must be occupied.

It is convenient to use the multiplier method of Lagrange to obtain a constrained extreme of a function. In this method a set of multipliers $\alpha(z)$, one for each constraint, is introduced and a new unconstrained function f is defined by adding to ln Ξ, for each layer, a term $\alpha(z)$ times the constraint:

$$f = \ln Q + \sum_i \frac{\mu_i n_i}{kT} + \sum_z \alpha(z)\left[L - \sum_{i,c} n_i^c r_i^c(z)\right] \qquad (1.11)$$

The unconstrained function f has a saddle point in the $(\{n_i^c\},\{\alpha(z)\})$ space, i.e., a maximum on $\{n_i^c\}$ combined with a minimum on $\{\alpha(z)\}$. Moreover, in this saddle point f satisfies the constraining relations, so that the added terms are zero. Hence, in this point the function f equals the maximum term of ln Ξ for the equilibrium set $\{n_i^c\}$.
The equilibrium set $\{n_i^c\}$ and the M multipliers $\alpha(z)$ are given by the set of equations

$$\frac{\partial f}{\partial n_j^d} = \frac{\partial \ln Q}{\partial n_j^d} + \frac{\mu_j}{kT} - \sum_z \alpha(z) r_j^d(z) = 0 \ , \qquad \text{for all } n_j^d \in \{n_i^c\}$$

$$\frac{\partial f}{\partial \alpha(z)} = 0 \ , \qquad z = 1,2,\ldots,M \qquad (1.12)$$

For the derivative $\partial \ln Q/\partial n_j^d$ we use equation (1.8). The differential of $-kT \ln Q^*$ with respect to n_j^d gives the chemical potential μ_j^* of a molecule j in the pure amorphous state. Hence, the first term of $\partial f/\partial n_j^d$ in equation (1.12) is

$$\frac{\partial \ln Q}{\partial n_j^d} = \ln \frac{L\lambda^d}{r_j n_j^d} - 1 - \frac{\partial (U - U^*)/kT}{\partial n_j^d} - \mu_j^*/kT \qquad (1.13)$$

We assume the energy U-U* to depend only on the segment density distribution of every segment type, irrespective of the type of molecule or conformation to which it belongs. The third term on the right hand side of equation (1.13) then becomes:

$$\frac{\partial (U - U^*)/kT}{\partial n_j^d} = -\frac{\partial U^*/kT}{\partial n_j} + \sum_{z,A} \frac{\partial U/LkT}{\partial \phi_A(z)} \frac{\partial L\phi_A(z)}{\partial n_j^d} \qquad (1.14)$$

Differentiating U* with respect to n_j^d is the same as differentiating U* with respect to n_j, since U* does not depend on the conformation of the molecules but only on the number of molecules of each type. The differential $\partial L\phi_A(z)/\partial n_j^d$ can be written as $r_{Aj}^d(z)$, the number of segments A in layer z originating from a molecule j in conformation d. In order to find the equilibrium set of conformations $\{n_i^c\}$, we substitute equations (1.13) and (1.14) into equation (1.12) and obtain the following set of equations

$$\ln \frac{L\lambda^d}{r_j n_j^d} - 1 + \left(\mu_j - \mu_j^*\right)/kT + \frac{\partial U^*/kT}{\partial n_j} - \sum_{z,A} r_{Aj}^d(z) \left[\alpha(z) + \frac{\partial U/LkT}{\partial \phi_A(z)}\right] = 0$$

$$\text{for all } n_j^d \in \{n_i^c\} \qquad (1.15)$$

$$L - \sum_{i,c} r_i^c(z) n_i^c = 0 \quad , \qquad z = 1,2,\ldots,M$$

Equation (1.15) gives the number n_j^d of molecules j in conformation d, i.e., the equilibrium distribution of conformations. From this

distribution all the equilibrium properties of the system can be derived, as will be shown in the following sections.

1.2.4 Segment Potential and Segment Weighting Factor

Equation (1.15) constitutes our central result for the equilibrium situation. Upon closer inspection, the term in between the square brackets can be interpreted as 1/kT times the potential $u_A(z)$ of a segment A in layer z with respect to an arbitrary reference potential u_A^{ref}. Hence, we define $u_A(z)$ as

$$u_A(z) = kT\,\alpha(z) + \frac{\partial U / L}{\partial \phi_A(z)} + u_A^{ref} \qquad (1.16)$$

The segment potential $u_A(z)$ depends only on the type of segment but not on the type of molecule or conformation to which it belongs. In section 1.2.8 we will discuss the physical meaning of the terms on the right hand side of equation (1.16).

From the definition of the segment potential $u_A(z)$ and equation (1.15) the number of molecules i in conformation c per surface site, n_i^c/L, is easily found. The result is

$$\frac{n_i^c}{L} = C_i \lambda^c \prod_{z,A} G_A(z)^{r_{Ai}^c(z)} \qquad (1.17)$$

where the segment weighting factor $G_A(z)$ for a segment of type A in layer z is defined as

$$G_A(z) = \exp[-u_A(z)/kT] \qquad (1.18)$$

and the normalization constant C_i, which depends only on the type of molecule, is given by

$$\ln C_i = (\mu_i - \mu_i^*)/kT - 1 + \sum_A \frac{r_{Ai} u_A^{ref}}{kT} + \frac{\partial U_i^*/kT}{\partial n_i} - \ln r_i \qquad (1.19)$$

where r_{Ai} is the number of A-segments in one molecule of type i. In fact, $G_A(z)$ is a Boltzmann factor depending on the segment type and the layer number but not on the molecule type. It gives the statistical weight to find a detached segment of type A in layer z, according to its local potential $u_A(z)$. That is the reason for calling $G_A(z)$ the segment weighting factor.

If we denote the segment weighting factor of segment s of a molecule i in conformation c by $G_i^c(s)$ we can rewrite equation (1.17) as

$$\frac{n_i^c}{L} = C_i \lambda^c G_i^c \qquad (1.20)$$

where G_i^c is a product of r_i segment weighting factors:

$$G_i^c = \prod_{s=1}^{r_i} G_i^c(s) \qquad (1.21)$$

If segment s of molecule i in conformation c is of type A, and finds itself in layer z, then $G_i^c(s)$ equals $G_A(z)$. The number n_i^c/L of molecules i per surface site in conformation c is given by the product of a normalization factor C_i, a weighting factor λ^c (i.e., r_i-1 bond weighting factors λ_0 or λ_1) for performing a walk over an empty lattice according to conformation c, and a multiple product of r_i segment weighting factors $G_i^c(s)$, one for each segment according to its type and layer number.

1.2.5 Segment Density Distributions

In this section we describe how the segment density distributions $\phi_i(z)$, $\phi_{Ai}(z)$, and $\phi_A(z)$ are found from the set $G_A(z)$ of segment weighting factors using equation (1.20), but without the need to generate all the configurations separately.

We start our derivation by introducing a chain end distribution function $G_i(z,s\,|\,1)$ for a chain part consisting of the segments 1,...,s of a molecule i. This distribution function gives the statistical weight of all possible walks starting from segment 1, which may be located anywhere in the lattice, and ending at segment s in layer z. In other words, $G_i(z,s\,|\,1)$ is the statistical weight of s-mers (of the same composition as the first s segments of a molecule i with the end segment s in layer z. We denote the segment weighting factor for segment s of molecule i in layer z by $G_i(z,s)$. The difference with $G_i^c(s)$ as given above is that in the latter case the layer number need not be specified because it is fully defined by the conformation c. The factor $G_i(z,s)$ equals $G_A(z)$ if segment s of molecule i is of type A and in layer z, whereas $G_i^c(s)$ equals $G_A(z)$ if s is of type A and if conformation c prescribes that s is in z.

Our aim is to express the chain end distribution function in the segment weighting factors $G_i(z,s)$. According to its definition, $G_i(z,r_i\,|\,1)$ is the statistical weight of molecules i ending with the last segment r_i in layer z. Summation over all z gives the statistical weight of all chains i, the chain weighting factor $G_i(r_i\,|\,1)$. In $G_i(r_i\,|\,1)$ all possible conformations of the chains i in the system are included. The same total weight is obtained by summing $\lambda^c G_i^c$, the weight of chains i in one particular conformation c, over all c. Hence,

$$G_i(r_i\,|\,1) = \sum_z G_i(z,r_i\,|\,1) = \sum_c \lambda^c G_i^c = \frac{n_i}{C_i L} \qquad (1.22)$$

The last identity in this equation follows from equation (1.20).
In order to obtain the chain end distribution function $G_1(z,r_1 \mid 1)$ itself, we sum only over those conformations c having the r_1^{th} segment located in layer z. We denote these conformations by $c(z,r_1)$:

$$G_1(z,r_1|1) = \sum_{c(z,r_1)} \lambda^c G_1^c \qquad (1.23)$$

which is part of the statistical weight $G_1(r_1 \mid 1)$ given in equation (1.22). For all conformations $c(z,r_1)$ the segment weighting factor $G_1^c(r_1)$ for segment r_1 equals $G_1(z,r_1)$, and this factor may be taken outside the summation. Moreover, λ^c may be separated in the bond weighting factor $\lambda^c(r_1 \mid r_1\text{-}1)$ for the last bond and the product of the first r_1-2 bond weighting factors, see equations (1.5) and (1.6):

$$G_1(z,r_1|1) = G_1(z,r_1) \sum_{c(z,r_1)} \left[\lambda^c(r_1|r_1-1)\lambda^c(r_1-1|1)G_1^c(r_1-1|1)\right] \qquad (1.24)$$

Because segment r_1 is found in layer z there are only three possible locations for segment r_1-1: z-1, z and z+1. If we allow for backfolding we can replace the sum in equation (1.24) by three terms, using equation (1.5): $\lambda_1 G_1(z\text{-}1,r_1\text{-}1 \mid 1)$, $\lambda_0 G_1(z,r_1\text{-}1 \mid 1)$, and $\lambda_1 G_1(z\text{+}1,r_1\text{-}1 \mid 1)$. Backfolding is included because the chain end distribution functions $G_1(z,r_1\text{-}1 \mid 1)$, $G_1(z\text{-}1,r_1\text{-}1 \mid 1)$, and $G_1(z\text{+}1,r_1\text{-}1 \mid 1)$ contain a few conformations other than $c(z,r_1)$, namely those in which one or more of the first r_1-2 segments occupy the same lattice site as segment r_1. We rewrite equation (1.24) by introducing an abbreviated notation <...> for a weighted average over three layers:

$$< G_1(z,s \mid 1) > = \lambda_1 G_1(z+1,s \mid 1) + \lambda_0 G_1(z,s \mid 1) + \lambda_1 G_1(z-1,s \mid 1) \qquad (1.25)$$

This average expresses the average weight of an s-mer with segment s adjacent to a site in layer z. Now equation (1.24) becomes simply

$$G_i(z,r_i \mid 1) = G_i(z,r_i) < G_i(z,r_i - 1 \mid 1) > \qquad (1.26)$$

According to equation (1.26) the chain distribution function for an r-mer of molecule type i can be expressed in terms of the distribution function of an r-1 mer. The same arguments can be used to obtain the following recurrence relations,

$$G_i(z,s \mid 1) = G_i(z,s) < G_i(z,s-1 \mid 1) > \qquad (1.27)$$

$$G_i(z,s \mid r_i) = G_i(z,s) < G_i(z,s+1 \mid r_i) > \qquad (1.28)$$

Starting at the first segment (s=1) of a molecule of type i, for which $G_i(z,1 \mid 1) = G_i(z,1)$, the chain end distribution functions $G_i(z,s \mid 1)$ are calculated by applying equation (1.27). The chain distribution functions $G_i(z,s \mid r_i)$ are calculated starting at the other end of the chain ($s=r_i$).

For the distribution functions of inner segments of chains i we use the connectivity law, also known as the composition law. Segment s joins the chain parts 1,2,...,s and s,s+1,...,r_i. If segment s is in layer z the first chain part has a statistical weight $G_i(z,s \mid 1)$, the other $G_i(z,s \mid r_i)$. The statistical weight of all chains i with segment s in layer z becomes $G_i(z,s \mid 1)G_i(z,s \mid r_i)/G_i(z,s)$, where the factor $G_i(z,s)$ comes in to correct for double counting of the weighting factor of segment s. The volume fraction $\phi_i(z,s)$ due to segments s of molecules i in layer z is proportional to this. With $\phi_i(z) = \Sigma_s \phi_i(z,s)$ we obtain

$$\phi_i = C_i \sum_{s=1}^{r_i} G_i(z,s \mid 1)\, G_i(z,s \mid r_i) \,/ G_i(z,s) \qquad (1.29)$$

If $\partial U_i^*/\partial n_i$ and the chemical potential of molecules i in the mixture between the two plates are known, the normalization constant C_i is directly obtained from equation (1.19). The choice of the reference potential u_A^{ref} in equations (1.16) and (1.19) is arbitrary, as it cancels in equation (1.29). Alternatively, if the total amount θ_i of molecules i is known, the normalization constant is directly obtained from equation (1.22).

$$C_i = \frac{\theta_i}{r_i G_i(r_i|\,1)} \tag{1.30}$$

where we have defined θ_i as the total number of segments of molecules i per surface site present between the two plates, which equals the number of equivalent monolayers of molecules i:

$$\theta_i = \sum_z \phi_i(z) = \frac{r_i n_i}{L} \tag{1.31}$$

The expression for the volume fraction given in equation (1.29) is a straightforward generalization of that given by Scheutjens and Fleer, which only applies to chains with inversion symmetry. If we want to obtain $\phi_{Ai}(z)$, we should include in the summation over s in equation (1.29) only those segments which are of type A.

1.2.6 Adsorbing, Bridging and Free Molecules

Scheutjens and Fleer[6] have shown how to obtain detailed information on adsorbing, bridging and free polymers between two plates in case of a mixture of homopolymer and solvent, once the segment weighting factors $\{G_A(z)\}$ are known. Their equations can easily be extended to the case of a multicomponent mixture containing block copolymers.

The amount θ_i of molecules i can be subdivided into five groups: $\theta_i^{a'}$ of molecules i adsorbed on the first plate; $\theta_i^{a''}$ of molecules i adsorbed on the second plate; θ_i^{f} of non-adsorbed (free) molecules i having no segments in layers 1 and M; $\theta_i^{b'}$ of bridging molecules i with the last chain end leaving from the first plate, and $\theta_i^{b''}$ of bridging molecules i with the last chain end leaving from the second plate. Obviously,

$$\sum_g \theta_i^g = \theta_i \tag{1.32}$$

where g denotes f,a',a'',b', or b''. For each group we can define a chain weighting factor $G_i^g(r_i \mid 1)$, so that

$$\sum_g G_i^g(r_i \mid 1) = G_i(r_i \mid 1) \tag{1.33}$$

From the conditions that $G_i(z,s \mid 1) = \Sigma_g G_i^g(z,s \mid 1)$ and $G_i(z,s \mid r_i) = \Sigma_g G_i^g(z,s \mid r_i)$, and the recurrence relations (1.27) and (1.28), we can calculate the chain end distribution functions $G_i^g(z,s \mid 1)$ and $G_i^g(z,s \mid r_i)$ for every group using equations 36-43 of reference (6). If all $G_i^g(z,s \mid 1)$ and $G_i^g(z,s \mid r_i)$ are known, the volume fraction profiles of segments in trains, loops, and tails of adsorbing and bridging molecules can be calculated, as well as their size distributions. Since we are dealing with block copolymers which, in general, show no inversion symmetry, the equations for the volume fraction profiles and for the average number of trains, loops, tails, etc. will be slightly different from those derived by Scheutjens and Fleer for homopolymers. Substitution of $\Sigma_g G_i^g(z,s \mid 1)$ for $G_i(z,s \mid 1)$ and $\Sigma_g G_i^g(z,s \mid r_i)$ for $G_i(z,s \mid r_i)$ into equation (1.29) and performing the multiplication $[\Sigma_g G_i^g(z,s \mid 1)]\,[\Sigma_g G_i^g(z,s \mid r_i)] \,/\, G_i(z,s)$ gives 25 terms which contribute to $\phi_i(z)$. These 25 terms can be recognized as the distribution of segments s in free chains, in trains (or loops) on

each of the surfaces, in tails of bridging or non-bridging chains, etc. For more details we refer to table I of reference (6). From these 25 terms we can calculate the volume fraction profiles of free chains, trains, loops, tails, etc. The complete equations are given in appendix II.

1.2.7 Flory-Huggins Approximation

In order to derive the potential $u_A(z)$ of segment A in layer z and the differential of U_l^* with respect to n_l (see equations 1.16 and 1.19), we have to find expressions for the total energy U of the mixture and the energies U_l^* of the reference states.

For the energy of mixing we use the familiar Flory-Huggins[15] interaction parameter χ_{AB}, defined as the energy change (in units of kT) associated with the transfer of a segment of type A from a solution of pure A to a solution of pure B. For segments of equal size, the same energy effect occurs upon the transfer of a segment B from pure B to a solution of pure A, so that $\chi_{AB} = \chi_{BA}$ and $\chi_{AA} = 0$. In this paper, we will only account for nearest neighbor interactions, although the incorporation of long range interactions is straightforward. If a segment is located in layer z, it can only be in contact with segments in the layers z+1, z, and z-1. Since we are using a mean field approximation within each layer, we need only the average number of contacts a segment in layer z will have with, for instance, segments of type B. This average number of contacts with B-segments is given by $\lambda_1 Z\phi_B(z-1) + \lambda_0 Z\phi_B(z) + \lambda_1 Z\phi_B(z+1) \equiv Z\langle\phi_B\rangle$. The use of the angular brackets is the same as in equation (1.25). If A would be fully surrounded by B-segments, the energy contribution to the system would be χ_{AB}. Hence, the contact energy of segments A in layer z with B-segments is $L\phi_A(z)\chi_{AB}\langle\phi_B(z)\rangle$, and the total energy of mixing U can be written as

$$U/kT = \frac{L}{2} \sum_{z,\,A,\,B} \phi_A(z)\,\chi_{AB} < \phi_B(z) > \qquad (1.34)$$

where $<\phi_B(z)>$ is called the contact fraction of B-segments for a segment in layer z, and is given by

$$< \phi_B(z) > = \lambda_1 \phi_B(z-1) + \lambda_0 \phi_B(z) + \lambda_1 \phi_B(z+1) \qquad (1.35)$$

The factor 1/2 in equation (1.34) corrects for double counting, because in the double summation over A and B each type of contact occurs twice. Note that the total number of contacts A-B in the system is

$$L \sum_z \phi_A(z) < \phi_B(z) > = L \sum_z \phi_B(z) < \phi_A(z) > \qquad (1.36)$$

Equation (1.34) includes the energy of adsorption U^a provided that the solid S is included in the summation over A and B. To show this, we define a Flory-Huggins parameter* for the interaction between a segment and a surface site. The energy change (in units of kT) resulting from bringing a segment A from pure A into an environment of pure S is given by χ_{AS}. Now the adsorption energy follows directly from equation (1.34). In this equation, both A and B may refer to the two solid surfaces S and S'. The four terms containing S and S' combine pairwise so that the factor 1/2 cancels:

---

* Scheutjens and Fleer, following Silberberg[16], use an adsorption energy parameter χ_s, which is defined as the dimensionless difference $-(u^a_A - u^a_O)/kT$, where u^a_A is the adsorption energy of a polymer segment A and u^a_O that of a solvent molecule. Thus, χ_s is positive if A adsorbs preferentially from the solvent. Since in the adsorption process only $\lambda_1 Z$ instead of Z contacts are formed, $u^a_A/kT = \lambda_1 \chi_{AS}$ and $u^a_O/kT = \lambda_1 \chi_{OS}$. Therefore, $\chi_s = -\lambda_1(\chi_{AS} - \chi_{OS})$.

$$U^a / kT = L \sum_{z,A} [\phi_A(z)\chi_{AS} < \phi_S(z) > + \phi_A(z)\chi_{AS'} < \phi_{S'}(z) >] \qquad (1.37)$$

For the remaining of this article we adopt the convention that, unless stated otherwise, the surfaces S and S' are included whenever a summation over segment types is taken. For S we assume that $\phi_S(z)$ is unity for $z \leq 0$ and zero for $z > 0$, so that $<\phi_S(1)> = \lambda_1$ and $<\phi_S(z)> = 0$ for $z > 1$. Similarly, $\phi_{S'}(z)$ is zero for $z \leq M$ and unity for $z > M$, and $<\phi_{S'}(M)> = \lambda_1$ and $<\phi_{S'}(z)> = 0$ for $z < M$. Equation (1.37) can thus also be written in the form

$$U^a / kT = L \sum_{A} [\phi_A(1)\chi_{AS}\lambda_1 + \phi_A(M)\chi_{AS'}\lambda_1] \qquad (1.38)$$

To obtain the differential of U/LkT with respect to $\phi_A(z)$, needed in equation (1.16), we differentiate the right hand side of equation (1.34). Since the volume fraction of type A segments is contained in both summations (over A and B) the factor 1/2 drops out.

$$\frac{\partial U / L}{\partial \phi_A(z)} = kT \sum_{B} \chi_{AB} < \phi_B(z) > \qquad (1.39)$$

For the fourth term of equation (1.19) we need an expression for the energy U_i^* of n_i molecules in the pure amorphous state, which may contain various segment types. This energy follows from equation (1.34) as

$$U_i^* / kT = \frac{L}{2} \sum_{z,A,B} \phi_{Ai}(z)\chi_{AB}\phi_{Bi}^* \qquad (1.40)$$

where ϕ_{Bi}^* is the volume fraction of segments B in pure amorphous i, or

$$\phi^*_{Ai} = \frac{r_{Ai}}{r_i} \tag{1.41}$$

When differentiating the right hand side of equation (1.40) with respect to n_i we should note that ϕ^*_{Ai} is independent of n_i, and the factor 1/2 is retained:

$$\frac{\partial U^*_i / kT}{\partial n_i} = \frac{r_i}{2} \sum_{A,B} \phi^*_{Ai} \chi_{AB} \phi^*_{Bi} \tag{1.42}$$

In order to choose a proper reference potential, we consider a homogeneous bulk solution which is in equilibrium with the mixture between the two plates, i.e., for every molecule type the chemical potential in the bulk solution and in the mixture between the two plates are equal. The volume fraction of molecules i in this bulk solution is denoted as ϕ^b_i. An obvious choice for the reference potential would be such that u^b_A becomes zero, i.e., all G's will be unity in the bulk solution. From the condition that all G's are unity and equation (1.29) we can express the normalization constant C_i in the bulk solution volume fraction ϕ^b_i.

$$C_i = \phi^b_i / r_i \tag{1.43}$$

In appendix I we have derived an expression for the chemical potential $\mu_i - \mu^*_i$ of molecules i in a homogeneous mixture, which is a generalization of the Flory-Huggins expression. The reference potential corresponding to the condition that all G's are unity in the bulk solution is found from substitution of equations (1.42), (1.43), and (A.I.8) into equation (1.19):

$$u_A^{ref}/kT = \sum_j \frac{\phi_j^b}{r_j} + \frac{1}{2}\sum_{B,C}\phi_B^b\chi_{BC}\phi_C^b - \sum_B \chi_{AB}\phi_B^b \qquad (1.44)$$

Since the choice of the reference potential u_A^{ref} is arbitrary, we can still use equation (1.44) for u_A^{ref} when applying it to an arbitrary chosen homogeneous bulk solution. However, if the chosen bulk solution is not in full equilibrium with the mixture between the two plates then equation (1.43) will no longer hold. Using this reference potential (equation 1.44) and equation (1.42) we can rewrite the expression for the normalization constant C_i given in equation (1.19) as

$$\ln C_i = (\mu_i - \mu_i^*)/kT - 1 + r_i\sum_j \frac{\phi_j^b}{r_j} - \ln r_i + \frac{r_i}{2}\sum_{A,B}\left(\phi_A^b - \phi_{Ai}^*\right)\chi_{AB}\left(\phi_B^b - \phi_{Bi}^*\right) \qquad (1.45)$$

This equation for the normalization constant is, like equation (1.30), generally valid. For the case of full equilibrium equation (1.45) reduces to the simple form of equation (1.43) which can be seen by substituting (A.I.8) in equation (1.45).

1.2.8 Hard Core Potential and Interaction Potential

Generally, the segment potential $u_A(z)$ of segment A in layer z can be expressed as:

$$u_A(z) = u'(z) + u_A^{int}(z) \qquad (1.46)$$

where both u'(z) and $u_A^{int}(z)$ can be defined with respect to the bulk solution by a suitable choice of the reference potential, so that $u_A^b = u'^b = 0$. For example, substituting equation (1.44) for the reference potential u_A^{ref} and equation (1.39) in equation (1.16) results in the following expression for the potential u'(z) in the Flory-Huggins approximation:

$$u'(z)/kT = \alpha(z) + \sum_j \frac{\phi_j^b}{r_j} + \sum_{A,B} \phi_A^b \chi_{AB} \phi_B^b \qquad (1.47)$$

and similarly, the potential $u_A^{int}(z)$ is given by

$$u_A^{int}(z)/kT = \sum_B \chi_{AB}\left(<\phi_B(z)> - \phi_B^b\right) \qquad (1.48)$$

As can be seen from equations (1.46-1.48), $u_A(z)$ contains a part u'(z), which is independent of the segment type, and a mixing contribution $u_A^{int}(z)$ which, obviously, depends on the type of segment. The potential u'(z) may be identified as the "hard core" potential. If there is no mixing energy (i.e., if all χ_{AB} are zero), only u'(z) remains. This is, for instance, the case in a polymer melt containing only one segment type. Now u'(z) is the potential in each layer that must be applied to ensure complete occupancy of the lattice. Without this potential, the surface region of a polymer melt would be depleted because of entropic restrictions. The hard core potential u'(z) prevents this depletion and makes $\Sigma_i \phi_i(z) = 1$ for any z. In fact, u'(z) gives, through equation (1.47), the physical meaning of the Lagrange multipliers $\alpha(z)$, that were introduced precisely to satisfy the volume filling constraint (1.10). The potential u'(z) is the same for any segment type. In appendix III it will be shown how u'(z) can be found selfconsistently.

A similar "hard core potential" occurs also in other theories. For example, Helfand and Tagami[8] and Hong and Noolandi[9] define a compressibility parameter $\omega(z)$, and Gruen and De Lacey[10] introduce a lateral pressure $\pi(z)$. Marqusee and Dill[11] use parameters ln q(z) and Theodorou[12,13] arrives at $\xi(z)$ as Lagrange parameters. All these parameters have a similar physical meaning as our u'(z).

The second part of $u_A(z)$, the interaction potential $u_A^{int}(z)$, corresponds to the energy of mixing. In the Flory-Huggins approximation it represents the energy associated with the transfer of a segment A from the bulk solution, with contact fractions ϕ_B^b, ϕ_C^b, ..., to layer z where the contact fractions are $\langle\phi_B(z)\rangle$, $\langle\phi_C(z)\rangle$, ..., see equation (1.48). Clearly, this mixing energy term depends on the segment type and on the actual model used for the interaction energies.

1.2.9 Free Energy and Surface Tension

The free energy A-A* of the mixture between the two surfaces with respect to the reference state is, according to standard statistical thermodynamics, given by

$$A - A^* = -kT \ln \frac{Q}{Q^*} \qquad (1.49)$$

The logarithm of the canonical partition function is given by equation (1.8). Let us rewrite the first term on the right hand side of equation (1.8), i.e. the entropic part of Q, using equations (1.17) and (1.18). Taking the logarithm of the former equation, multiplying by n_i^c and summing over i and c gives after some rearrangement:

$$\sum_{i,c} n_i^c \ln \frac{L\lambda^c}{r_i n_i^c} = -L\sum_i \frac{\theta_i}{r_i} \ln r_i C_i + L \sum_{z,A'} \phi_{A'}(z) u_{A'}(z) / kT \qquad (1.50)$$

In the summation over A' the surfaces S and S' are *not* included. Substitution of equation (1.8) into equation (1.49), using equations (1.34), (1.40), and (1.50), results in the following expression for the free energy A-A*:

$$\frac{A - A^*}{LkT} = \sum_i \frac{\theta_i}{r_i} \ln r_i C_i - \sum_{z,A'} \phi_{A'}(z) u_{A'}(z) / kT + \frac{1}{2} \sum_{z,A,B} \phi_A(z) \chi_{AB} < \phi_B(z) >$$

$$- \frac{1}{2} \sum_i \left(\theta_i \sum_{A,B} \phi^*_{Ai} \chi_{AB} \phi^*_{Bi} \right) \qquad (1.51)$$

For the normalization constant C_i we can substitute $\theta_i / r_i G_i(r_i | 1)$, according to equation (1.30), so that the free energy is written in terms of the segment potentials and segment densities only.
We can also express the free energy in terms of hard core potentials, chemical potentials, and segment densities, by substituting equations (1.45), (1.46), and (1.48) in equation (1.51).

$$\frac{A - A^*}{LkT} = -\sum_i \frac{\theta_i^{ex}}{r_i} - \sum_z u'(z) / kT - \frac{1}{2} \sum_{z,\, A',\, B'} \chi_{A'B'} \left(\phi_{A'}(z) < \phi_{B'}(z) > - \phi^b_{A'} \phi^b_{B'} \right)$$

$$+ \sum_i \frac{\theta_i}{r_i kT} (\mu_i - \mu_i^*) \qquad (1.52)$$

where θ_i^{ex} is, analogous to equation (1.31), the excess amount of molecules i, expressed as equivalent monolayers:

$$\theta_i^{ex} = \sum_i \left(\phi_i(z) - \phi_i^b \right) \tag{1.53}$$

Again, the primes in the third term on the right hand side of equation (1.52) indicate that the surfaces S and S' are *not* included in the double summation.

The surface tensions γ_S and $\gamma_{S'}$ are the excess surface free energies per unit area for the two surfaces. At constant volume V = ML and surface areas A_S and $A_{S'}$, standard thermodynamics gives $-pV + \gamma_S A_S + \gamma_{S'} A_{S'} = -kT \ln \Xi(\{\mu_i\},M,L,T)$, where p is the pressure. In the reference state, containing only bulk phases, we have $-p\Sigma_i V_i = -kT\Sigma_i \ln \Xi_i^*$. Hence,

$$\gamma_S A_S + \gamma_{S'} A_{S'} = -kT \ln\left(\frac{\Xi}{\Xi^*}\right) = A - A^* - \sum_i n_i(\mu_i - \mu_i^*) \tag{1.54}$$

Substituting equation (1.52) into equation (1.54) gives the following result for the excess surface free energy per surface site:

$$\begin{aligned} \frac{\gamma_S A_S + \gamma_{S'} A_{S'}}{LkT} = &- \sum_i \frac{\theta_i^{ex}}{r_i} - \sum_z u'(z) / kT \\ &- \frac{1}{2} \sum_{z,A',B'} \chi_{A'B'} \left(\phi_{A'}(z) < \phi_{B'}(z) > - \phi_{A'}^b \phi_{B'}^b \right) \end{aligned} \tag{1.55}$$

Obviously, the value of $\gamma_S A_S + \gamma_{S'} A_{S'}$ depends on the plate separation M. In the case of two equal surfaces, the excess surface free energy can be written as $2\gamma_S A_S$. If the volume fractions in each layer are the same as in the bulk solution, equation (1.55) reduces to $\gamma_S A_S + \gamma_{S'} A_{S'} = -L\Sigma_z u'(z)$. This implies, e.g., to a one component system, for which the volume fraction at any z is unity.

1.3 RESULTS and DISCUSSION

In this section we present a selection of numerical results on the segment distributions of adsorbed block copolymers in relation to parameters like solvent quality, surface affinity, and bulk concentration. In another publication[14] we will give detailed and systematic results on the effect of the chain composition of block copolymers on the adsorbed amount and the hydrodynamic layer thickness.

All results presented here have been calculated for a hexagonal lattice (Z=12, λ_0=6/12).

1.3.1 Segment Density Distributions

In order to illustrate the structure of an adsorbed layer on one surface, we examine the segment weighting factors $G_A(z)$ and $G_B(z)$, and the segment density profiles $\phi(z)$, $\phi_A(z)$, and $\phi_B(z)$ of an $A_{50}B_{50}$ diblock copolymer. The 50 A-segments are given a high affinity for the surface (χ_{AS} = -10 kT) and the 50 B-segments have the same affinity for the surface as the solvent O ($\chi_{BS} = \chi_{OS} = 0$). The solvent quality is taken poor for the A-segments (χ_{AO} = 0.5) and good for the B-segments (χ_{BO} = 0). Figure (1.2a) gives the segment weighting factors G(z) for the A and B-segments. Near the surface $G_A(z)$ is higher than 1 since the A-segments adsorb preferentially on the surface because of the high surface affinity (χ_{AS} = -10). For $G_B(z)$ low values (< 1) are found near the surface because B-segments are displaced by the preferentially adsorbing A-segments.

From the volume fraction profiles in figure (1.2b,c,d) we may conclude that the A-segments are mainly found in trains and loops, whereas the B-segments contribute predominantly to the density profile of tails. It

is instructive to compare the density profiles of the A-segments of the $A_{50}B_{50}$ diblock copolymer with those of an A_{50} homopolymer (figure 1.2e) at the same adsorbed amount of A-segments. The (total) volume fraction profile of A-segments is nearly equal for both types of

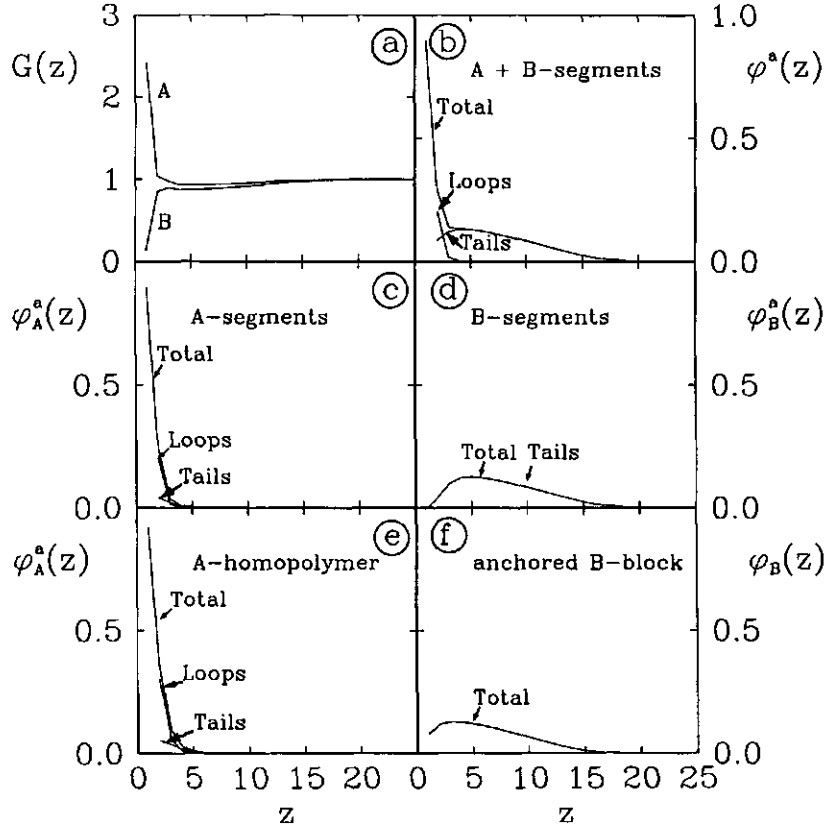

Figure 1.2. *Segment weighting factor profiles of the A and B-segments for an $A_{50}B_{50}$ diblock copolymer (a), the corresponding (total) segment density profile for the copolymer (b), and the separate segment density profiles for A and B-segments (c,d).The latter profiles may be compared with those of an A_{50}-homopolymer (e) and a B_{50} terminally attached homopolymer (f). The A segments are strongly adsorbing (χ_{AS} = -10), χ_{AO} = 0.5, all other χ parameters are zero.*

molecules. However, the volume fraction of A-segments in loops is slightly higher for the A-homopolymer and, consequently, that of A-segments in tails lower than for the $A_{50}B_{50}$ copolymer. Hence, the distribution of A-segments in the homopolymer is more homogeneous (i.e., depends less on the ranking number). In the next section we will study the distribution of the individual segments of adsorbed molecules over the layers in more detail.

As adsorbed block copolymers are often treated as anchored chains, it is also interesting to compare the profile of B-segments with that of an anchored B-block. Cosgrove et al.[17] and Hirz[18] have extended the theory of Scheutjens and Fleer to the case of anchored tails. We used this modification of the theory to calculate the profile of a terminally attached B-block (figure 1.2f). The amount of anchored B-blocks of 50 segments is taken equal to the adsorbed amount of B-segments of the $A_{50}B_{50}$ diblock copolymers. The shape of both density profiles is essentially the same, with the profile of the B-segments of the block copolymer shifted about 2 layers further into the solution than the profile of the anchored B-block. There is a significant difference between both profiles in the first two layers since the B-segments of the copolymer interpenetrate the adsorbed layer of A-segments.

The effect of the surface affinity of the A and B-segments and that of the solvent quality for the B-segments on the segment density profiles of an adsorbing AB block copolymer is shown in figure (1.3), for a longer copolymer $A_{250}B_{250}$. In this case χ_{AB} was chosen as 0.3, the other parameters are $\chi_{OS} = 0$, $\chi_{AO} = 0.5$, and $\phi^b = 10^{-4}$. In figure (1.3a) the A-segments are weakly adsorbing ($\chi_{AS} = -2$) whereas in figure (1.3b) the A-segments have a high surface affinity ($\chi_{AS} = -10$); in both cases the B-segments are non-adsorbing ($\chi_{BS} = 0$). When the surface affinity is high (figure 1.3b) more extended adsorbed layers than for $\chi_{AS} = -2$ are found due to a higher adsorbed amount. This higher adsorbed amount for $\chi_{AS} = -10$ gives also higher segment densities. If

the solvent quality is good for the B-segments (χ_{BO} = 0), a very extended profile is found for χ_{AS} = -10: up to 45 layers. In case of a low surface affinity for the A-segments (χ_{AS} = -2), lowering the solvent quality for the B-segments results primarily in higher segment densities. A poor (χ_{BO} = 0.5, Θ-solvent) or bad (χ_{BO} = 0.6) solvent

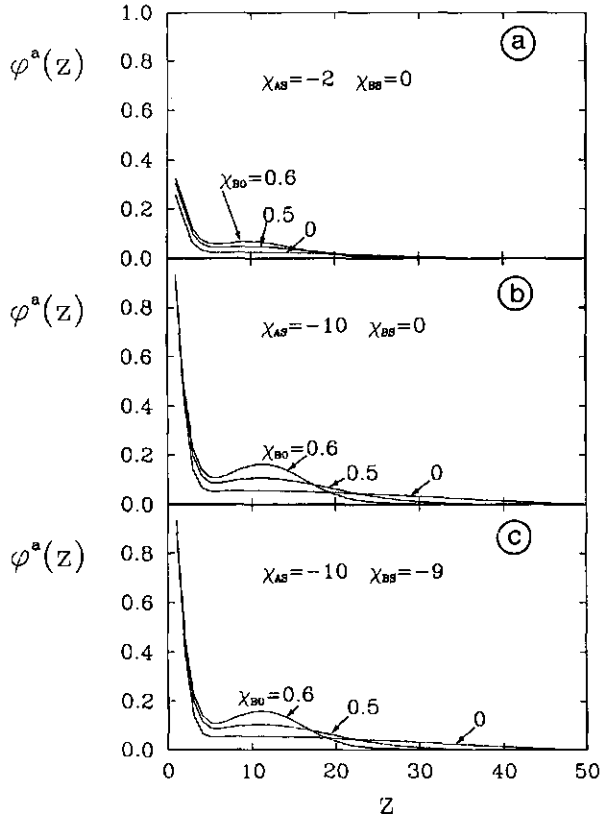

Figure 1.3. *Segment density profiles of an $A_{250}B_{250}$ diblock copolymer for a low (a) and a high (b,c) surface affinity of A-segments (χ_{AS} = -2 and -10, respectively) and three different solvent qualities for the B-segments (indicated). The B-segments are non-adsorbing (χ_{BS} = 0) in (a) and (b), and are given a surface affinity χ_{BS} = -9 in (c). Other parameters: χ_{OS} = 0, χ_{AO} = 0.5, χ_{AB} = 0.3, and $\phi^b = 10^{-4}$.*

quality for the B segments, but just below the critical χ value where phase separation occurs between B-chains of 250 segments and the surface affinity is high (figure 1.3b) more extended adsorbed layers than for χ_{AS} = -2 are found due to a higher adsorbed amount. This higher adsorbed amount for χ_{AS} = -10 gives also higher segment densities. If the solvent quality is good for the B-segments (χ_{BO} = 0), a very extended profile is found for χ_{AS} = -10: up to 45 layers. In case of a low surface affinity for the A-segments (χ_{AS} = -2), lowering the solvent quality for the B-segments results primarily in higher segment densities. A poor (χ_{BO} = 0.5, Θ-solvent) or bad (χ_{BO} = 0.6) solvent quality for the B segments, but just below the critical χ value where phase separation occurs between B-chains of 250 segments and solvent molecules, makes it less favorable for these segments to be surrounded by solvent molecules. However, there is no substantial collapse of the B-block because the surface affinity is too low to compensate for the loss of entropy. If the surface affinity is high for the A-segments (χ_{AS} = -10), a lower solvent quality for the B-segments results in less extended segment density profiles (25-30 layers) and the density in the tail region increases. In this case the loss of entropy due to the partial collapse of the B-tail is compensated by the strongly adsorbing A-segments. There is hardly any effect on the segment density profiles if the B-segments have a surface affinity somewhat lower than the A-segments (χ_{AS} = -10 and χ_{BS} = -9), as is seen from figure (1.3c). Since the A and B-blocks are equally long and the adsorbed amount is high because of the high surface affinity of the A-segments, displacement of A-segments from the surface by B-segments is not likely, even if the difference in surface affinity is rather low.

1.3.2 Distribution of Individual Segments

In order to obtain more detailed information on the structure of the adsorbed layer, we present in this subsection some typical results of the distribution of individual segments of adsorbed molecules over the various layers.

For every individual segment s the ratio $\phi_i^a(z,s)/\Sigma_z\phi_i^a(z,s)$ gives the normalized distribution of segment s over the various layers. In fact, this ratio gives the probability $P_i^a(z,s)$ to find segment s of an adsorbed molecule i in layer z.

$$P_i^a(z,s) = \frac{\phi_i^a(z,s)}{\sum_z \phi_i^a(z,s)} \qquad (1.56)$$

For showing the dependence of $P_i^a(z,s)$ on the layer number z and the segment ranking number s, we will give contour plots of $100*P_i^a(z,s)$ as a function of z and s. The curves in these contour plots represent points of equal $P_i^a(z,s)$ values.

Figure (1.4) gives the individual segment distributions of an A_{100} homopolymer, an $A_{100}B_{100}$ diblock copolymer, and an $A_{100}B_{100}A_{100}$ triblock copolymer. The A-segments are the adsorbing segments (χ_{AS} = -10), all other χ parameters are zero, and the solution concentration is $\phi^b = 10^{-4}$. From comparing the $P_i^a(z,s)$ profile of the A_{100} homopolymer with the profile of the A_{100}-block of the diblock copolymer we may conclude the following.

Obviously, the segment probability profile for the A_{100} homopolymer is symmetric with respect to s. The end segments are distributed over a larger distance from the surface than the middle segments. The average tail length of the homopolymer is found to be 6.2 segments long. The segment probability profile of the A-block of the $A_{100}B_{100}$ diblock copolymer is asymmetric (figure 1.4b), since the A-segment

with s=100 is connected to the non-adsorbing B-block. The A-block is closer to the surface except the A-segments close to s=100, and the effect of the ranking number is weaker than in the A_{100} homopolymer. This is due to the fact that the adsorbed amount of A-segments is lower for the diblock copolymer than for the A-homopolymer. As already concluded from the volume fraction profiles of the B-segments in figure (1.2d), the B-block is found in one dangling tail, which is also seen in the segment probability profile of the B-blocks. The loops in

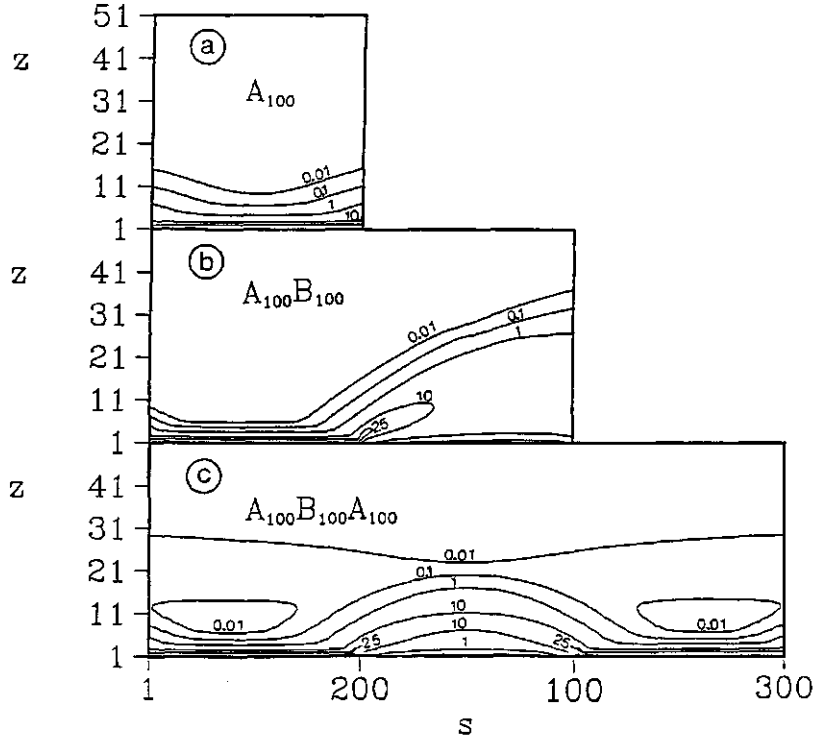

Figure 1.4. *Contour plots of 100 * $P_t^a(z,s)$ as a function of segment ranking number s and layer number z for an A_{100} homopolymer (a), an $A_{100}B_{100}$ diblock copolymer (b), and an $A_{100}B_{100}A_{100}$ triblock copolymer (c). The A-segments are strongly adsorbing (χ_{AS} = -10), all other χ-parameters are zero, and $\phi^b = 10^{-4}$.*

the probability curves for the B-segments (s>100) indicate that the distance from the surface where B-segments have the highest probability increases with increasing ranking number. The strongest increase is found for the B-segments near the A-block.

For the $A_{100}B_{100}A_{100}$ triblock copolymer a symmetric profile is found (figure 1.4 c). From the profile of the B-block we can conclude that most B-segments are found in one loop. For the first 10 layers we obtain a profile for the A-blocks very similar to that of the A-blocks of

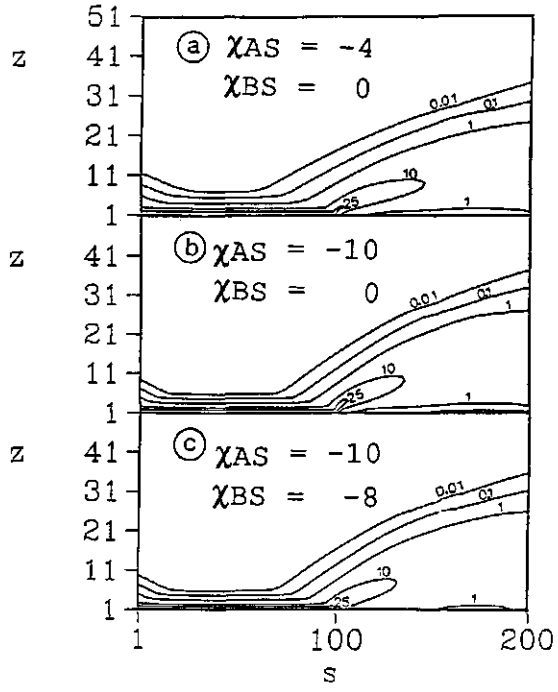

Figure 1.5. *Contour plots of 100 * $P^{\alpha}(z,s)$ as a function of segment ranking number s and layer number z of an $A_{100}B_{100}$ diblock copolymer for two different values of χ_{AS} and χ_{BS} (indicated). As in figure (1.4) all other χ parameters are zero. Figure (1.5b) is the same as figure (1.4b).*

the $A_{100}B_{100}$ diblock copolymer. However, at larger distance from the surface the profile of the end-segments of the copolymer shows a hump. This originates from a few chains with one A-block adsorbed and a "sticky" tail containing both the B-block and the other A-block. A second interesting point is the extension of the profile of the A-blocks into the solution as compared with the diblock copolymer. The conformation of the A-blocks of the $A_{100}B_{100}A_{100}$ triblock copolymer is less "flat" than that of the A block of the $A_{100}B_{100}$ diblock copolymer, because the adsorbed amount of A segments is higher for the triblock copolymer.

The effect of surface affinity of the A-segments on an $A_{100}B_{100}$ diblock copolymer is shown in parts a and b of figure (1.5). The segment probability profile of the diblock copolymer is given for two different surface affinities for the A-segments (χ_{AS} = -4, and -10). When χ_{AS} becomes more negative the A-block is found closer to the surface and the B-block is somewhat more stretched out. This is easily understood since a higher surface affinity gives a better compensation for the loss of entropy. Hence, more copolymers adsorb, the B-blocks are in a more extended conformation because of lateral interactions, and the A-blocks will be found in a more closely packed and relatively collapsed conformation on the surface.

Similarly, the effect of the surface affinity of the B-segments is given in figure (1.5b,c). For the two χ_{BS} values used (χ_{BS} = 0 and -8) there is hardly any effect on the profile of the A-block. The profile of the B-block becomes slightly less extended as χ_{BS} becomes more negative, especially for the B-segments with a low ranking number, i.e., close to the A-block. As the difference in surface affinity between A and B-segments decreases, more B-segments will be found in long loops and in short trains.

The solvent quality for the B-segments has a drastic effect on the conformation of the B block as is seen in figure (1.6). The B-segments are found closer to the surface when the solvent quality for

these segments decreases. This is especially the case for the B-segments with a higher ranking number, near the chain end. Since the adsorbed amount increases with increasing χ_{BO}, the profile for A-block becomes somewhat more extended.

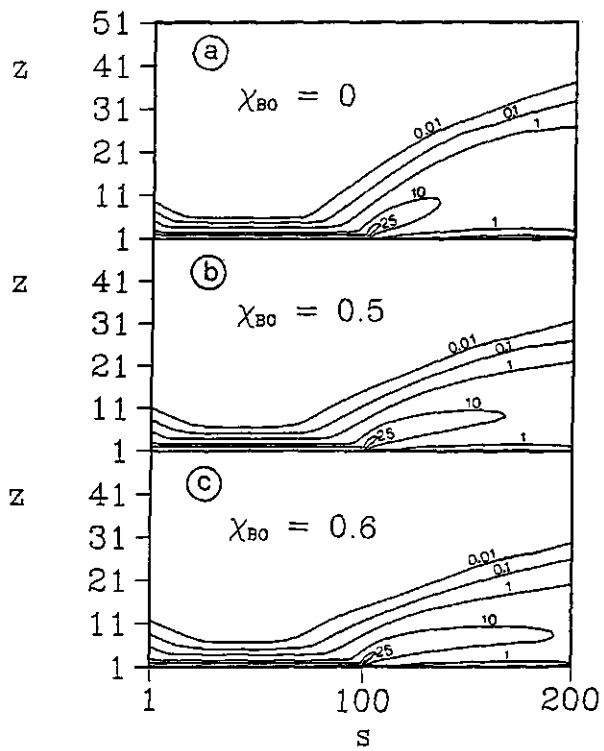

Figure 1.6. *Contour plots of 100 * $P^{\alpha}(z,s)$ as a function of segment ranking number s and layer number z of an $A_{100}B_{100}$ diblock copolymer for three different values of χ_{BO}. All other χ-parameters are zero.*

1.4 CONCLUSIONS

We have shown how the self-consistent field theory of Scheutjens and Fleer for adsorption of homopolymers from a binary mixture can be generalized to describe adsorption of block copolymers of any composition from a multicomponent mixture. Also, we have shown how the surface tension of adsorbed block copolymers in a multicomponent mixture can be calculated.

Detailed information on the structure of the adsorbed layer of block copolymers has been obtained. Diblock copolymers tend to adsorb with the adsorbing block rather flat on the surface. The density profile of the adsorbing A-segments is similar to that of an A-homopolymer of the same length. The less or non-adsorbing adsorbing block is found in one dangling tail and protrudes far out into the solution. The segment density profile of this block resembles that found for terminally anchored chains. For high adsorbed amounts the extension of the segment density profile of the less or non-adsorbing adsorbing block depends highly on the solvent quality for the segments of this block. Triblock copolymers with adsorbing end blocks form dangling tails with "sticky" ends.

APPENDIX I Derivation of a generalized Flory-Huggins formula for the chemical potential

Flory[15] has derived a formula for the chemical potential of a homopolymer in binary and ternary mixtures. His expression for a binary mixture can be written as

$$\left(\mu_1 - \mu_1^*\right)/kT = \ln\phi_1 + 1 - r_1\left(\phi_1/r_1 + \phi_2/r_2\right) + r_1\chi_{12}\phi_2^2 \qquad \text{(A.I.1)}$$

By interchanging the indices 1 and 2, μ_2 is obtained.

We need a general equation for the chemical potential of a copolymer in a homogeneous multicomponent mixture. The chemical potential μ_j of a molecule j in a mixture containing n_j molecules j is obtained by differentiating the free energy A of the mixture with respect to n_j:

$$(\mu_j - \mu_j^*) / kT = \frac{\partial(A - A^*)}{\partial n_j} \qquad \text{(A.I.2)}$$

The free energy of the pure unmixed liquid phases of the same molecules is denoted by A^*. The free energy difference $A-A^*$ is simply given by:

$$\frac{A - A^*}{kT} = \sum_i n_i \ln \phi_i + \frac{1}{2} \sum_{i,A,B} n_i r_{Ai} \chi_{AB} (\phi_B - \phi_{Bi}^*) \qquad \text{(A.I.3)}$$

This equation can be derived as $A-A^* = -kT \ln (\Omega/\Omega^*) = -kT \ln(\Omega/\Omega^*) + U - U^*$, applied to a homogeneous bulk solution along the lines given in sections 1.2.3 and 1.2.8. It is easily verified that equation (1.7) reduces to the first term (the entropy part) of equation (A.I.3), whereas equations (1.34) and (1.40) give the second (energetic) term.

The physical process corresponding to the differentiation in equation (A.I.2) is the transfer of a molecule j from the reference state to the mixture. During this transfer the number of molecules of component j in both phases will change. For the entropy part of the free energy difference we obtain:

$$\frac{\partial \sum_i n_i \ln \phi_i}{\partial n_j} = \ln \phi_j + 1 - r_j \sum_i \frac{\phi_i}{r_i} \qquad \text{(A.I.4)}$$

For the derivative of the energy part we make use of the expressions given in equations (A.I.5) and (A.I.6). Note that $\phi_j = r_j n_j / n$, where n is the total number of molecules in the mixture, and r_{Ai} is the number of segments A per molecule of type i.

$$\frac{\partial \phi_B}{\partial n_j} = (r_{Bj} - \phi_B r_j) / \sum_i r_i n_i \qquad \text{(A.I.5)}$$

$$\frac{\partial \phi^*_{Bj}}{\partial n_j} = 0 \qquad \text{(A.I.6)}$$

Equation (A.I.6) follows from the fact that the segment volume fractions of pure liquid molecules j ($\phi^*_{Aj} = r_{Aj}/r_j$) is independent of the number of molecules. With equations (A.I.5) and (A.I.6) we obtain

$$\frac{\partial (U - U^*)}{\partial n_j} = \tfrac{1}{2} kT \sum_{A,B} \chi_{AB} \left[r_{Aj} \left(\phi_B - \phi^*_{Bj} \right) + \phi_A \left(r_{Bj} - \phi_B r_j \right) \right] \qquad \text{(A.I.7)}$$

where $\Sigma_i n_i r_{Ai} / \Sigma_i n_i r_i$ was replaced by ϕ_A. Combining equations (A.I.7) and (A.I.4) we obtain for $\mu_j - \mu^*_j$

$$\frac{\mu_j - \mu^*_j}{kT} = \ln \phi_j + 1 - r_j \sum_i \frac{\phi_i}{r_i} - \frac{r_j}{2} \sum_{A,B} \left(\phi_A - \phi^*_{Aj} \right) \chi_{AB} \left(\phi_B - \phi^*_{Bj} \right) \qquad \text{(A.I.8)}$$

where we used the relation $r_{Aj} = r_j \phi^*_{Aj}$.
It is easily verified that equation (A.I.8) reduces to equation (A.I.1) for the case of a binary mixture.

APPENDIX II Adsorbing, Bridging and Free Molecules

The equations for the chain end distribution functions of adsorbed (a), bridging (b) and free (f) chains are given below, where a prime (') indicates the surface adjacent to layer 1 and a double prime (") the surface adjacent to layer M. The equations are straightforward generalizations of those given in reference (6).

The chain end distribution function $G^f_i(z,s \mid 1)$ of segment s of non-adsorbed (free) molecules i is given by:

$$
\begin{aligned}
&G_i^f(1, s|\,1) = 0 \\
&G_i^f(z, s|\,1) = G_i(z, s) < G_i^f(z, s-1|\,1) > , \qquad \text{for } 1 < z < M \\
&G_i^f(M, s|\,1) = 0
\end{aligned}
\tag{A.II.1}
$$

For $z = 1$ we have $G_i(1,s)<G_i^f(1,s-1|\,1)>$, but this term contributes to adsorbing chains. The equations for the chain end distribution functions $G_i^f(z,s|\,r_i)$ are similar.

The chain end distribution function $G_i^{a'}(z,s|\,1)$ of segment s of molecules i adsorbed on the first surface is given by:

$$
\begin{aligned}
&G_i^{a'}(1, s|\,1) = G_i(1, s) < G_i^{a'}(1, s-1|\,1) + G_i^f(1, s-1|\,1) > , \text{ for } M > 1 \\
&G_i^{a'}(z, s|\,1) = G_i(z, s) < G_i^{a'}(z, s-1|\,1) > , \qquad \text{for } 1 < z < M \\
&G_i^{a'}(M, s|\,1) = 0
\end{aligned}
\tag{A.II.2}
$$

The equations for the chain end distribution functions $G_i^{a'}(z,s|\,r_i)$ are similar.

The chain end distribution function $G_i^{a''}(z,s|\,1)$ of segment s of molecules i adsorbed on the second surface is given by:

$$
\begin{aligned}
&G_i^{a''}(1, s|\,1) = 0 \\
&G_i^{a''}(z, s|\,1) = G_i(z, s) < G_i^{a''}(z, s-1|\,1) > , \qquad \text{for } 1 < z < M \\
&G_i^{a''}(M, s|\,1) = G_i(M, s) < G_i^{a''}(M, s-1|\,1) + G_i^f(M, s-1|\,1) > , \text{ for } M > 1
\end{aligned}
\tag{A.II.3}
$$

The equations for the chain end distribution functions $G_i^{a''}(z,s|\,r_i)$ are similar.

The chain end distribution function $G_i^{b'}(z,s|\,1)$ of segment s of bridging molecules i with the last chain end leaving from the first surface is given by:

$$
\begin{aligned}
&G_i^{b'}(1, s|\,1) = G_i(1, s) \\
&\qquad < G_i^{b'}(1, s-1|\,1) + G_i^{b''}(1, s-1|\,1) + G_i^{a''}(1, s-1|\,1) > , \text{ for } M > 1 \\
&G_i^{b'}(z, s|\,1) = G_i(z, s) < G_i^{b'}(z, s-1|\,1) > , \qquad \text{for } 1 < z < M \\
&G_i^{b'}(M, s|\,1) = 0, \qquad \text{for } M > 1
\end{aligned}
\tag{A.II.4}
$$

The equations for the chain end distribution functions $G_i^{b'}(z,s|\,r_i)$ are similar.

The chain end distribution function $G_i^{b''}(z,s|1)$ of segment s of bridging molecules i with the last chain end leaving from the second surface is given by:

$$G_i^{b''}(1, s|1) = 0, \qquad \text{for } M > 1$$
$$G_i^{b''}(z, s|1) = G_i(z, s) < G_i^{b''}(z, s-1|1) >, \qquad \text{for } 1 < z < M$$
$$G_i^{b''}(M, s|1) = G_i(M, s) < G_i^{b'}(M, s-1|1) + G_i^{b''}(M, s-1|1) + G_i^{a'}(M, s-1|1) >, \text{ for } M > 1 \qquad \text{(A.II.5)}$$

For M=1 all chains are bridging:

$$G_i^{b'}(1, s|1) = G_i^{b''}(1, s|1) = G_i(1, s) < G_i^{b'}(1, s-1|1) >, \qquad \text{for } M = 1 \qquad \text{(A.II.6)}$$

The equations for the chain end distribution functions $G_i^{b''}(z,s|r_i)$ are similar.

All starting values of the various chain end distribution functions $G_i^{g}(z,1|1)$, where g = a', a'', f , b', or b'', are zero except the following nonzero terms:

$$G_i^{a'}(1, 1|1) = G_i(1, 1), \qquad \text{for } M > 1$$
$$G_i^{f}(z, 1|1) = G_i(z, 1), \qquad \text{for } 1 < z < M \qquad \text{(A.II.7)}$$
$$G_i^{a''}(M, 1|1) = G_i(M, 1), \qquad \text{for } M > 1$$
$$G_i^{b'}(1, 1|1) = G_i^{b''}(1, 1|1) = \tfrac{1}{2}G_i(1, 1), \text{ for } M = 1$$

For the starting values of $G_i^{g}(z,s|r_i)$ we have similar equations.

From the chain end distribution functions $G_i^{g}(z,s|1)$ and $G_i^{g}(z,s|r_i)$ the volume fractions in trains (tr), loops (lp), and tails (tl) may be calculated with the following equations.

$$\phi_{tr,i}^{a'}(1) = C_i \sum_{s=1}^{r_i} G_i^{a'}(1, s|1) G_i^{a'}(1, s|r_i) \; / \; G_i(1, s) \qquad \text{(A.II.8)}$$

$$\phi_{tr,i}^{a''}(M) = C_i \sum_{s=1}^{r_i} G_i^{a''}(M, s|1) G_i^{a''}(M, s|r_i) \; / \; G_i(M, s) \qquad \text{(A.II.9)}$$

$$\phi^{a'}_{lp,i}(z) = C_i \sum_{s=1}^{r_i} G_i^{a'}(z, s|1) G_i^{a'}(z, s|r_i) / G_i(z, s), \qquad \text{for } 1 < z < M \qquad \text{(A.II.10)}$$

$$\phi^{a''}_{lp,i}(z) = C_i \sum_{s=1}^{r_i} G_i^{a''}(z, s|1) G_i^{a''}(z, s|r_i) / G_i(z, s), \qquad \text{for } 1 < z < M \qquad \text{(A.II.11)}$$

$$\phi^{a'}_{tl,i}(z) = C_i \sum_{s=1}^{r_i} [G_i^{a'}(z, s|1) G_i^{f}(z, s|r_i) + G_i^{f}(z, s|1) G_i^{a'}(z, s|r_i)] / G_i(z, s), \qquad \text{for } 1 < z < M$$

(A.II.12)

$$\phi^{a''}_{tl,i}(z) = C_i \sum_{s=1}^{r_i} [G_i^{a''}(z, s|1) G_i^{f}(z, s|r_i) + G_i^{f}(z, s|1) G_i^{a''}(z, s|r_i)] / G_i(z, s), \qquad \text{for } 1 < z < M$$

(A.II.13)

For the volume fraction $\phi_{br,i}(z)$ of segments in bridges we obtain:

$$\phi_{br,i}(z) = C_i \sum_{s=1}^{r_i} [\left(G_i^{a'}(z, s|1) + G_i^{b'}(z, s|1)\right)\left(G_i^{a''}(z, s|r_i) + G_i^{b''}(z, s|r_i)\right)$$
$$+ \left(G_i^{a''}(z, s|1) + G_i^{b''}(z, s|1)\right)\left(G_i^{a'}(z, s|r_i) + G_i^{b'}(z, s|r_i)\right)] / G_i(z, s), \qquad \text{for } 1 < z < M$$

(A.II.14)

The volume fractions of segments in trains (tr), loops (lp), and tails (tl) of bridging molecules are given by

$$\phi^{b'}_{tr,i}(1) = C_i \sum_{s=1}^{r_i} [G_i^{a'}(1, s|1) G_i^{b'}(1, s|r_i) + G_i^{b'}(1, s|1) G_i^{a'}(1, s|r_i) + G_i^{b'}(1, s|1) G_i^{b'}(1, s|r_i)] / G_i(1, s) \qquad \text{(A.II.15)}$$

$$\phi^{b''}_{tr,i}(M) = C_i \sum_{s=1}^{r_i} [G_i^{a''}(M, s|1)G_i^{b''}(M, s|r_i) + G_i^{b''}(M, s|1)G_i^{a''}(M, s|r_i) + G_i^{b''}(M, s|1)G_i^{b''}(M, s|r_i)] \; / \; G_i(M, s) \qquad \text{(A.II.16)}$$

$$\phi^{b'}_{lp,i}(z) = C_i \sum_{s=1}^{r_i} [G_i^{a'}(z, s|1)G_i^{b'}(z, s|r_i) + G_i^{b'}(z, s|1)G_i^{a'}(z, s|r_i) + G_i^{b'}(z, s|1)G_i^{b'}(z, s|r_i)] \; / \; G_i(z, s), \qquad \text{for } 1 < z < M \qquad \text{(A.II.17)}$$

$$\phi^{b''}_{lp,i}(z) = C_i \sum_{s=1}^{r_i} [G_i^{a''}(z, s|1)G^{b''}(z, s|r_i) + G_i^{b''}(z, s|1)G_i^{a''}(z, s|r_i) + G_i^{b''}(z, s|1)G_i^{b''}(z, s|r_i)] \; / \; G_i(z, s), \qquad \text{for } 1 < z < M \qquad \text{(A.II.18)}$$

$$\phi^{b'}_{tl,i}(z) = C_i \sum_{s=1}^{r_i} [G_i^{b'}(z, s|1)G_i^{f}(z, s|r_i) + G_i^{f}(z, s|1)G_i^{b'}(z, s|r_i)] \; / \; G_i(z, s), \qquad \text{for } 1 < z < M \qquad \text{(A.II.19)}$$

$$\phi^{b''}_{tl,i}(z) = C_i \sum_{s=1}^{r_i} [G_i^{b''}(z, s|1)G_i^{f}(z, s|r_i) + G_i^{f}(z, s|1)G_i^{b''}(z, s|r_i)] \; / \; G_i(z, s), \qquad \text{for } 1 < z < M \qquad \text{(A.II.20)}$$

The volume fraction $\phi^f(z)$ of free molecules, for $1 < z < M$, is simply given by

$$\phi^{f}_{i}(z) = C_i \sum_{s=1}^{r_i} G_i^{f}(z, s|1)G_i^{f}(z, s|r_i) \; / \; G_i(z, s) \qquad \text{(A.II.21)}$$

The equations for the average number of trains, loops, and tails per adsorbing chain are

$$n^{a'}_{lp,i} = \frac{\lambda_1}{G_i^{a'}(r_1|1)} \sum_{s=2}^{r_i - 1} G_i^{a'}(2, s|1)G_i^{a'}(1, s+1|r_i) \qquad \text{(A.II.22)}$$

$$n^{a''}_{lp,i} = \frac{\lambda_1}{G_i^{a''}(r_1|1)} \sum_{s=2}^{r_i - 1} G_i^{a''}(M-1, s|1)G_i^{a''}(M, s+1|r_i) \qquad \text{(A.II.23)}$$

$$n^{a'}_{tr,i} = n^{a'}_{lp,i} + 1 \qquad \text{(A.II.24)}$$

$$n^{a''}_{tr,i} = n^{a''}_{lp,i} + 1 \qquad \text{(A.II.25)}$$

$$n^{a'}_{tl,i} = 2 - \frac{G_i^{a'}(1, r_1 | 1) + G_i^{a'}(1, 1 | r_1)}{G_i^{a'}(r_1 | 1)} \qquad \text{(A.II.26)}$$

$$n^{a''}_{tl,i} = 2 - \frac{G_i^{a''}(M, r_1 | 1) + G_i^{a''}(M, 1 | r_1)}{G_i^{a''}(r_1 | 1)} \qquad \text{(A.II.27)}$$

The average number of bridges per molecule i is given by

$$n_{br,i} = \frac{\lambda_1}{G_i^{b'}(r_1 | 1) + G_i^{b''}(r_1 | 1)} \times$$

$$\sum_{s=1}^{r_1 - 1} [\left(G_i^{a''}(2, s | 1) + G_i^{b''}(2, s | 1)\right)\left(G_i^{a'}(1, s+1 | r_1) + G_i^{b'}(1, s+1 | r_1)\right)$$

$$+ \left(G_i^{a'}(1, s | 1) + G_i^{b'}(1, s | 1)\right)\left(G_i^{a''}(2, s+1 | r_1) + G_i^{b''}(2, s+1 | r_1)\right)]$$

(A.II.28)

The equations for the average number of trains, loops, and tails per bridging molecule are

$$n^{b'}_{lp,i} = \frac{\lambda_1}{G_i^{b'}(r_1 | 1) + G_i^{b''}(r_1 | 1)} \times$$

$$\sum_{s=1}^{r_1 - 1} [G_i^{b'}(2, s | 1)\left(G_i^{a'}(1, s+1 | r_1) + G_i^{b'}(1, s+1 | r_1)\right) + G_i^{a'}(1, s | 1) G_i^{b'}(2, s+1 | r_1)]$$

(A.II.29)

$$n_{lp,i}^{b''} = \frac{\lambda_1}{G_i^{b'}(r_i|1) + G_i^{b''}(r_i|1)} \sum_{s=1}^{r_i-1} [G_i^{b''}(M-1, s|1)\left(G_i^{a''}(M, s+1|r_i) + G_i^{b''}(M, s+1|r_i)\right) + G_i^{a''}(M, s|1)G_i^{b''}(M-1, s+1|r_i)]$$

(A.II.30)

$$n_{tr,i}^{b'} = n_{lp,i}^{b'} + \frac{n_{br,i}}{2} + \frac{G_i^{b'}(r_i|1)}{G_i^{b'}(r_i|1) + G_i^{b''}(r_i|1)} \quad \text{(A.II.31)}$$

$$n_{tr,i}^{b''} = n_{lp,i}^{b''} + \frac{n_{br,i}}{2} + \frac{G_i^{b''}(r_i|1)}{G_i^{b'}(r_i|1) + G_i^{b''}(r_i|1)} \quad \text{(A.II.32)}$$

$$n_{tl,i}^{b'} = \frac{G_i^{b'}(r_i|1) + G_i^{b'}(1|r_i) - G_i^{b'}(1, r_i|1) - G_i^{b'}(1, 1|r_i)}{G_i^{b'}(r_i|1) + G_i^{b''}(r_i|1)} \quad \text{(A.II.33)}$$

$$n_{tl,i}^{b''} = \frac{G_i^{b''}(r_i|1) + G_i^{b''}(1|r_i) - G_i^{b''}(M, r_i|1) - G_i^{b''}(M, 1|r_i)}{G_i^{b'}(r_i|1) + G_i^{b''}(r_i|1)} \quad \text{(A.II.34)}$$

The average fraction of segments, ν, in trains, loops, tails, and bridges of molecule i is given by

$$\nu_{sq,i}^{g} = \sum_{z=1}^{M} \frac{\phi_{sq,i}^{g}(z)}{\theta_i^{g}} \quad \text{(A.II.35)}$$

where g (=a',a",b) refers to one of the molecule fractions: adsorbed molecules on the first surface, adsorbed molecules on the second surface, or bridging molecules, and sq (=tr,lp,tl) denotes the sequence type: either trains, loops or tails.
The average length $l_{sq,i}^{g}$ for chain part sq of the molecule fractions g of molecules i is then given by

$$l_{sq,i}^{g} = \frac{r_i \nu_{sq,i}^{g}}{n_{sq,i}^{g}} \quad \text{(A.II.36)}$$

APPENDIX III

Numerical Method

The segment density profiles $\{\phi_A(z)\}$ can be calculated according to equations (1.18) and (1.29) once the potentials $\{u_A(z)\}$ are known. These potentials are given by equation (1.46) and depend on the segment densities and u'(z). Hence, we are dealing with an implicit set of equations, which can be solved numerically, for instance with the FORTRAN program of Powell[19].

We define a set of unconstrained variables $x_A(z)$ which we relate to the deviation of $u_A(z)$ from the average segment potential $\bar{u}$ and a term independent of A and z:

$$x_A(z) = -\frac{u_A(z) - \bar{u}}{kT} + \frac{\sum_i \ln G_i(r_i|1)}{\sum_{z,A} 1} \qquad \text{(A.III.1)}$$

where the average segment potential $\bar{u}$ is defined as

$$\bar{u} = \frac{\sum_{z,A} u_A(z)}{\sum_{z,A} 1} \qquad \text{(A.III.2)}$$

From the definition of the unconstraint variables $x_A(z)$ in equation (A.III.1) it follows immediately that the following relations must hold:

$$\sum_{z,A} x_A(z) = \sum_i \ln G_i(r_i|1) \qquad \text{(A.III.3)}$$

and

$$x_A(z) - \bar{x} = -\frac{u_A(z) - \bar{u}}{kT} \qquad \text{(A.III.4)}$$

where $\bar{x}$ is the average of all $x_A(z)$ defined in the same way as $\bar{u}$. We introduce a (reduced) segment weighting factor $\tilde{G}_A(z)$. It is defined as

$$\tilde{G}_A(z) = G_A(z)\exp[\bar{u}/kT] \qquad \text{(A.III.5)}$$

With the help of equations (1.18) and (A.III.4) we can rewrite equation (A.III.5) and express $\tilde{G}_A(z)$ in terms of the unconstraint variables $x_A(z)$.

$$\tilde{G}_A(z) = \exp\left[x_A(z) - \bar{x}\right] \qquad \text{(A.III.6)}$$

From the set $\{x_A(z)\}$ we calculate the (reduced) segment weighting factors $\tilde{G}_A(z)$ according to equation (A.III.6), the corresponding reduced chain distribution functions $\tilde{G}_i(z,s|1)$ and $\tilde{G}_i(z,s|r_i)$ according to the equivalents of equations (1.27) and (1.28), and the reduced chain weighting factors $\tilde{G}_i(r_i|1)$ according to the equivalent of equation (1.22). Note that $\tilde{G}_i(r_i|1) = G_i(r_i|1)\exp[r_i\bar{u}/kT]$, so that $\bar{u}/kT$ may be obtained from equation (A.III.3) as

$$\frac{\bar{u}}{kT} = \frac{\sum_i \ln \tilde{G}_i(r_i|1) - \sum_{z,A} x_A(z)}{\sum_i r_i} \qquad \text{(A.III.7)}$$

The segment densities $\phi_i(z)$ are found with the equivalent of equation (1.29) in reduced weighting factors:

$$\phi_i(z) = \tilde{C}_i \sum_{s=1}^{r_i} \tilde{G}_i(z,s|1)\,\tilde{G}_i(z,s|r_i) / \tilde{G}_i(z,s) \qquad \text{(A.III.8)}$$

where the reduced normalization constant $\tilde{C}_i$ is related to C_i by

$$\tilde{C}_i = \frac{C_i}{\exp[r_i\bar{u}/kT]} \qquad \text{(A.III.9)}$$

If θ_i is given we can substitute equation (1.30) in equation (A.III.9).

$$\tilde{C}_i = \frac{\theta_i}{r_i\,\tilde{G}_i(r_i|1)} \qquad \text{(A.III.10)}$$

It is easily verified that the factors $\exp[\bar{u}/kT]$ cancel out in equation (A.III.8).
The Lagrange multipliers $\alpha(z)$ may be calculated from equations (1.16) and (1.39). During the iterations $\alpha(z)$ may depend on the type of segment. Therefore we define $\alpha_A(z)$ as

$$\alpha_A(z) = u_A(z)/kT - \sum_B \chi_{AB} \frac{<\phi_B(z)>}{\sum_C \phi_C(z)} - u_A^{ref} \qquad \text{(A.III.11)}$$

For u_A^{ref} we use the expression given in equation (1.44). The division by $\Sigma_C \phi_C(z)$ damps strong fluctuations in $\alpha_A(z)$ during the iterations (when the boundary conditions $\Sigma_C \phi_C(z) = 1$ are not yet satisfied) and has no effect on the final result.
For every layer z we have to satisfy the boundary condition $\Sigma_A \phi_A(z) = 1$. In addition, $\alpha(z)$ must have the same value for every type of segment in layer z. We have formulated the following function $f_A(z)$, which combines the boundary conditions and has turned out to be reasonably linear in $u_A(z)$ for most cases.

$$f_A(z) = 1 - \frac{1}{\sum_A \phi_A(z)} + \alpha(z) - \alpha_A(z) \qquad \text{(A.III.12)}$$

where $\alpha(z) = \Sigma_A \alpha_A(z)/\Sigma_A 1$ is the average of $\alpha_A(z)$ in layer z. This function $f_A(z)$ is only zero if the boundary conditions are satisfied and if $\{u_A(z)\}$ is consistent with $\{\phi_A(z)\}$.
Initial values of $\{x_A(z)\}$ are obtained as follows. The potentials $u_A(z)$ for $1 < z < M$ are set to zero. Only $u_A(1)$ and $u_A(M)$ are given a small negative value. From these initial values of $\{u_A(z)\}$ we can calculate $\{G_A(z)\}$ and, from them, $G_i(r_i \mid 1)$ of every molecule type i. The corresponding initial values of $\{x_A(z)\}$ are then found from equation (A.III.1). Then the iteration procedure is started to find the set of $\{x_A(z)\}$ for which the functions $\{f_A(z)\}$ are zero. The iteration is stopped when the tolerance $\sqrt{(\Sigma_z \Sigma_A [f_A(z)]^2)}$ is typically less than 10^{-7}.

For each component either θ_i or μ_i (or ϕ_i^b) should be given. However, in order to avoid that the functions $f_A(z)$ become overdetermined because of $\Sigma_i \theta_i = \Sigma_{1,z} \phi_1(z)$, at least one component, e.g. a solvent, should be free to adapt its θ_i during the iterations.

REFERENCES

(1) G. Hadziioannou, S. Patel, S. Granick, and M. Tirrell, J.Amer.Chem.Soc. 108, 2869 (1986)

(2) P.G. de Gennes, Macromolecules 13, 1069 (1980)

(3) S.J. Alexander, J.Phys. (Paris) 38, 983 (1977)

(4) J.M.H.M. Scheutjens, and G.J. Fleer, J.Phys.Chem. 83, 1619 (1979)

(5) J.M.H.M. Scheutjens, and G.J. Fleer, J.Phys.Chem. 84, 178 (1980)

(6) J.M.H.M. Scheutjens, and G.J. Fleer, Macromolecules 18, 1882 (1985)

(7) F.A.M. Leermakers, J.M.H.M. Scheutjens, and J. Lyklema, Biophys.Chem. 18, 353 (1983)

(8) E. Helfand and Y. Tagami, J.Chem.Phys. 56, 3592 (1972)

(9) K.M. Hong and J. Noolandi, Macromolecules 13, 964 (1980)

(10) D.W.R. Gruen and E.H.B. de Lacey, in "Surfactants in Solution" (K.L. Mittal and B. Lindman, Eds.), Plenum, New York (1984), Vol. 1, 279.

(11) J.A. Marqusee and K.A. Dill, J.Chem.Phys. 85, 434 (1986)

(12) D.N. Theodorou, Macromolecules 21, 1391 (1988)

(13) D.N. Theodorou, Macromolecules 21, 1400 (1988)

(14) O.A. Evers, PhD thesis, Wageningen (1989), Chapter 2.

(15) P.J. Flory, "Principals of Polymer Chemistry", Cornell University Press, Ithaca, NY (1953).

(16) A. Silberberg, J.Chem.Phys.,48, 2835 (1968).

(17) T. Cosgrove, T. Heath, B. van Lent, F. Leermakers, and J. Scheutjens, Macromolecules 20, 1692 (1987).

(18) S. Hirz, MSc. Thesis, University of Minnesota (1987).

(19) M.J.D. Powell, in "Numerical Methods for Nonlinear Algebraic Equations" (P.Rabinowitz, Ed.), Gordon and Breach, London (1970), 115.

CHAPTER 2

Effect of chain composition on the adsorption of block copolymers

ABSTRACT

Recently, we presented a self-consistent field theory for the adsorption of block copolymers[1]. The physical background of this theory is briefly reviewed and a number of results on the adsorbed amount and the hydrodynamic layer thickness of adsorbed di- and triblock copolymers are presented.

The adsorbed amount and the hydrodynamic layer thickness of adsorbed block copolymers depend strongly on the chain composition. When the total length of a diblock copolymer is kept constant, a maximum is found in the adsorbed amount as a function of the fraction of adsorbing segments. This maximum is found at a lower fraction of adsorbing segments with increasing chain length, bulk solution concentration, and surface affinity.

Usually thick adsorbed layers are found. For diblock copolymers the hydrodynamic layer thickness is of the order of 10 to 30% of the length of the non-adsorbing block, depending on the solvent quality.

For BAB-triblock copolymers with adsorbing A-segments and non-adsorbing B-segments we find lower adsorbed amounts as compared to an AB-block copolymer with the same number of A- and B-segments.

$$u_A^{int}(z) = kT\sum_B \chi_{AB}\left(<\phi_B(z)> - \phi_B^b\right) \qquad (2.3)$$

The first term in the summation of equation (2.3) is the mixing energy of a segment A in layer z with neighboring B-segments. The second term gives the same for a segment A in the homogeneous bulk solution. Obviously, $<\phi_B^b> = \phi_B^b$. The summation is taken over all types of segments present in the mixture. A segment in the first layer is also in contact with surface sites. Using a Flory-Huggins parameter χ_{AS} for the interaction of an A-segment with surface sites of the adsorbent we find from equation (2.3) for z = 1:

$$u_A^{int}(1) = kT\chi_{AS}\lambda_1 + kT\sum_B \chi_{AB}\left(<\phi_B(z)> - \phi_B^b\right) \qquad (2.4)$$

since the number of contacts of an adsorbed segment with the surface is only $\lambda_1 Z$. If desired, the first term of equation (2.4) could be included in the summation by considering S as a separate component[1].

Let us first consider the case of monomer adsorption. For a monomer we have the following simple Boltzmann type relation between the volume fraction $\phi_A(z)$ of monomers A in layer z and the volume fraction ϕ_A^b in the bulk of the mixture:

$$\phi_A(z) = \phi_A^b \exp\left[-u_A(z)/kT\right] \qquad (2.5)$$

We can write equation (2.5) in terms of a weighting factor $G_A(z)$ as follows:

$$\phi_A(z) = \phi_A^b G_A(z) \qquad (2.6)$$

where

$$G_A(z) = \exp[-u_A(z)/kT] \tag{2.7}$$

The Boltzmann factor $G_A(z)$ is called the "segment weighting factor" for a segment of type A in layer z. By definition, all the weighting factors are unity in the bulk solution.

For dimers the situation is slightly more complex. If we want to calculate the segment density profile $\{\phi_A\}$ of A-segments of AB-dimers we have to satisfy the condition that a B-segment must be in an lattice site adjacent to the A-segment. The average Boltzmann factor for dimers with segment A in z will be $G_A(z)$ times the neighbor average $<G_B(z)>$ of the segment weighting factor for B-segments. Note that in this way all possible positions of the B-segment (hence, all possible conformations of the dimer) are taken into account. Therefore,

$$\phi_A(z) = \frac{\phi^b_{AB}}{2} G_A(z) < G_B(z) > \tag{2.8}$$

where $<G_B(z)>$ is defined in the same way as the neighbor average $<\phi_B(z)>$ (see equation 2.2), ϕ^b_{AB} is the bulk solution volume fraction of the AB-dimer, and $\phi^b_{AB}/2$ gives the bulk solution volume fraction of A-segments. For a BAB trimer the segment density $\phi_A(z)$ would be given by $\phi^b_{BAB}/3$ times the Boltzmann factor $<G_B(z)>G_A(z)<G_B(z)>$, because segment A in layer z is connected with B-segments in layers z-1, z, or z+1.

We may follow a more general scheme to obtain the volume fraction $\phi_i(z,s)$ in layer z of the s^{th} segment of a block copolymer of type i, with a total length of r_i segments. The Boltzmann factor necessary to calculate $\phi_i(z,s)$ reflects three events. First, segment s must be located in layer z. The weighting factor for this event is $G_i(z,s)$, the segmental weighting factor of segment s in layer z. For example, if the s^{th} segment is of type D, then $G_i(z,s)$ equals $G_D(z)$. Secondly, the chain part starting from the first segment up to segment

s-1 must have its last segment (s-1) in one of the layers z-1, z, or z+1. Finally, the chain part starting from segment r_i and ending at segment s+1 must also have its last segment (s+1) in one of the layers z-1, z, or z+1. We introduce $G_i(z,s \mid 1)$ as the weighting factor for a chain of s segments long starting at segment 1 anywhere in the lattice and ending with its last segment (s) in layer z. The weighting factor $G_i(z,s \mid r_i)$ is defined in the same way but now for a chain starting at segment r_i and ending at segment s in layer z. The weighting factors $G_i(z,s \mid 1)$ and $G_i(z,s \mid r_i)$ are easily calculated. Obviously, $G_i(z,1 \mid 1) = G_i(z,1)$ and $G_i(z,r_i \mid r_i) = G_i(z,r_i)$. If segment s is in layer z, then the adjacent segment s-1 must be in one of the layers z-1, z, z+1. Thus the weighting factor $G_i(z,s \mid 1)$ can be divided into two factors:

$$G_i(z,s \mid 1) = G_i(z,s) < G_i(z,s-1 \mid 1) > \tag{2.9}$$

where $<G_i(z,s \mid 1)>$ is the neighbor average of $G_i(z,s \mid 1)$. Equation 2.9 is a recurrence relation, valid for $s > 1$. First, the relation is applied for $s = 2$: $G_i(z,2 \mid 1)$ is calculated from the appropriate segment weighting factors in the layers z-1, z, and z+1. Next $G_i(z,3 \mid 1)$ is found from $G_i(z,3)$ and $<G_i(z,2 \mid 1)>$, etc. For $G_i(z,s \mid r_i)$ we have a similar recurrent relation:

$$G_i(z,s \mid r_i) = G_i(z,s) < G_i(z,s+1 \mid r_i) > \tag{2.10}$$

which applies for any $s < r_i$.

In analogy with the trimer BAB, $\phi_i(z,s)$ for a copolymer is $(\phi_i^b / r_i) < G_i(z,s-1 \mid 1) > G_i(z,s) < G_i(z,s+1 \mid r_i)$. Using equations (2.9) and (2.10) we can write for the volume fraction in layer z due to segment s of component i:

$$\phi_i(z,s) = \frac{\phi_i^b}{r_i} G_i(z,s \mid 1)\, G_i(z,s \mid r_i) \,/\, G_i(z,s) \tag{2.11}$$

The volume fraction $\phi_i(z)$ of all segments of block copolymer i in layer z is simply given by the summation of $\phi_i(z,s)$ over all segments of the molecule.

$$\phi_i(z) = \sum_{s=1}^{r_i} \phi_i(z,s) \qquad (2.12)$$

The volume fraction $\phi_{Ai}(z)$ due to A-segments in layer z belonging to molecules of type i is obtained by performing the summation in equation (2.12) only over those segments s which are of type A. The total volume fraction $\phi_A(z)$ of all segments A in layer z is then obtained by summation of $\phi_{Ai}(z)$ over all molecule types i.

2.2.3. Adsorbed Amount and Hydrodynamic Layer Thickness

We will use the definition for the adsorbed amount θ^a given by Scheutjens and Fleer[2]. Let $\{\phi_i^f(z)\}$ be the volume fraction profile of free molecules i, i.e., the molecules of type i which are not in contact with the surface. The volume fraction profile of adsorbed chains $\{\phi_i^a(z)\}$ is then given by $\{\phi_i(z)-\phi_i^f(z)\}$. The adsorbed amount θ_i^a is defined as the sum of $\phi_i^a(z)$ over all layers z:

$$\theta_i^a = \sum_{z=1}^{M} \left[\phi_i(z) - \phi_i^f\right] \qquad (2.13)$$

Since $\phi_i^a(z)$ is zero in the bulk solution the only requirement is to choose the number of layers M large enough. The quantity ϕ_i^a gives the number of segments of adsorbed molecules i per surface site; if $\theta_i^a = 1$, one equivalent monolayer is adsorbed. To find $\phi_i^f(z)$ we may use the same equations as for $\phi_i(z)$. However, we must account for the

condition that no segment of a free molecule i may be in the first layer, so we have to set $G_i(1,s) = 0$ for any s of molecule i.

For the calculation of the hydrodynamic layer thickness δ_h from the adsorption profiles we use the theory of Cohen Stuart et al.[5], which is based on the Debye-Brinkman equation for the solvent flow near a flat surface. The layer thickness is obtained from the condition that the flux of the solvent flow for the case of adsorbed polymer is equal to the flux when only a hard wall of thickness δ_h is present. An analytical solution is given by Scheutjens et al.[18] The hydrodynamic layer thickness δ_h in this analytical method is given as the difference between the total number of layers M, which reflects the free lumen when no adsorbed polymer is present, and the effective number of permeable layers $\Phi(M)$ in the presence of the adsorbed polymer:

$$\delta_h = M - \Phi(M) \tag{2.14}$$

The term $\Phi(M)$ can be calculated by a recurrence relation between $\Phi(z)$ for z layers and $\Phi(z-1)$ for z-1 layers, starting with $\Phi(0) = 0$, because there is no solvent flow inside the surface:

$$\Phi(z) = \frac{q(z)\tanh\left(q(z)^{-1}\right) + \Phi(z-1)}{1 + \Phi(z-1)q(z)^{-1}\tanh\left(q(z)^{-1}\right)}, \qquad \text{for } z \geq 1 \tag{2.15}$$

For the factor q(z) we extend the expression given in reference (5) which applies only for one type of adsorbed polymer:

$$q(z)^2 = C_h \frac{1 - \sum_i \phi_i^a(z)}{\sum_i \phi_i^a(z)} \tag{2.16}$$

For large z, $q(z) \rightarrow \infty$ and $\Phi(z) = 1 + \Phi(z-1)$. Hence, the outcome for δ_h does not depend on the number M of layers taken into account.

The hydrodynamic layer thicknesses presented in this article are calculated with C_h equal to unity, which is in accordance with results of Mijnlieff and Wiegel[5,19].

2.2.4. Numerical Method

From an initial guess for the segment potentials $u_A(z)$ we can calculate the corresponding segment densities $\phi_A(z)$ from equations (2.7), (2.11), and (2.12). With these $\phi_A(z)$ values the M boundary conditions $\Sigma_A\phi_A(z) = 1$ are checked. Moreover, in combination with an initial guess for the M hard core potentials u'(z) the initial guess for the segment potentials is checked on its consistency with the $\phi_A(z)$ values, using equations (2.1) and (2.3).
As shown in reference (1), an implicit set of simultaneous equations can be formulated from which the segment potentials $u_A(z)$ and the hard core potentials u'(z) are evaluated by standard numerical techniques.

2.3 RESULTS and DISCUSSION

2.3.1 Adsorption of Diblock Copolymers

A large difference in adsorption behaviour between AB block copolymers and homopolymers can be expected. For homopolymers some general trends are known. For instance, the adsorbed amount increases with longer chain length, higher surface affinity of the segments, decreasing solvent quality, and increasing bulk concentration of polymer. These trends will be more complex for

block copolymers because they depend highly on the composition of the copolymer and on the difference in interaction parameters for A and B segments. In this section we will present a selection of numerical results for the adsorption of AB block copolymers. We will concentrate on some characteristic parameters of the adsorbed layer, such as the adsorbed amount and the hydrodynamic layer thickness. All results are calculated using a hexagonal lattice, $\lambda_0 = 6/12$.

2.3.1.1 Potential Profiles and Segment Density Profiles

In sections 2.2.2 and 2.2.4 we related the segment densities $\{\phi_A\}$ to the potential profiles $\{u_A\}$ and described shortly how these are obtained in a self-consistent way.

To illustrate how the potential profiles look like and how the adsorbed layer is built up, we give in figure (2.2) an example of the adsorption of an $A_{100}B_{400}$ block copolymer. The 100 A segments have a high affinity for the surface ($\chi_{AS} = -10$) and the 400 B segments have the same affinity for the surface as the solvent monomers ($\chi_{BS} = \chi_{OS} = 0$). The solvent O is a poor solvent for A-segments and an athermal solvent for B-segments ($\chi_{AO} = 0.5$ and $\chi_{BO} = 0$). These parameters result in potential profiles for the A and B segments as shown in figure (2.2a).

For the adsorbing A-segments an attractive potential is present at $z \leq 5$. The potential profile for B-segments is positive for small z, which means that there is a barrier for these segments near the surface. Obviously, this is due to the high concentration of A-segments. The corresponding volume fraction profiles are given in figure (2.2b). A high volume fraction of A-segments is found in the first layer: $\phi_A(1) = 0.87$. This is to be expected because of the high surface affinity of A-segments. The profile of A-segments shows a steep decay in the first few layers. About 99% of the A-segments are in loops and trains. The

average conformation of the A-blocks is very flat. The trains are on average 7 segments long and the mean loop size is only 2 segments. On the other hand, the segment density profile of the B-segments is very wide, up to about 80 layers. There is little overlap between A and B-segments, even in this case, where $\chi_{AB} = 0$. The B-segments cannot adsorb because of the higher surface affinity of A-segments. Hence, the

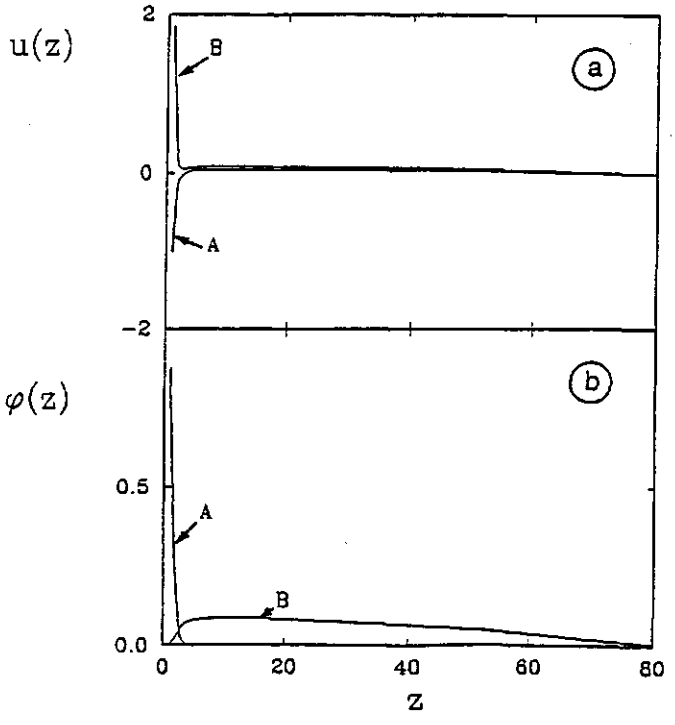

Figure 2.2. *Potential profiles (a) and volume fraction profiles (b) for strongly adsorbing A-segments (χ_{AS} = -10) and non-adsorbing B-segments (χ_{BS} = 0) of a block copolymer $A_{100}B_{400}$. The solvent is athermal for the B-segments (χ_{BO} = 0) and poor for A-segments (χ_{AO} = 0.5). Other parameters are: χ_{AB} = 0 and $\phi^b = 10^{-4}$.*

B-segments, forming one end of the chain, are found in one dangling tail per molecule. In fact, the density profile of the B-segments resembles closely that found for anchored chains.[1,20,21,22]

We may conclude that diblock copolymers having one strongly adsorbing block tend to adsorb with this block lying flat on the surface and with the other block (for which the solvent quality is good) sticking far out into the solution. In the next section we will examine how this picture depends on the lengths of the blocks.

2.3.1.2 Effect of Chain Composition

In this section we want to investigate the effect of the composition of diblock copolymers on the adsorbed amount θ^a and the hydrodynamic layer thickness δ_h. There are two ways of varying the composition of an AB block copolymer. First we can vary the fractions of A and B-segments, keeping the total length of the copolymer constant. Second, we can change the length of the A or B-block at constant length of the other block. We will present both types of results.

In figure (2.3a) the adsorbed amount is given as a function of the fraction ν_A of adsorbing A-segments (χ_{AS} = -8) at various chain lengths; figure (2.3c) gives the analogous $\delta_h(\nu_A)$-plot. The B-segments are non-adsorbing (χ_{BS} = 0) and the solvent O is a poor solvent for A-segments and a good solvent for B-segments. For chains longer than 15 segments a maximum in the adsorbed amount is observed. The fraction of A-segments corresponding to this maximum will be referred to as the "optimal fraction" ν_A^{opt}.

At low ν_A the total adsorption energy of the polymer molecule is low, as there are not many A-segments per chain. This results in a low adsorbed amount. As long as the number of adsorbed chains is low, increasing the fraction A-segments results in a higher adsorbed

amount. As the amount increases, the tail containing the B-block will be more stretched out into the solution as is seen in figure (2.3c,d): up to 20 % of the contour length of the B-block. If the fraction of A-segments is increased beyond the optimal fraction, the adsorbed amount decreases since the long A-blocks tend to lie flat on the surface, leaving less place for other adsorbed chains. At the adsorption

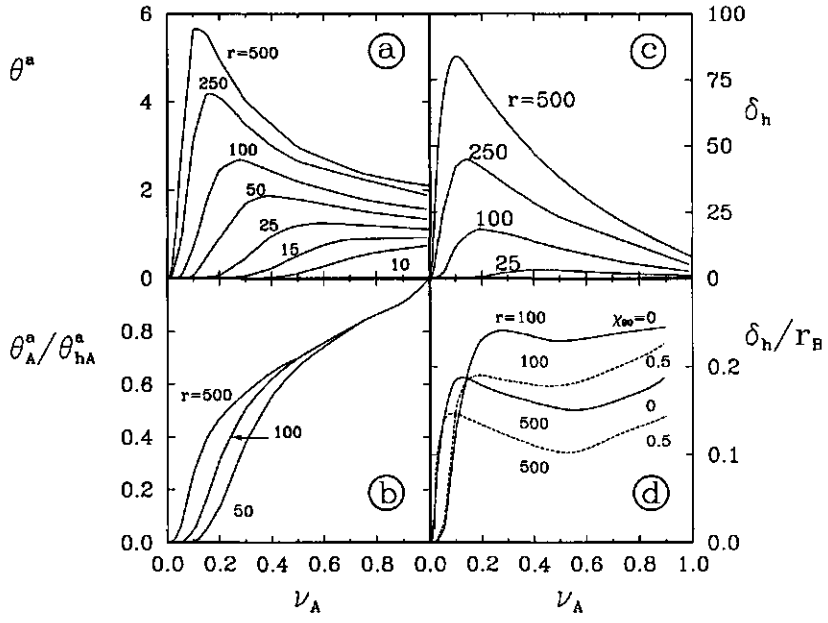

Figure 2.3. *The adsorbed amount θ^a (a), the ratio θ^a_A/θ^a_{hA} between the amount of A-segments θ^a_A in adsorbed AB-copolymer and the adsorbed amount θ^a_{hA} of A-homopolymer (b), the hydrodynamic layer thickness δ_h (c), and the degree of stretching δ_h/r_B (d), as a function of the fraction ν_A of A-segments in the AB-copolymer. The total chain length r is indicated. The A-segments are strongly adsorbing (χ_{AS} = -8), the B-segments are non-adsorbing ($\chi_{BS} = \chi_{OS}$ = 0). Other parameters: $\chi_{AO} = \chi_{AB}$ = 0.5, $\phi^b = 10^{-4}$, C_h = 1. In figures a-c, χ_{BO} = 0, in figure d χ_{BO} = 0 or 0.5.*

maximum for r = 500 we have in average one molecule per 73 surface sites, whereas the number of A-segments equals 60. For r = 100 this is one molecule per 36 surface sites and 26 A-segments. It is found that at the adsorption maximum the fraction of A-segments in trains is around 85 %, independent of the chain length. Hence at this maximum the A-blocks are rather closely packed on the surface. Experimentally an adsorption maximum as a function of the fraction of adsorbing segments has been found by Hopkins and Howard[6] for styrene-methyl methacrylate random and block copolymers adsorbed on carbon. Similarly, Diaz Barrios and Howard[11] reported an adsorption maximum for random styrene-vinylferrocene copolymers adsorbed on SiO_2 and TiO_2.

To gain some insight in the relation between the adsorption of an AB-block copolymer and an A-homopolymer of equal length, the adsorption data of figure (2.3a) are replotted in figure (2.3b). The latter figure (2.3b) shows the dependence of the ratio θ^a_A/θ^a_{hA} as a function of ν_A for three different chain lengths, where $\theta^a_A = \nu_A\theta^a$ and θ^a_{hA} is the adsorbed amount at $\nu_A = 1$, i.e., the adsorbed amount of a homopolymer consisting of r A-segments. If ν_A equals unity, the ratio θ^a_A/θ^a_{hA} is, by definition, also unity. With decreasing ν_A, this ratio decreases because the block copolymer contains an increasing fraction of non-adsorbing B-segments. From figure (2.3b) it appears that this decrease is approximately linear in ν_A and independent of chain length, provided ν_A is not too low. For small values of ν_A, around the maximum in figure (2.3a), the number of anchoring A-segments becomes too small to maintain this linearity. We interpret these trends with the following simple picture.

If the B-segments would be identical to the A-segments, $\theta^a = \theta^a_A + \theta^a_B$ would be equal to θ^a_{hA} and the ratio θ^a_A/θ^a_{hA} would be equal to ν_A. For ν_A nearly unity the behaviour is close to this limit even if the B-segments do not adsorb: the effect of replacing a few A-segments in the tails by B-segments is quite small. For higher values of $\nu_B = 1 - \nu_A$,

the ratio θ_A^a/θ_{hA}^a is higher than ν_A because the B-segments do not compete for surface sites and relatively more A-blocks can adsorb. As a first approximation we assume that each B-segment gives the same contribution to this increment, so that the additional adsorption of A-segments is proportional to ν_B: $\theta_A^a/\theta_{hA}^a = \nu_A + \alpha\nu_B$ or:

$$\frac{\theta_A^a}{\theta_{hA}^a} = (1-\alpha)\nu_A + \alpha \qquad (2.17)$$

The effect of the chain length is accounted for in θ_{hA}^a. Figure (2.3c) shows that this linear decrease of θ_A^a/θ_{hA}^a is approximately obeyed down to $\nu_A \approx 0.5$ for short chains and even further ($\nu_A \approx 0.2$) for long chains (r = 500). Under the conditions of figure (2.3), $\alpha = 0.4$. The value of α is (mainly) determined by $\chi_{BS} - \chi_{AS}$. If the latter difference is zero (A and B identical), $\alpha = 0$ as discussed above.

From equation (2.17) the dependence of the total adsorbed amount θ^a on ν_A may be found from $\theta^a = \theta_A^a/\nu_A$. Replacing $(1 - \nu_A)/\nu_A$ by r_B/r_A we obtain the simple expression:

$$\theta^a = \theta_{hA}^a\left(1 + \frac{\alpha r_B}{r_A}\right) \qquad (2.18)$$

which describes $\theta^a(\nu_A)$ in figure (2.3a) to the right of the maximum quite accurately for chains longer than 50. Left of the maximum, θ^a decreases steeply because the number of anchoring segments becomes too low. For small chain lengths, the adsorbed amount decreases with decreasing ν_A, even for high values of ν_A, because the total adsorption energy per chain becomes to small.

Equation (2.17) may be used to estimate ν_A^{opt}, i.e., the position of the maximum in figure (2.3a) as a function of chain length (or θ_{hA}^a) if we assume that this equation applies up to the maximum and that $\theta_A^a \approx 1$ in this maximum. Then $\nu_A^{opt} \approx [1/\theta_{hA}^a - \alpha]/[1-\alpha]$, showing a decrease of

ν_A^{opt} with increasing θ_{hA}^a or with increasing chain length. This estimate for ν_A^{opt} is rather accurate for long chains, but less so for r = 50 or 100, for which $\theta_A^a(\nu_A)$ deviates considerably from the linear dependence of equation (2.17) around ν_A^{opt}.

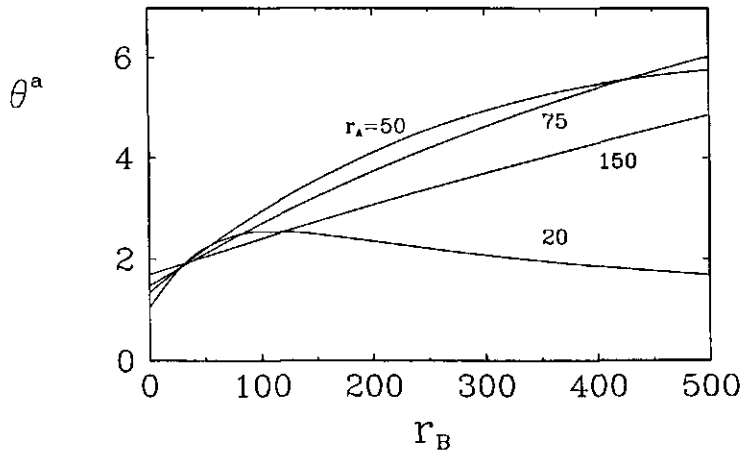

Figure 2.4. *The adsorbed amount θ^a as a function of the number r_B of B-segments per chain at various values of r_A. In this case χ_{BO} = 0 and all other parameters are the same as in figure 2.3.*

The extent of stretching of the tails into the solution may be expressed by the ratio δ_h/r_B, since mainly the B-blocks determine δ_h. Figure (2.3d) shows δ_h/r_B as a function of ν_A for two solvent qualities for the B-segments and two chain lengths (r = 100 and r = 500). As can be expected, the degree of stretching is higher for the good solvent than for the poor solvent. A maximum is observed at a fraction ν_A equal to the optimum composition ν_A^{opt} where the maximum adsorbed amount is found. As long as there is no saturation of the surface with adsorbed A-blocks (below ν_A^{opt}), increasing ν_A results in a higher adsorbed amount and a higher degree of stretching. When ν_A equals ν_A^{opt} saturation of the surface with A-blocks is reached, and further increase of ν_A (lower r_B) will then result in a lower adsorbed

amount and more lateral space for the B-block. This in turn will decrease δ_h/r_B until r_B becomes so low that δ_h depends also (or predominantly) on r_A, so that δ_h/r_B increases again. It is interesting to note that shorter chains are more highly stretched. Adsorption of shorter chains results in a higher density of B-blocks near the surface, which gives a higher δ_h/r_B ratio.

Up till now we have investigated the effect of the composition on the adsorbed amount by varying the fraction of A-segments, at constant total chain length r. The adsorbed amount as a function of the length r_B of the B-block is shown in figure (2.4) at various but constant lengths r_A of the A-block. In this case the total chain length $r = r_A + r_B$ is not constant. At constant r_A the adsorbed amount increases initially approximately linearly with r_B. The slope of this linear part decreases with increasing r_A, in agreement with equation (2.18) which predicts a slope of $\alpha\theta^a_{hA}/r_A$. The physical picture is that at low r_A more molecules adsorb than at higher r_A. Making the B-block longer will then result in a stronger increase of θ^a. However, at a certain value of r_B a maximum in the adsorbed amount occurs (see the curve for $r_A = 20$); then v_A becomes so low that θ^a_A and θ^a deviate downwards from the linear relations given in equations (2.17) and (2.18). At high r_B more adsorbing A-segments are necessary to compensate for the loss of entropy due to adsorption. Hence, if we keep r_A constant the adsorbed amount will decrease if the B-block becomes too long and a maximum will be found. This maximum is higher for longer A-blocks (i.e., stronger anchoring) and the corresponding r_B-value increases drastically. For r_A=150 the linear dependence of equation (2.18) is quite accurate over this range of r_B; in this case the maximum occurs at much higher r_B-values.

The adsorbed amount as a function of both the length r_A of the A-block and the length r_B of the B-block is shown in the contour plot in figure (2.5a). The contour lines are points of equal adsorbed amount

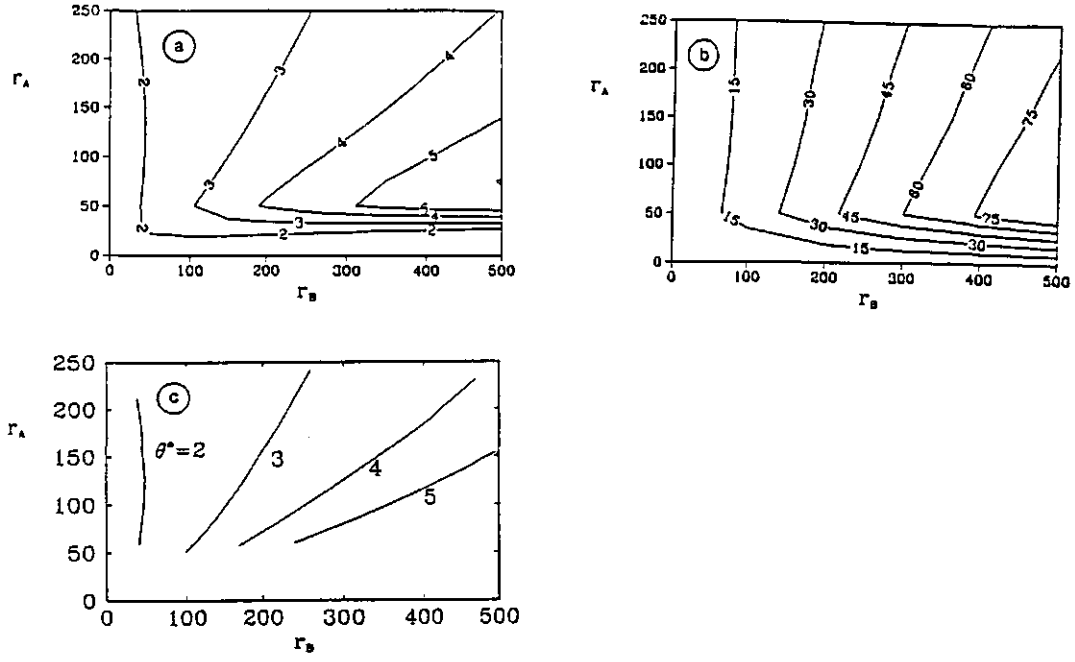

Figure 2.5. *Contour plots of θ^a (a) and the corresponding hydrodynamic layer thickness δ_h (b) as a function of the number r_A of A-segments and the number r_B of B-segments per chain. Contour plots of θ^a obtained with equation (2.18) are shown in (c). The parameters are the same as in figure 2.3. The value of θ^a or δ_h corresponding to each contour line is indicated.*

θ^a, the value of which is indicated. A similar contour plot for δ_h is given in figure (2.5b). The parameters used are the same as in figure (2.3a). We observe that the maximum adsorbed amount at given r_B is found around r_A = 50. This almost coincides with the maximum in the hydrodynamic thickness δ_h as can be seen in figure (2.5b). If at constant r_B the number of A-segments is increased above 50 segments, the adsorbed amount decreases because each anchoring block will occupy more surface sites. To follow the contour line (i.e.,

maintain the same adsorbed amount), one has to increase the number of B-segments per chain. In this region there is an almost linear dependence between r_A and r_B. As has been shown in equation (2.18) the adsorbed amount of an AB-block copolymer scales linearly with the ratio r_B/r_A for chain lengths above 50 and for not to low fractions of A-segments. For constant θ^a, this equation can be rewritten as $r_A = \alpha r_B \theta^a_{hA}/[\theta^a - \theta^a_{hA}]$. Using the appropriate θ^a_{hA} values, we are able to predict the contour lines of equal adsorbed amount in figure (2.5a) quite accurately for values of r_A above 50, as is shown in figure (2.5c).Since θ^a_{hA} is not constant but changes slightly if one follows a contour line (i.e., changes $r = r_A + r_B$) the resulting curves are not linear. From the above equation it is clear that with increasing θ^a the slope of the contour lines decreases.

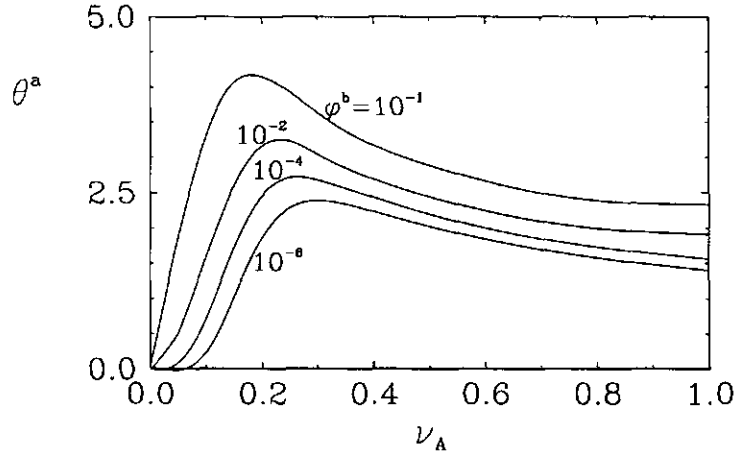

Figure 2.6. *The effect of the volume fraction in the bulk solution on the adsorbed amount. The adsorbed amount is plotted versus ν_A for various solution concentrations ϕ^b (indicated). Other parameters are the same as in figure 2.3.*

In figure (2.6) the adsorbed amount θ^a for a chain of 100 segments is plotted as a function of the fraction ν_A of A-segments for various values of the solution concentration ϕ^b. A higher equilibrium solution concentration will lead to higher adsorbed amounts. The adsorption maximum occurs at a lower fraction of A-segments when ϕ^b becomes higher. As for homopolymers, the dependence of the adsorption on ϕ^b is only weak, considering the large range of ϕ^b values.

2.3.1.3 Effect of Surface Affinity

In figure (2.7a) the adsorbed amount as a function of ν_A is shown for various values of the surface affinity χ_{AS} of the A-segments, for a chain of 500 segments. The B-segments are non-adsorbing (χ_{BS} = 0). Increasing the surface affinity for the A-segments, i.e., making χ_{AS} more negative, results in a higher adsorbed amount and a lower optimal fraction ν_A^{opt} since less A-segments are necessary to compensate for the loss of entropy. At low surface affinities (e.g. χ_{AS} = -2) the optimal fraction ν_A^{opt} is equal to one. Thus, there is a critical value of - χ_{AS} above which an adsorption maximum is found. Below this critical value the maximum is situated at ν_A=1: then a homopolymer of A-segments adsorbs more strongly than an AB-block copolymer.

In figure (2.7b) the adsorption data of figure (2.7a) are replotted. The ratio θ_A^a/θ_{hA}^a is given as a function of ν_A for four different surface affinities. We find linear parts in these curves like in figure (2.3b). The slope of this linear part (which is 1-α) increases with decreasing -χ_{AS}. For χ_{AS} = -10 or -8 (fig 2.3), α is around 0.4, for χ_{AS} = -5 and -4, respectively, α is 0.3 and 0.25, and for χ_{AS} = -2 α becomes negative (α = -0.15); this is the situation that the block copolymer adsorbs more weakly than an A-homopolymer. As - χ_{AS} increases, more A-segments per lattice site will adsorb and θ^a increases; according to

equation (2.17) this corresponds to an increase of α and, consequently, to a decreasing slope (1-α).

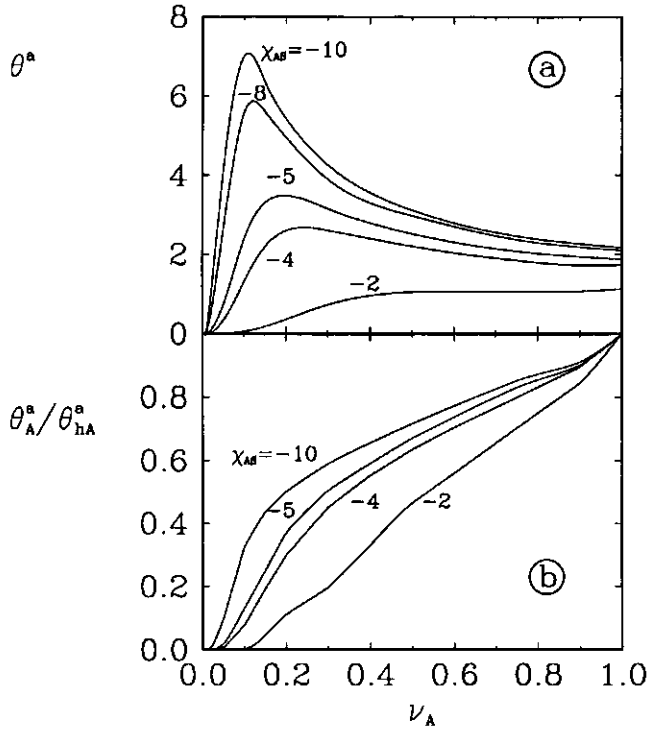

Figure 2.7. *The effect of the surface affinity of the A-segments on the adsorbed amount. The adsorbed amount θ^a (a) and the ratio θ^a_A/θ^a_{hA} (b) are plotted as a function of the fraction of A-segments per chain, for r = 500 and for different adsorption affinities of the A-segments. All other parameters are the same as in figure 2.3.*

In the results dicussed so far, it was assumed that the B-segments have the same affinity for the surface as the solvent monomers ($\chi_{BS} = \chi_{OS} = 0$). Figure (2.8) shows the effect of χ_{BS} on the $\theta^a(\nu_A)$ curves for r = 500. The curve for χ_{BS} = -10 represents in fact a

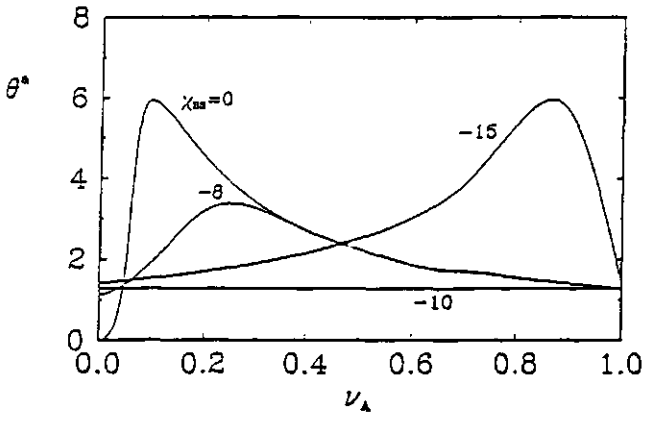

Figure 2.8. *The effect of the surface affinity of B-segments on the adsorbed amount. The adsorbed amount is plotted as a function of the fraction of A-segments per chain, for r = 500 and four different surface affinities for B-segments (χ_{BS} = 0, -8, -10, -15, as indicated). Other parameters: χ_{AS} = -10, $\chi_{AO} = \chi_{BO} = \chi_{AB} = 0$, and $\phi^b = 10^{-4}$.*

homopolymer, because all the interaction parameters are the same for A and B-segments. For the χ_{BS} = -8 curve the maximum is less pronounced than for χ_{BS} = 0, and is found at a higher fraction of A-segments as compared to the curve for χ_{BS} = 0. This can be explained by the fact that the B-segments will compete with the A-segments for surface sites when they have a surface affinity (χ_{BS} = -8) not much below that of the A-segments (χ_{AS} = -10). Hence, the average conformation of the adsorbed molecules will contain more loops and trains, and the tail containing segments of the B-block will be shorter when χ_{BS} differs less from χ_{AS}, leaving less place for adsorbed molecules on the surface. For small ν_A the curve for χ_{BS} = -8 is intermediate between χ_{BS} = 0 and χ_{BS} = -10, whereas for high ν_A the curves for χ_{BS} = 0 and χ_{BS} = -8 coincide. If there are sufficient A-segments, the B-tails will be completely desorbed, even if χ_{BS} - χ_{AS} is as low as 2. For χ_{BS} = -15, the B-segments have the stronger surface

affinity and now the A-segments are found in the tails. The curve is more or less a mirror image of that for $\chi_{BS} = 0$, except near $v_A = 0$ and $v_A = 1$.

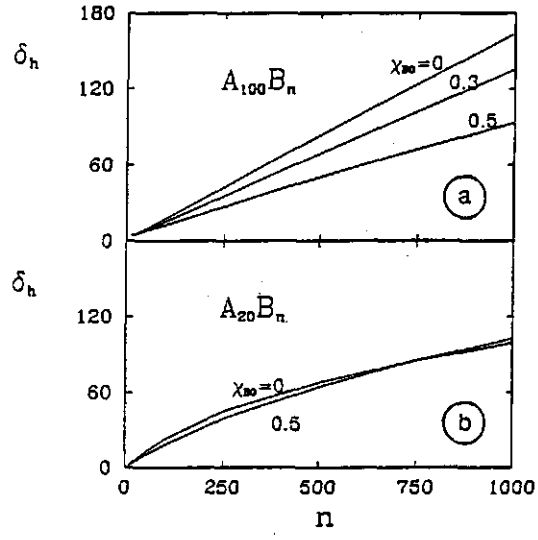

Figure 2.9. *The hydrodynamic layer thickness as a function of the length of the B-block for an $A_{100}B_n$ (a) and an $A_{20}B_n$ (b) copolymer for different values of χ_{BO} (indicated). The A-segments are strongly adsorbing (χ_{AS} = -10), the B-segments do not adsorb ($\chi_{BS} = \chi_{OS} = 0$), $\chi_{AO} = \chi_{AB} = 0$, $C_h = 1$, and $\phi^b = 10^{-4}$.*

2.3.1.4 Effect of Solvent Quality

In this section some results on the effect of the solvent quality for the non-adsorbing segments on the hydrodynamic layer thickness δ_h are shown. In figure (2.9a) δ_h is given as a function of n, the length of the non-adsorbing block, for an $A_{100}B_n$ diblock copolymer and three different solvent qualities χ_{BO} for the B-segments (indicated). The A-

segments are strongly adsorbing (χ_{AS} = -10) and the B-segments do not adsorb ($\chi_{BS} = \chi_{OS} = 0$), $\chi_{AB} = \chi_{AO} = 0$, and $\phi^b = 10^{-4}$. In figure (2.9b) the same parameters are used but now for an AB-block copolymer with a shorter adsorbing block, $A_{20}B_n$, and for two different χ_{BO} values. For the $A_{100}B_n$ block copolymer a nearly linear dependence of δ_h on the length of the B-block is found as a result of the linear increase of the adsorbed amount on n, see for example figure (2.4). Apparently, δ_h scales linearly with n (=r_B), in a similar way as θ^a (see equation 2.18). As the solvent quality decreases, lower δ_h values are obtained, i.e., the adsorbed layer is more compressed. A linear dependence of the layer thickness on the length of the non-adsorbing block has also been found by Hadziioannou et al.[23,24] who applied the Alexander-de Gennes scaling theory[25,26] for anchored chains to the adsorption of block copolymers. The linear relation between δ_h and n is no longer found for the $A_{20}B_n$ copolymer because in this case the A-block is too small. The adsorbed amount increases initially linearly with n, but, as in figure (2.4), levels off for high n (n > 75). This effect of a very small adsorbing A-block was also predicted by Munch and Gast[27], using a mean-field theory in which the layer thickness, the adsorbed amount, and the volume fraction in the tail region for a fixed density profile are found by minimization of the free energy. Hadziioannou et al.[23,24] do not find this effect since in their analysis the adsorbed amount is not affected by the length of the non-adsorbing block.

For $A_{20}B_n$ the effect of χ_{BO} is less than for the $A_{100}B_n$ copolymer. If n is low, δ_h decreases slightly as the solvent quality decreases. However, for high n we find the opposite effect: extension instead of compression. In this case two compensating effects play a role. If the solvent becomes poorer for B-segments, the adsorbed amount (and, hence, the number of tails) is higher because in this way less unfavourable BO-contacts occur. On the other hand, the extension of the tails is less. Apparently, for low n the compression of the tails is

the stronger effect, whereas for high n the increasing number of tails prevent their compression.

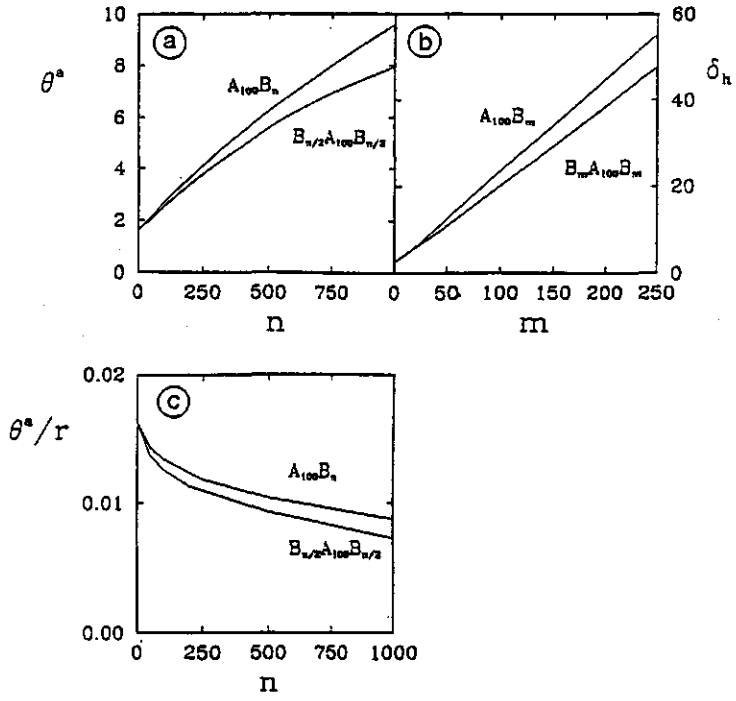

Figure 2.10. *(a) The adsorbed amount as a function of the total number n of B-segments for an $A_{100}B_n$ and a $B_{n/2}A_{100}B_{n/2}$ block copolymer. The di- and triblock copolymers have the same number n of B-segments per chain. (b) The hydrodynamic layer thickness as a function of the length m of the B-block(s). The length m of the B-block(s) is the same for the di- and triblock copolymer. (c) The number of adsorbed molecules per surface site as a function of the total number of B-segments. The A-segments are strongly adsorbing (χ_{AS} = -10) and the B-segments are non-adsorbing ($\chi_{BS} = \chi_{OS} = 0$), the other parameters are $\chi_{AO} = \chi_{AB} = \chi_{BO} = 0$, $C_h = 1$, and $\phi^b = 10^{-4}$.*

2.3.2 Adsorption of Triblock Copolymers

In figure (2.10a) the adsorbed amount of a BAB triblock copolymer and an AB diblock copolymer, both having 100 A-segments, is shown as a function of the total number n of B-segments per chain. The A-segments are strongly adsorbing (χ_{AS} = -10) and the B-segments do not adsorb (χ_{BS}= χ_{OS} = 0), the other parameters are χ_{AB} = χ_{AO} = 0.5, χ_{BO} = 0, and ϕ^b = 10^{-4}. For equal n lower adsorbed amounts are found for the triblock copolymer. The difference in adsorbed amount between the di- and triblock copolymer increases with increasing n. A lower adsorbed amount for the triblock copolymer with the same total number of B-segments as an AB diblock copolymer can be expected since adsorbed triblock copolymers will occupy more lateral space than adsorbed diblock copolymers, because of the two dangling B-blocks. Hence the number of adsorbed chains is lower, which is shown in figure (2.10c). The adsorption data of figure (2.10a) are replotted in figure (2.10c) where the number θ^a/r of adsorbed chains per surface site is given as a function of n. A similar dependence for the diblock copolymer has been found by Munch and Gast[27]. The hydrodynamic layer thickness δ_h is given in figure (2.10b) as a function of the number m of B-segments per B-block, instead of per chain as in figure (2.10a). We find for equal lengths of the B-blocks a lower hydrodynamic layer thickness for the triblock copolymer. Due to the lower number of adsorbed tails, the B-blocks in the triblock copolymer are less stretched than in the diblock copolymer.

2.4 Conclusions

The adsorbed amount and the hydrodynamic layer thickness of adsorbed block copolymers depend strongly on the composition of the copolymer. When the total length of an AB block copolymer is kept

constant, a maximum is found in the adsorbed amount as a function of the fraction of adsorbing segments. The optimal fraction (i.e., the fraction of adsorbing segments corresponding to this adsorption maximum) decreases with increasing chain lenght, increasing bulk solution volume fraction, increasing surface affinity of the more strongly adsorbing block, and decreasing surface affinity for the non- or weakly adsorbing block. From our results it is possible to relate in a relatively simple way the adsorbed amount of an AB-block copolymer to the adsorbed amount of an A-homopolymer of equal length, for fractions of adsorbing A-segments above the optimal fraction. One obtains a linear relation between the adsorbed amount of AB-block copolymer (as compared with an A-homopolymer) and the block length ratio r_B/r_A.

Usually thick adsorbed layers are found and the hydrodynamic layer thickness is of the order of 10 to 30% of the length of the non-adsorbing block. The hydrodynamic layer thickness is found to depend strongly on the adsorbed amount. For most cases, this thickness decreases with decreasing solvent quality for the non-adsorbing segments. The opposite effect occurs for diblock copolymers with a short adsorbing block and a very long non-adsorbing block.

Adsorption of BAB-triblock copolymers with adsorbing A-segments and non-adsorbing B-segments results in a lower adsorbed amount as compared to an AB-block copolymer with the same (total) number of A- and B-segments. If the two B-blocks in the triblock copolymer have the same length as the B-block in the diblock copolymer, the hydrodynamic layer thickness is higher for the diblock copolymer.

REFERENCES

(1) O.A. Evers, PhD thesis, Wageningen (1989), chapter 1; Macromolecules, submitted.

(2) J.M.H.M. Scheutjens and G.J. Fleer, J.Phys.Chem. 83, 1619 (1979).

(3) J.M.H.M. Scheutjens and G.J. Fleer, J.Phys.Chem. 84, 178 (1980).

(4) J.M.H.M. Scheutjens and G.J. Fleer, Macromolecules 18, 1882 (1985).

(5) M.A. Cohen Stuart, F.H.W.H. Waajen, T. Cosgrove, B. Vincent and T.L. Crowley, Macromolecules 17, 1825 (1984).

(6) A. Hopkins and G.J. Howard, J.Polym.Sci. A-2, 9, 841 (1971).

(7) G.J. Howard and M.J. McGrath, J.Polym.Sci.Polym.Chem.Ed. 15, 1705 (1977).

(8) G.J. Howard and M.J. McGrath, J.Polym.Sci.Polym.Chem.Ed 15, 1721 (1977).

(9) M. Kawaguchi, M. Aoki and A. Takahashi, Macromolecules 16, 635 (1983).

(10) A. Diaz-Barrios and A. Rengel, J.Polym.Sci.Polym.Chem.Ed. 22, 519 (1984).

(11) A. Diaz-Barrios and G.J. Howard, Macromol.Chem. 182, 1081 (1981).

(12) J.A. Baker, and J.C. Berg, Langmuir 4, 1055 (1988).

(13) K.G. Mathai and R.H. Ottewil, Trans.Faraday Soc., 62, 750, ibid. 759 (1966).

(14) J.M. Corkhill, J.F. Goodman and J.R. Tate, Trans. Faraday Soc., 62, 979 (1966).

(15) Th. van den Boomgaard, Th. F. Tadros and J. Lyklema, J.Colloid Interface Sci. 116, 8 (1987).

(16) B. Kronberg, J. Kuortti and P. Stenius, Colloids Surfaces. 18, 411

(1986).

(17) B. van Lent and J.M.H.M. Scheutjens, Macromolecules 22, 1931 (1989).

(18) J.M.H.M. Scheutjens, G.J. Fleer and M.A. Cohen Stuart, Colloids Surfaces. 21, 285 (1986)

(19) P.F. Mijnlieff and F.W.J. Wiegel, J.Polym.Sci.Polym.Phys.Ed. 16, 245 (1978)

(20) T. Cosgrove, T. Heath, B. van Lent, F. Leermakers, and J. Scheutjens, Macromolecules 20, 1692 (1987)

(21) T. Cosgrove, T.G. Heath, K. Ryan, and B. van Lent, Polymer Communications 28, 64 (1987)

(22) S. Hirz, MSc thesis, University of Minnesota (1987)

(23) G. Hadziioannou, S. Patel, S. Granick, and M. Tirrell, J.Amer.Chem.Soc. 108, 2869 (1986).

(24) S. Patel, M. Tirrell, and G. Hadziioannou, Colloids Surfaces 31, 157 (1988).

(25) P.G. de Gennes, Macromolecules 13, 1069 (1980).

(26) S.J. Alexander, J.Phys. (Paris) 38, 983 (1977).

(27) M.R. Munch and A.P. Gast, Macromolecules 21, 1366 (1988).

CHAPTER 3

Interaction between adsorbed layers of block copolymers

ABSTRACT

Recently, we presented a self-consistent field theory for the adsorption of block copolymers from a multicomponent mixture. In this papar the theory is applied to the interaction between two layers of adsorbed block copolymers. The free energy of interaction is derived for two types of equilibrium: (i) all molecules are free to diffuse out of the gap (full equilibrium) and (ii) the amount between the surfaces of some or all molecules is constant (restricted equilibrium).

For diblock copolymers with one strongly and one weakly adsorbing or non-adsorbing block we find repulsive interaction curves at full equilibrium because bridging is unfavorable. This is in contrast with homopolymers. which always lead to attraction in full equilibrium. If the total amount of diblock copolymer is kept constant, the interaction in a good solvent is always repulsive. With increasing amounts the interaction becomes stronger repulsive. The onset of interaction is found at a surface separation which is approximately twice the hydrodynamic layer thickness. This separation depends highly on the length of both blocks. We show how the interaction curves at different block lengths can be scaled onto one master curve. In a poor solvent attraction is found at large separations due to osmotic forces.

For ABA-triblock copolymers with adsorbing A-segments and non-adsorbing B-segments in a good solvent for B, we find attraction at large separations due to bridging.

3.1 INTRODUCTION

Polymers are widely used to modify the surface of colloidal particles. The main goal is to stabilize or flocculate these particles.[1-4] Diblock copolymers, like non-adsorbing terminally attached chains, are found to form very extended adsorption layers.[5-15] The amount on the surface can be higher than in the case homopolymers (consisting of the adsorbing segments). As a result of these extended layers, colloidal particles covered with block copolymers in solvents that are better than Θ-solvents experience a strong steric repulsion when they approach each other. Formation of polymer bridges of adsorbing blocks is prevented by steric hindrance due to the non-adsorbing blocks. Hence, block copolymers are very effective in stabilizing colloidal suspensions and are utilized in many industrial products like paints, inks, lubricants, coatings, blends, etc.

Recently, force measurements between mica sheets bearing adsorbed diblock copolymer[5,9-14] and triblock copolymer[9,11] have been reported. In good solvents long range repulsive forces are found. The onset of repulsion is detected at separations between the mica sheets of upto 10 times the unperturbed radius of gyration of the non-adsorbing block. In solvents that are worse than Θ-solvents attraction between the surfaces occurs. The magnitude of the attraction between adsorbed diblock copolymer layers as compared to the corresponding homopolymer varies considerably between the various experiments. For PV2P-PS (60,000-60,000 molecular weight) block copolymers in cyclohexane at 21°C Hadziioannou et al.[10] found a magnitude of attraction that was 5 to 10 times weaker than for a corresponding PS homopolymer. For PEO-PS (20,000-250,000) block copolymers in a solution of heptane-toluene (2:1 v/v) Marra et al.[12] found the same order of magnitude for the attraction as for PS (300,000) homopolymer.

In a previous paper[16] we introduced a self-consistent (mean) field theory for the adsorption of block copolymers (between two plates) from a multicomponent mixture, as a generalization of the

Scheutjens-Fleer theory.[17,18] The theory is based on a lattice model in which no a priori assumptions are made about the conformations of the molecules. The probabilities of the various possible conformations are derived from the partition function, resulting in the segment density profile near the surface. We have shown[16] how the conformation probabilities can be expressed in the potentials of every segment in the copolymer molecule. In this paper we will apply the theory to the case of the interaction between two adsorbed layers of block copolymers. The theory will be shortly reviewed in sections 3.2.1 and 3.2.2. In section 3.2.3 the concepts of full equilibrium and restricted equilibrium are introduced, and equations for the free energy of interaction are obtained from equations derived in reference (16). A collection of numerical results on the interaction between layers of adsorbed diblock and triblock copolymers are presented for both types of equilibrium. Special attention is paid to the effect of chain composition on the interaction.

3.2. THEORY

3.2.1 Model

A lattice between two parallel plates is used so that the number of possible conformations of the various molecules is finite. The lattice is divided into equidistant layers parallel to the surfaces (see figure 3.1), numbered z=1,2,...,M, and having L lattice sites each. Every lattice site has Z nearest neighbors a fraction λ_0 of which is found in the same layer and a fraction λ_1 in each of the adjacent layers. For example, in a hexagonal lattice $\lambda_0 = 6/12$ and $\lambda_1 = 3/12$.

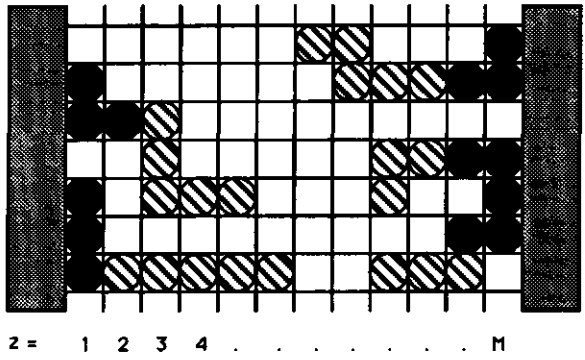

Figure 3.1. *Three chains AAABBBBB and one chain BBBAAAAABBB in a lattice between two surfaces*

We will use the subscript i to denote a particular type of molecule. A polymer molecule of type i is represented as a chain of connected segments numbered $s=1,2,...,r_i$. Since block copolymers contain in general more than one type of segment it is necessary to know the type, denoted by A,B,C,..., of each segment s. We assume that every lattice site is occupied by a segment or a solvent molecule and that every type of segment in the mixture has the same volume.

A density gradient in the mixture between the two plates will be found as a result of spatial restrictions, of mutual interactions between segments, and of interactions between segments and the surfaces. We use a mean field approximation within each layer, i.e., we neglect density fluctuations parallel to the surfaces. In this approximation, only the distance to the surfaces is relevant. The volume fraction of molecules i in layer z is denoted by $\phi_i(z)$.

Apart from the mixture between the two surfaces we introduce an infinitely large bulk solution as a reference. As shown in reference (16) it is not necessary that this bulk solution is in equilibrium with the mixture between the plates. The volume fraction of molecules i in the bulk solution is denoted by $\phi^{b;i}$.

3.2.2 Segment Density Distribution

Every individual segment is subjected to a local potential, which depends on its physical nature and on the distance to the surfaces. We denote the local potential for a segment of type A in layer z as $u_A(z)$. In a previous paper[16] we derived an expression for $u_A(z)$ from the grand canonical partition function of the system. This potential can be subdivided into a part u'(z) which only depends on z and a part $u_A^{int}(z)$ which also depends on the type of segment.

$$u_A(z) = u'(z) + u_A^{int}(z) \tag{3.1}$$

The potentials are defined with respect to the infinitely large homogeneous bulk solution: $u_A^b = 0$. The "hard core" potential u'(z) results from the fact that every segment has the same finite volume and is determined by the packing constraint $\Sigma_A \phi_A(z) = 1$. The potential $u_A^{int}(z)$ accounts for the energetic interactions a segment of type A in layer z has with neighboring segments or surface sites. We use the familiar Flory-Huggins interaction parameter χ_{AB} to account for the energetic interaction between A- and B-segments, and χ_{AS} for the interaction between A-segments and surface-sites. In average, a segment in layer z has $<\phi_B(z)>Z$ contacts with B-segments, where the contact fraction with B-segments $<\phi_B(z)>$ is given by

$$<\phi_B(z)> = \lambda_1 \phi_B(z-1) + \lambda_0 \phi_B(z) + \lambda_1 \phi_B(z+1) \tag{3.2}$$

We introduce a fixed density profile for both surfaces S and S': $\phi_S(z)$ equals 1 for $z < 1$ and 0 for $z \geq 1$, and $\phi_{S'}(z)$ equals 1 for $z > M$ and 0 for $z \leq M$. In the bulk solution $\phi_S^b = \phi_{S'}^b = 0$. The interaction potential $u_A^{int}(z)$ is given by

$$u_A^{int}(z) = \sum_B \chi_{AB}\left(<\phi_B(z)> - \phi_B^b\right) \tag{3.3}$$

where S and S' are also included in the summation over B. The summation on the right hand side of equation (3.3) is to be taken over all segment types and surfaces if they are present in layers z-1, z, or z+1.

Let us first consider the case of monomer adsorption. For the segment density profile of monomers A in the mixture between the two plates in equilibrium with an infinite large bulk solution b we have the following Boltzmann equation

$$\phi_A(z) = \phi_A^b \exp[-u_A(z)/kT] \tag{3.4}$$

This equation can be rewritten in terms of a segment weighting factor $G_A(z)$.

$$\phi_A(z) = \phi_A^b G_A(z) \tag{3.5}$$

where the segment weighting factor $G_A(z)$ is defined as

$$G_A(z) = \exp[-u_A(z)/kT] \tag{3.6}$$

For a chain molecule we have to take into account that the successive segments are connected to each other. First we introduce $G_i(z,s)$, the segment weighting factor of segment s in layer z. For example, if segment s is of type D, then $G_i(z,s)$ equals $G_D(z)$. The chain end distribution function $G_i(z,s \mid 1)$ is defined as the average weighting factor of all possible conformations of a chain of s segments long starting at segment 1 anywhere in the lattice and ending with its last segment (s) in layer z. The weighting factor for a chain starting at segment r_i anywhere in the lattice and ending at segment s in layer z is denoted as $G_i(z,s \mid r_i)$. To obtain the volume fraction $\phi_i(z,s)$ of segment s of molecules i in layer z we should multiply the weighting factors of the two chain parts $G_i(z,s \mid 1)$ and $G_i(z,s \mid r_i)$. However, we have to correct for double counting of the segment weighting factor

$G_i(z,s)$ of segment s (which is in layer z), since this weighting factor is contained in both chain end distribution functions.

$$\phi_i(z,s) = C_i G_i(z,s|1) G_i(z,s|r_i) / G_i(z,s) \tag{3.7}$$

where C_i is a normalization constant depending on the type of molecule and which will be derived in section 3.2.3. The chain end distribution functions $G_i(z,s|1)$ and $G_i(z,s|r_i)$ are found in a relatively easy way. Obviously, $G_i(z,1|1) = G_i(z,1)$ and $G_i(z,r_i|r_i) = G_i(z,r_i)$. If segment s finds itself in layer z then the connected segment s-1 should be located in one of the layers z-1, z, or z+1. Thus we can divide the chain end distribution function $G_i(z,s|1)$ into two factors:

$$G_i(z,s|1) = G_i(z,s) < G_i(z,s-1|1) > \tag{3.8}$$

where $<G_i(z,s-1|1)>$ is the neighbour average of $G_i(z,s-1|1)$, defined in the same way as $<\phi_B(z)>$ in equation (3.2). In fact, equation (3.8) is a recurrence relation, valid for $s > 1$. For $G_i(z,s|r_i)$ we have a similar recurrence relation.

$$G_i(z,s|r_i) = G_i(z,r_i) < G_i(z,s+1|r_i) > \tag{3.9}$$

The volume fraction profile $\phi_i(z)$ of all segments of molecules i in layer z is simply given by the summation of $\phi_i(z,s)$ over all r_i segments:

$$\phi_i(z) = \sum_{s=1}^{r_i} \phi_i(z,s) \tag{3.10}$$

If we want to calculate the volume fraction of, for instance, only the A segments of molecules i, $\phi_{Ai}(z)$, we perform the summation of $\phi_i(z,s)$ only over those segments s which are of type A.

restricted equilibrium is for many cases physically more realistic than full equilibrium. For a two component mixture containing polymer and solvent Scheutjens and Fleer[18] defined a restricted equilibrium by the condition that the total amount of polymer between the two plates is independent of the plate distance.

For a multicomponent mixture a restricted equilibrium is more complex to describe. The situation is essentially analogous to a membrane equilibrium, where some of the molecules (j) can pass a membrane and others (k) cannot. We define a restricted equilibrium by the condition that the total amount of every molecule type which can not leave the gap is independent of the plate distance. The total amount θ_i of molecules i between the two plates, irrespective of their equilibrium condition and expressed in number of equivalent monolayers of segments, is given by

$$\theta_i = \sum_z \phi_i(z) \tag{3.15}$$

The total amount of end segments per lattice site is θ_i/r_i. Using equations (3.7), with $s=r_i$, and (3.15) we find another expression for C_i which is independent of the choice of the reference state of $u_A(z)$.

$$C_i = \frac{\theta_i}{r_i G_i(r_i|1)} \tag{3.16}$$

where the chain weighting factor $G_i(r_i|1)$ is given by

$$G_i(r_i|1) = \sum_z G_i(z,r_i|1) = \sum_z G_i(z,1|r_i) \tag{3.17}$$

If the total amount θ_i of a certain molecule type is known, the volume fraction profile is calculated using equation (3.16) for the normalization constant. This is the case for the molecules for which the system is closed. For the molecules which can leave the gap we can always apply the general equation (3.12) or, if the segment potentials are defined with respect to a bulk solution in which these

molecules have the same chemical potential as in the gap, equation (3.11) can be used.

3.2.4 Free Energy of Interaction

The free energy of interaction $A^{int}(M)$ at plate distance M is given by the difference between the excess surface free energy $A^{\sigma}(M)$ at plate distance M and $A^{\sigma}(\infty)$ at a plate separation so large that the adsorption layers do not affect each other.

$$A^{int}(M) = A^{\sigma}(M) - A^{\sigma}(\infty) \tag{3.18}$$

The excess surface free energy $A^{\sigma}(M)$ with respect to the pure amorphous bulk states is given by A(M) - $\sum_j n_j\mu_j$, where the summation over j is taken over the molecules that are in full equilibrium with the bulk solution:

$$\frac{A^{\sigma}(M)}{L} = \frac{A(M) - A^{*}}{L} - \sum_{j} \frac{\theta_j\left(\mu_j - \mu_j^{*}\right)}{r_j} \tag{3.19}$$

The free energy A(M) has been derived before[16],

$$\frac{A(M) - A^{*}}{LkT} = -\sum_{i} \frac{\theta_i^{ex}}{r_i} - \sum_{z} \frac{u'(z)}{kT} - \frac{1}{2} \sum_{z,A',B'} \chi_{A'B'}\left(\phi_{A'}(z) < \phi_{B'}(z) > - \phi_{A'}^{b}\phi_{B'}^{b}\right) + \sum_{i} \frac{\theta_i\left(\mu_i - \mu_i^{*}\right)}{r_i kT} \tag{3.20}$$

where θ_i^{ex} is, analogous to equation (3.15), the excess amount of molecules i, expressed as equivalent monolayers:

$$\theta_i^{ex} = \sum_{z}\left(\phi_i(z) - \phi_i^{b}\right) \tag{3.21}$$

As before, the summation over i in equation (3.20) includes all molecule types present in the mixture and in the bulk solution, both the "mobile" and "restricted" components. The primes in the third term on the right hand side of equation (3.20) indicate that the surfaces S and S' are not included in the double summation. In fact, the terms containing the bulk solution volume fraction cancel out against the first two terms of u_A^{ref} (equations (3.14) which are included in u'(z), since u'(z) is defined with respect to the bulk solution $u'^b = 0$.

Full Equilibrium:

In case of full equilibrium, i.e., the chemical potentials of all molecules are constant when the plates are brought closer, the surface excess free energy is found by substitution of equation (3.20) into equation (3.19):

$$\frac{A^{\sigma}(M)}{LkT} = -\sum_i \frac{\theta_i^{ex}}{r_i} - \sum_z \frac{u'(z)}{kT} - \frac{1}{2}\sum_{z,A',B'} \chi_{A'B'}\left(\phi_{A'}(z) < \phi_{B'}(z) > - \phi_{A'}^{b}\phi_{B'}^{b}\right) \qquad (3.22)$$

Again, the summation over i runs over all molecule types and the primes in the third term on the right hand side indicates that the surfaces S and S' are not included in the double summation.

Restricted Equilibrium

As deined above, we will use the subscript k for the subset of molecule types i which can not diffuse out of the gap between the two plates. Substitution of equation (3.20) into equation (3.19) and realizing that the molecules of type k are not included in the summation over the complementary subset j in the second term of equation (3.19) we obtain for the surface excess free energy:

$$\frac{A^{\sigma}(M)}{LkT} = -\sum_{i}\frac{\theta_i^{ex}}{r_i} - \sum_{z}\frac{u'(z)}{kT} - \frac{1}{2}\sum_{z,A',B'}\chi_{A'B'}\left(\phi_{A'}(z) < \phi_{B'}(z) > - \phi_{A'}^{b}\phi_{B'}^{b}\right) + \sum_{k}\frac{\theta_k(\mu_k - \mu_k^{*})}{r_k kT} \qquad (3.23)$$

3.2.5 Computational Aspects

We have related the segment potentials $u_A(z)$ to the segment densities $\phi_A(z)$ in a self-consistent way. From an initial guess for the segment potential profiles $u_A(z)$ the corresponding segment density profiles $\phi_A(z)$ are calculated with equations (3.6), (3.7), and (3.10). To calculate the normalization constant C_l necessary in equation (3.7) we use equation (3.11) or (3.14), depending whether the molecules are free to diffuse out of the gap between the two plates or not. The values obtained for $\phi_A(z)$ are checked on the M boundary conditions $\Sigma_A\phi_A(z) = 1$ and, in combination with an initial guess for the M hard core potentials u'(z) the initial guess for the segment potentials is checked on its consistency with the $\phi_A(z)$ values, using equations (3.1) and (3.3).

In reference (16) we introduced an implicit set of simultaneous equations from which the equilibrium values of $u_A(z)$ and u'(z) are calculated by standard numerical techniques.

3.3 RESULTS

In this section we present numerical results for some typical cases of interaction between adsorbed layers of copolymers for a hexagonal lattice ($\lambda_0 = 6/12$). The effect of chain composition on the free energy of interaction will be discussed in relation to the effect of parameters such as solvent quality and surface affinity. Both in case of full

equilibrium and restricted equilibrium will be considered. We will only deal with two-component mixtures, a copolymer in a monomeric solvent.

3.3.1 Full Equilibrium

For adsorbing homopolymers in full equilibrium with a constant bulk solution the interaction between two plates has been found to be always attractive[18]. With decreasing plate separation desorption of the homopolymer occurs in order to maintain equilibrium between the mixture in the gap and the bulk solution, eventually resulting in one monolayer of polymer segments and solvent monomers in contact with both surfaces. The attractive force between the adsorbed layers of homopolymer at full equilibrium is due to bridging, i.e., chains are simultaneously adsorbed on both surfaces. At the smallest separation of one monolayer between the plates, all polymer segments are bridging segments. Because of this bridging, desorption is not complete.

As we have shown in an earlier publication[16], diblock copolymers adsorb with the adsorbing block in a relatively flat conformation close to the surface and the more weakly (or non-) adsorbing block in one dangling tail. These copolymers are not likely to form bridges. When formation of bridges is negligible, repulsive forces are likely to be found even in full equilibrium. Therefore, with decreasing plate separation we expect these copolymers to desorb more strongly than homopolymers.

In figure (3.2) the total amount θ of diblock copolymer between the two plates and the free energy of interaction A^{int} are given as a function of the plate separation M, for an $A_{50}B_{100}$ diblock copolymer under various conditions. Unless indicated otherwise, the A-segments are adsorbing (χ_{AS} = -4) and the B-segments non-adsorbing ($\chi_{BS} = \chi_{OS}$ = 0). All other χ-parameters are zero, and $\phi^b = 10^{-6}$. Under most conditions the interaction between the plates is found to be repulsive. When the total amount of diblock copolymer (which in this case is

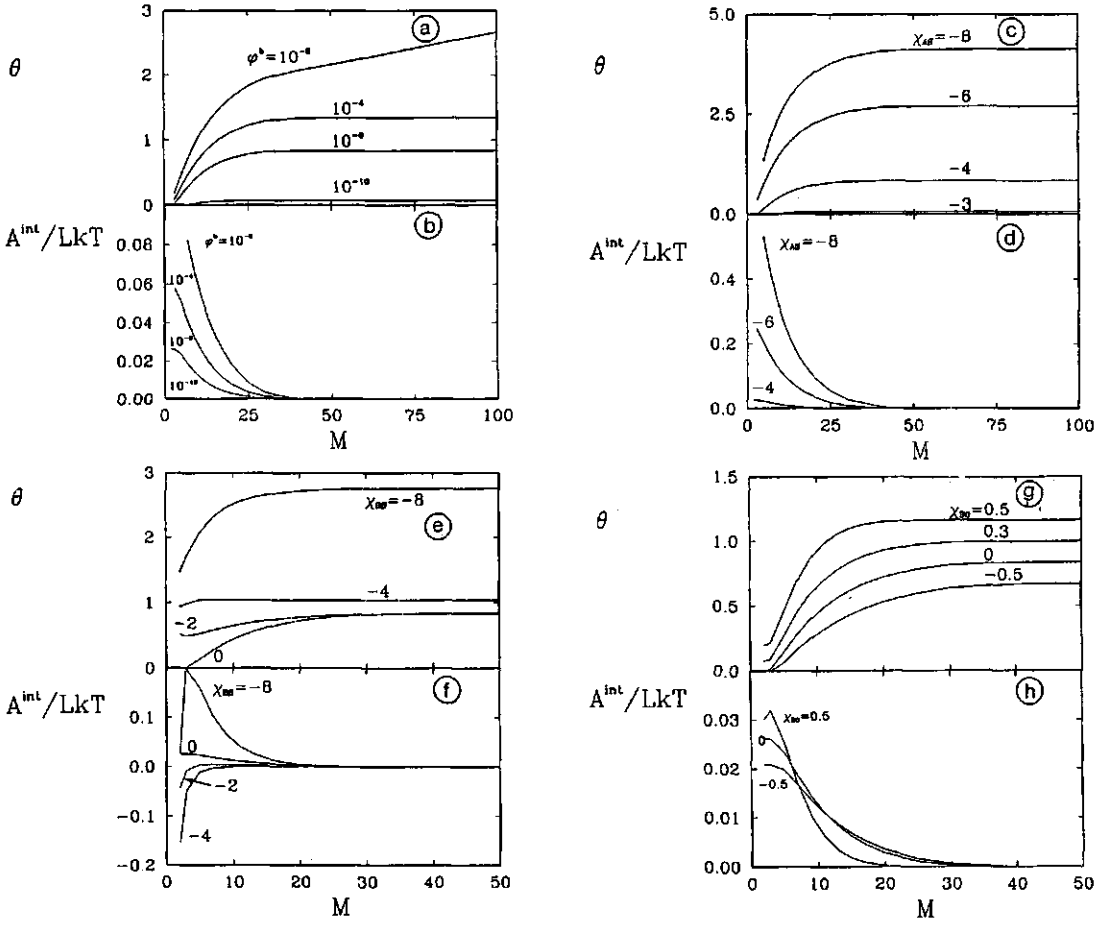

Figure 3.2. *Amount of polymer between the plates (a,c,e,g) and interaction curves (b,d,f,h) of an $A_{50}B_{100}$ diblock copolymer at full equilibrium. If not otherwise indicated the A-segments are adsorbing (χ_{AS} = -4) and the B-segments do not adsorb (χ_{BS} = 0). All the other χ-parameters are zero, and $\phi^b = 10^{-6}$. The effect of the solution concentration is shown in a and b, that of χ_{AS} in c and d, and that of χ_{BS} in e and f. Finally the effect of the solvent quality for the B-segments is given in g and h.*

nearly equal to the adsorbed amount) is increased, the interaction becomes more repulsive because a higher amount of copolymer at the same plate separation results in a stronger steric hindrance between the non-adsorbing blocks. Increasing the total amount θ can be achieved by increasing ϕ^b, increasing χ_{BO}, or decreasing χ_{AS}.

Interaction curves for four different solutions concentrations ϕ^b are shown in diagram b. In all cases the interaction between the adsorbed layers is repulsive, the more so as ϕ^b increasing. We will discuss the onset of interaction in connection with figures (3.2h) and (3.3). In parts c and d the effect of surface affinity of the adsorbing A-segments is shown. As the surface affinity increases, i.e. decreasing χ_{AS}, the total amount increases as can be expected since a higher surface affinity gives a better compensation of the loss of entropy when a copolymer molecule adsorbs. As a result of the higher adsorbed amounts the interaction becomes more repulsive when χ_{AS} decreases.

The effect of the surface affinity of the B-segments is displayed in parts e and f. The A-segments are adsorbing (χ_{AS} = -4). For χ_{BS} = 0 the interaction is repulsive as in parts b and d. When the B-segments have half the adsorption energy of the A-segments (χ_{BS} = -2) the interaction between the adsorbed layers is slightly repulsive arround M = 7 but becomes attractive at very small M due to formation of bridges. The desorption upon approach of the plates is less than in case of χ_{BS} = 0 because the easier bridge formation opposes desorption. The interaction curve for χ_{BS} = -4 is found to be attractive and represents in fact a homopolymer of 150 segments since χ_{AS} is also -4 and all other χ-parameters are zero. The maximum in θ in this case has been discussed by Scheutjens and Fleer[18] and is due to the contribution of bridging chains to θ in addition to the chains adsorbing on one of the plates only. The total amount θ of homopolymers (χ_{BS} = -4) is higher than of block copolymers in case of χ_{BS} = 0 or -2; diblock copolymers of the same length as a homopolymer can achieve a much higher adsorbed amount because of the dangling B-block, provided the chains are sufficiently strongly anchored. We have shown this effect in reference (19). Such a situation occurs for χ_{BS} = -8, where the A-block becomes the weakly-adsorbing block. At large plate separation the

interaction is strongly repulsive, but around M = 4 it passes a maximum. At smaller plate separation the energy of interaction decreases due to bridge formation but it remains weakly repulsive at M = 2.

Not only the adsorption energy, but also the solvent quality affects the adsorption and interaction curves. Diagrams g and h show the effect of varying the solvent quality χ_{BO} for the non-adsorbing B-block. When the solvent quality becomes poor ($\chi_{BO} > 0$) the dangling B-blocks assume a more collapsed conformation and, hence, the thickness of the adsorbed layer decreases. Therefore the onset of interaction decreases with increasing χ_{BO} as is seen in figure (3.2h). Because the adsorbed amount of copolymer is higher for poorer solvents, the interaction between the plates at small M becomes more repulsive when the solvent quality decreases (increasing χ_{BO}).

The adsorbed amount and the free energy of interaction of an AB-diblock for different adsorption energies of the B-segments are shown in figure (3.3) as a function of the chain composition. The diblock copolymer is 250 segments long, $\phi^b = 10^{-4}$, the A-segments are strongly adsorbing ($\chi_{AS} = -8$), χ_{BS} is 0, -4, or -6, and all other χ-parameters are zero. In diagram a the adsorbed amount θ^a is shown as a function of the fraction ν_A of A-segments per chain at three different values of χ_{BS}. A maximum in the adsorbed amount is observed. As already explained in reference (19), at low ν_A the attachement is too weak. The leveling off towards the maximum is due to saturation of the surface with A-segments, and the decrease beyond the maximum occurs because, at full surface satuaration, the length of the non-adsorbed B-tails decreases. Because the interaction between the adsorbed layers depends highly on the adsorbed amount we expect a strong effect of the composition of the copolymer on the free energy of interaction. This is indeed the case as can be seen from parts b,c, and d. Interaction curves for four (a and b) or three (d) different values of ν_A are shown. The strongest repulsion is found for those values of ν_A that correspond to the highest adsorbed amount. Thus, for χ_{BS} equal to zero or -4 we find the strongest repulsion for $\nu_A = 0.2$, whereas for $\chi_{BS} = -6$ the repulsion is stronger for $\nu_A = 0.5$ than that for $\nu_A = 0.2$. In

this latter case, the strongest repulsion is for ν_A arround 0.35 (not shown). With increasing length of the B-block (i.e., decreasing ν_A) and sufficient adsorption the adsorbed layer becomes thicker and therefore the onset of interaction will be found at larger plate separations.

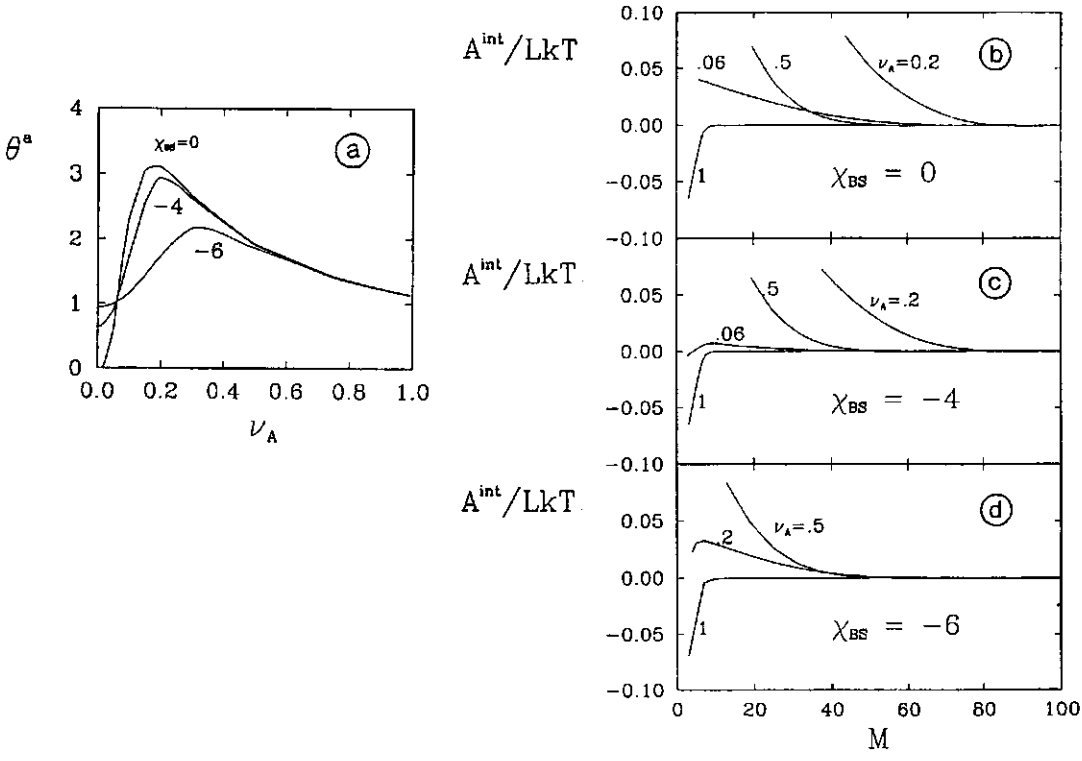

Figure 3.3. *The adsorbed amount of an AB-block copolymer as a function of the fraction ν_A of A-segments (a) and interaction curves at full equilibrium (b,c,d) for different values of ν_A at three surface affinities of the more weakly (or non-)adsorbing B-block. The A-segments are strongly adsorbing (χ_{AS} = -8). Other parameters: $\chi_{AO} = \chi_{AB} = \chi_{BO} = 0$, and $\phi^b = 10^{-4}$.*

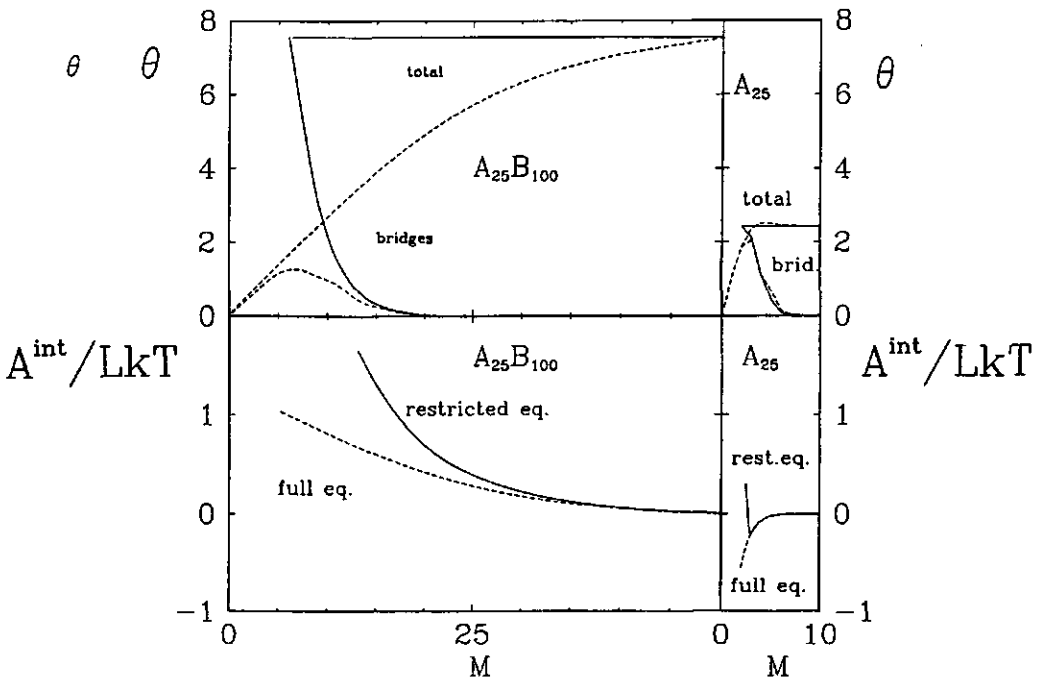

Figure 3.4. *Comparison between adsorption and interaction curves at full equilibrium (dashed curves) and restricted equilibrium (full curves) of an $A_{25}B_{100}$ diblock copolymer (left hand side) and an A_{25} homopolymer (right hand side). The total amounts of polymer at large surface separation correspond to equilibrium adsorption at $\phi^b = 10^{-4}$. The A-segments are strongly adsorbing ($\chi_{AS} = -10$) and the B-segments do not adsorb ($\chi_{BS} = 0$). Other parameters: $\chi_{AO} = \chi_{AB} = 0.5$, $\chi_{BO} = 0$.*

3.3.2 *Restricted Equilibrium*

When the polymer is unable to diffuse out of the gap between the two plates the mixture is in a restricted equilibrium. In this case the total amount θ of polymer is constant when the surface are brought closer and the chemical potential of the polymer varies with plate

separation. The free energy of interaction is zero at large plate separation and infinite when $M < \theta$ (the segments are incompressible).

The difference between a block copolymer $A_{25}B_{100}$ (with $\chi_{BS} = 0$) and the corresponding homopolymer A_{25} is shown in figure (3.4), both for the adsorbed amount (top) and for the interaction curves (bottum) in full equilibrium and restricted equilibrium. The A-segments are strongly adsorbing ($\chi_{AS} = -10$), and the solvent quality is good for the B-segments ($\chi_{BO} = 0$) and poor for the A-segments ($\chi_{AO} = \chi_{AB} = 0.5$). The equilibrium volume fraction ϕ^b is 10^{-4} which corresponds for the $A_{25}B_{100}$ copolymer with an equilibrium adsorption at large plate separation of $\theta = 7.6$ and for the A_{25} homopolymer $\theta = 2.4$. To obtain the same reference free energy in case of restricted equilibrium we used $\theta = 7.6$ for the diblock copolymer and $\theta = 2.4$ for the homopolymer. Since the solvent quality is poor for the A-segments, a maximum in θ is found for the A_{25} homopolymer in case of full equilibrium as a result of additional adsorption due to bridging at the onset of the interaction. An attractive minimum in the restricted equilibrium interaction curve of the homopolymer is observed because of bridging. For the diblock copolymer repulsive interaction curves are obtained, both in full and restricted equilibrium, as a result of the steric repulsion between the non-adsorbing B-blocks. The repulsion is stronger in the case of restricted equilibrium since the copolymers can not leave the gap between the plates. In full equilibrium, the relative number of bridging molecules in case of the $A_{25}B_{100}$ diblock copolymer is much lower (by a factor of 10) as compared to the A_{25} homopolymer. The steric hindrance caused by the B-blocks strongly reduces the possibility of bridging by the adsorbing A-segments. Therefore, like in case of restricted equilibrium where the chains are forced to bridge when the plates are brought closer together, the copolymer chains which are in contact with both surfaces do not contribute a significant attractive term to the free energy of interaction.

Figure (3.5) shows interaction curves for an $A_{50}B_{100}$ diblock copolymer in restricted equilibrium at different (constant) amounts θ,

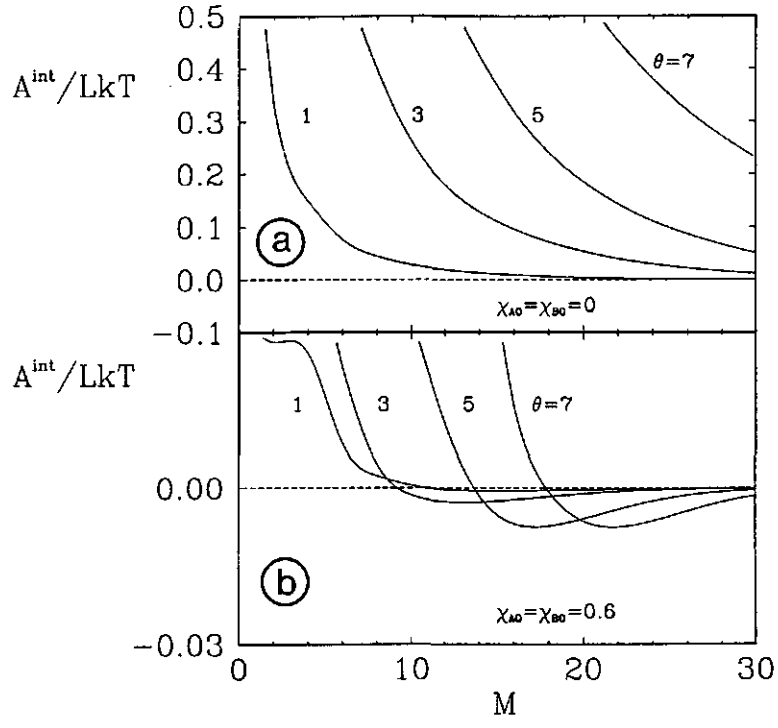

Figure 3.5. *Interaction curves at different (constant) amounts of an $A_{50}B_{100}$ diblock copolymer between the surfaces in case of a good solvent (a) and a poor solvent (b) for the A- and B-segments. χ_{AS} = -10, χ_{BS} = 0, χ_{AB} = 0.*

for two solvent qualities for the A- and B-segments. The A-segments are strongly adsorbing (χ_{AS} = -10, χ_{BS} = 0). If the solvent quality is good for the A- and B-segments (figure 3.5a) we find only repulsion. As the amount of copolymer increases the interaction becomes more repulsive because of the higher density and, consequently, increasing steric hindrance between the copolymers. At very poor solvent quality (χ = 0.6) for the A- and B-segments (figure 3.5b) the interaction curves have an attractive minimum at large plate separations. The reason for this attractive minimum is not bridging but osmotic attraction in the very poor solvent which causes the surface act as a nucleus for phase separation. This effect is shown in more detail in figure (3.6).

In this figure, interaction curves of an $A_{15}B_{200}$ diblock copolymer in restricted equilibrium (θ = 21.5) are given, for various solvent qualities for the A- and B-segments. The A-segments adsorb strongly (χ_{AS} = -20) and the B-segments do not adsorb (χ_{BS} = 0). An attractive minimum occurs when the solvent quality for the A- and B-segments (χ_{AO}, χ_{BO}) becomes just above 0.5. Hence, the phase separation

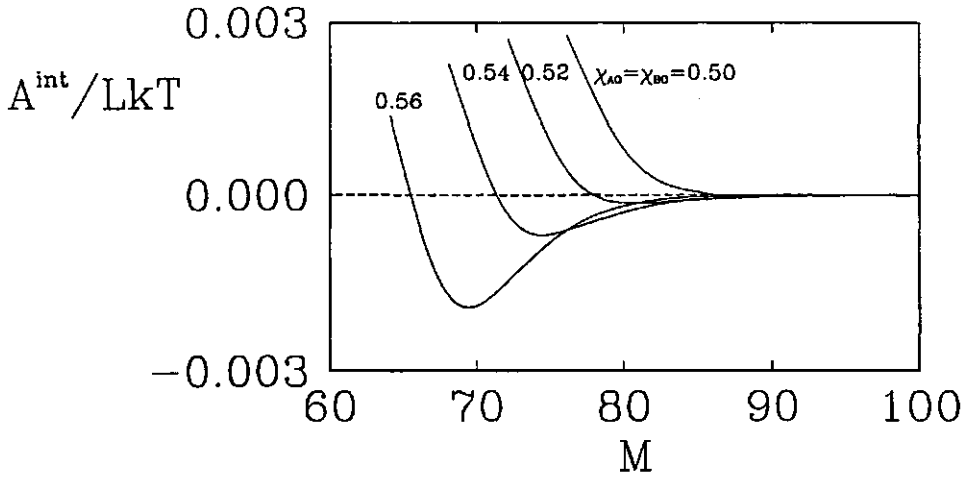

Figure 3.6. *The effect of the solvent quality for the A- and B-segments on the interaction curves of an $A_{15}B_{200}$ diblock copolymer at constant amount of polymer (θ = 21.5). χ_{AS} = -20, χ_{BS} = 0, χ_{AB} = 0.*

behaviour of strongly adsorbed diblock copolymers is similar to that of infinitely long chains in solution for which the critical χ-value for phase separation equals 0.5. This can be expected since adsorbed diblock copolymers, like anchored chains[20], have essentially no translational entropy. At weaker adsorption, a slightly higher χ-value is necessary for attraction to occure (not shown).

Next we consider the influence of the chain composition of block copolymers. Interaction curves of an AB-diblock copolymer and a BAB-triblock copolymer with an A-block of 100 segments and varying length of the B-block(s) are shown in figure (3.7) in the case of restricted equilibrium. As before, the A-segments adsorb strongly (χ_{AS}

= -10) and the B-segments have no affinity for the surface (χ_{BS} = 0). The solvent quality is good for the B-segments (χ_{BO} = 0) and poor for the A-segments (χ_{AO} = 0.5). The equilibrium adsorbed amounts at large plate separations are calculated at a fixed solution volume fraction of 10^{-4}. Since the solvent quality is good for the non-adsorbing block we obtain, as discussed before, only repulsive interaction curves. Figures (3.7a) and (b) give results for the diblock copolymer, figures (3.7c) and (d) for the triblock copolymer. Figure (3.7e) shows the hydrodynamic layer thickness of the adsorbed block copolymers calculated with the method of Scheutjens et al.[21]. The thickness increases linearly with the length of the non-adsorbing B-block. Hence, the plate separation at which the adsorbed layers overlap, i.e., the onset of interaction, will increase with increasing length of the B-block. If we assume the onset of interaction to be located at twice the hydrodynamic layer thickness δ_h, we might expect the curves to merge into one master curve by plotting A^{int} versus $M/2\delta_h$. To show this, we replotted the data of figure (3.7a) and (3.7c), respectively, with logarithmic scales in figures (3.7b) and (3.7d). The curves nearly merge into one master curve. At plate separations below δ_h ($M/2\delta_h$ < 0.5) the free energy of interaction A^{int} for the diblock copolymer scales approximately with $(M/2\delta_h)^{-2}$. At larger plate separations where the adsorbed layers just overlap we do not find a simple scaling relation between A^{int} and $M/2\delta_h$, but the dependence is then much stronger.

For the BAB-triblock copolymer, the onset of interaction is found at much smaller plate separations as compared to the AB-diblock copolymer. We have shown in an earlier publication[19] that the number of adsorbed chains of a BAB-triblock copolymer is lower than of the corresponding AB-diblock copolymer. Therefore, the hydrodynamic layer thickness (figure 3.7e) is also much lower for the BAB-triblock copolymer, as is the plate separation at the onset of the interaction (figure 3.7c). Like in case of the AB-diblock copolymer the interaction curves nearly merge into one master curve.

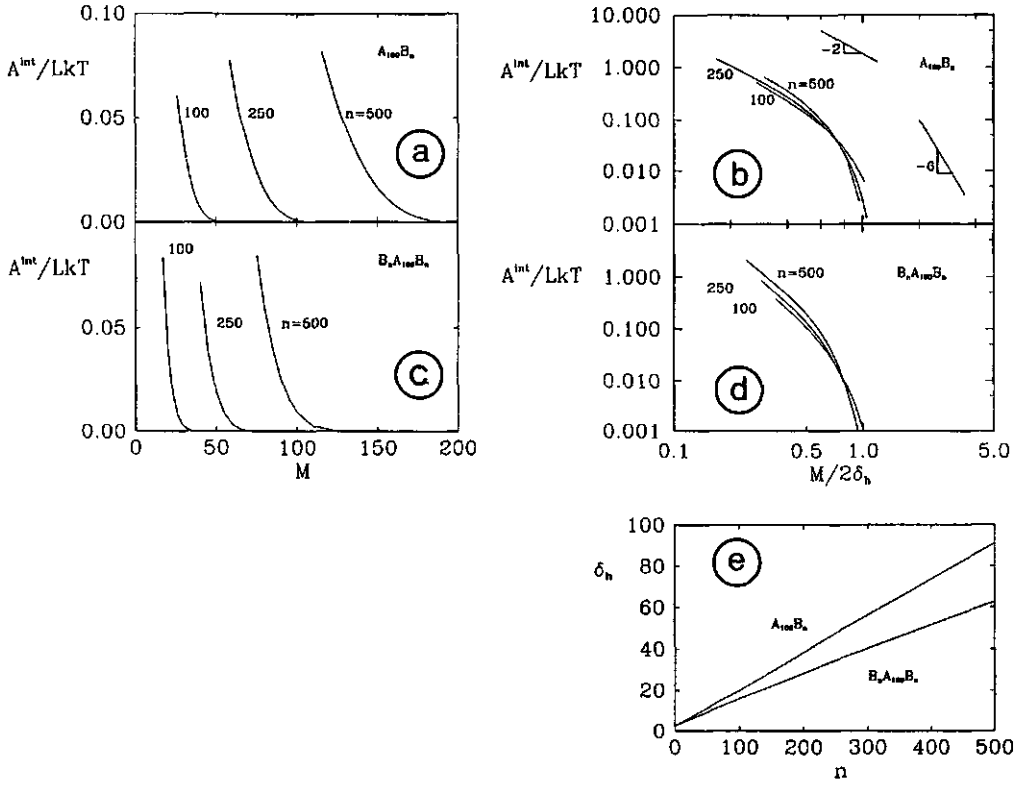

Figure 3.7. *The effect of the length n of the non-adsorbing B-block on the interaction curves at restricted equilibrium of an AB-diblock copolymer (a,b) and a BAB-triblock copolymer (c,d). The A-block contains 100 strongly adsorbing A-segments (χ_{AS} = -10). The total amounts correspond to an equilibrium adsorption at large plate separation from a bulk solution with $\phi^b = 10^{-4}$. The dependence of the hydrodynamic layer thickness of the adsorbed layers at large plate separation are shown in (e). χ_{BS} = 0, χ_{AO} = 0.5, $\chi_{AB} = \chi_{BO}$ = 0.*

Figure (3.8) shows the effect of varying the length of the adsorbing A-block on the adsorbed amount, the hydrodynamic layer thickness, and the interaction between layers of adsorbed AB-diblock copolymer in restricted equilibrium. The interaction parameters are

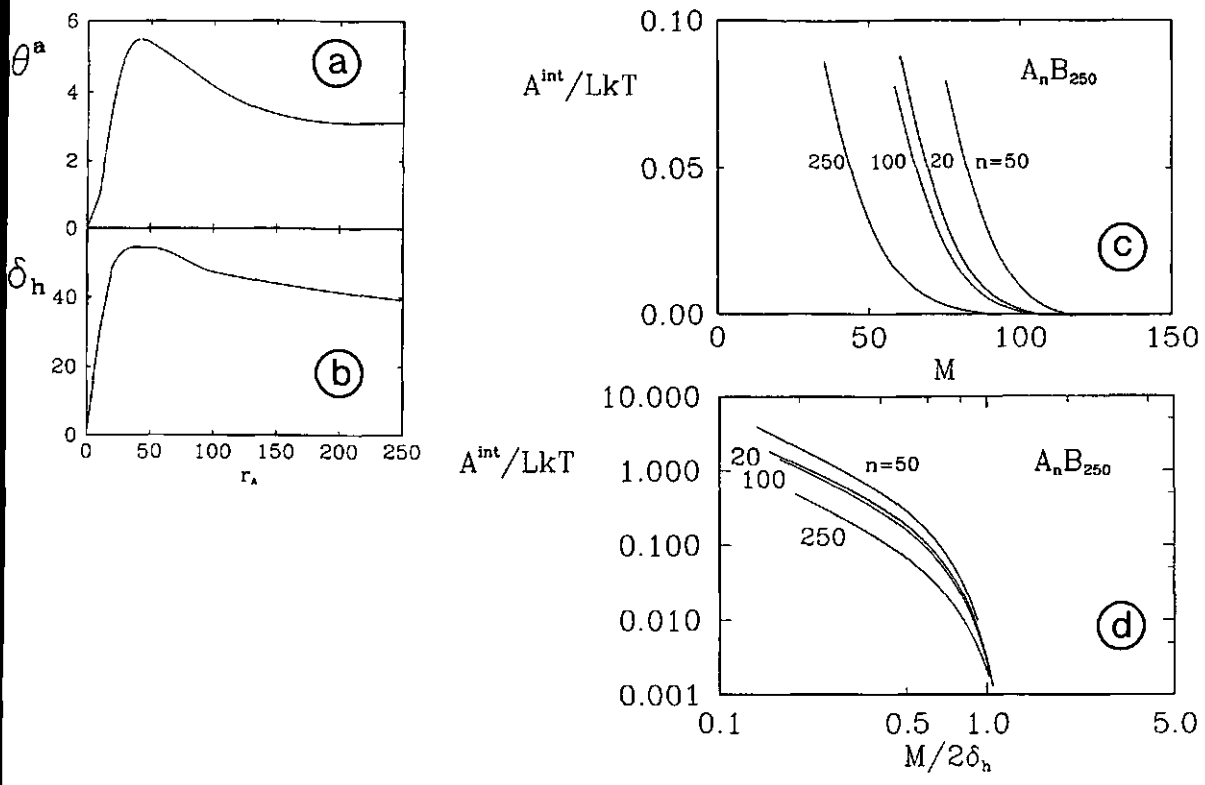

Figure 3.8. *The equilibrium adsorbed amount (a) and the hydrodynamic layer thickness (b) as a function of the length of the adsorbing A-block (χ_{AS} = -10) of an AB-diblock copolymer having 250 non-adsorbing B-segments (χ_{BS} = 0). In (c) interaction curves are given for four different lengths of the A-block. In (d) the curves of (c) are scaled with δ_h and replotted on logarithmic scales. The total amount (which is virtually equal to the adsorbed amount) corresponds to an equilibrium adsorption at $\phi^b = 10^{-4}$. χ_{AO} = 0.5, $\chi_{AB} = \chi_{BO}$ = 0.*

the same as in figure (3.7), the length of the non-adsorbing B-block is equal to 250. The equilibrium adsorbed amount at large plate separation shows a maximum as a function of r_A (figure 3.8a). The value of r_A corresponding to this maximum will be referred to as the "optimal A-block length". At very low lengths of the A-block the total adsorption energy is low. As r_A increases the number of adsorbed chains will increase until the surface is saturated with A-blocks. After passing the optimal A-block length the adsorbed amount decreases because each anchoring block will occupy more surface sites leaving less place for other chains to adsorb so that the number of dangling B-blocks decreases. The hydrodynamic layer thickness follows closely the adsorbed amount as can be seen in figure (3.8b). In figure (3.8c) interaction curves are given for four values of r_A. For $r_A = 50$ we find the most repulsive interaction curve and the largest interaction range. This is easily understood since a block length of 50 A-segments is close to the optimal A-block length (figure 3.8a). In figure (3.8d) we have replotted the data of figure (3.8c) on logarithmic scales as in figure (3.7b,d). We note that for r_A values upto 100 and for $M/2\delta_h$ near 1 the curves nearly merge into one master curve. For all curves a slope of -2 is found when $M < \delta_h$. For larger values of M the slope decreases far more steeply.

In figure (3.9) interaction curves are shown for an ABA-triblock copolymer at various lengths of the adsorbing A-blocks under the same conditions as in figure (3.7). Again, the length of the non-adsorbing B-block is kept constant at 250 segments. Because these triblock copolymers have adsorbing blocks at both sides of the molecule they are able to form bridges. Therefore, the curves show an attractive minimum at large plate separations. The highest onset of interaction and the lowest
attractive minimum is found for an A-block length of 50 segments because this block length is close to the maximum adsorption in equilibrium.

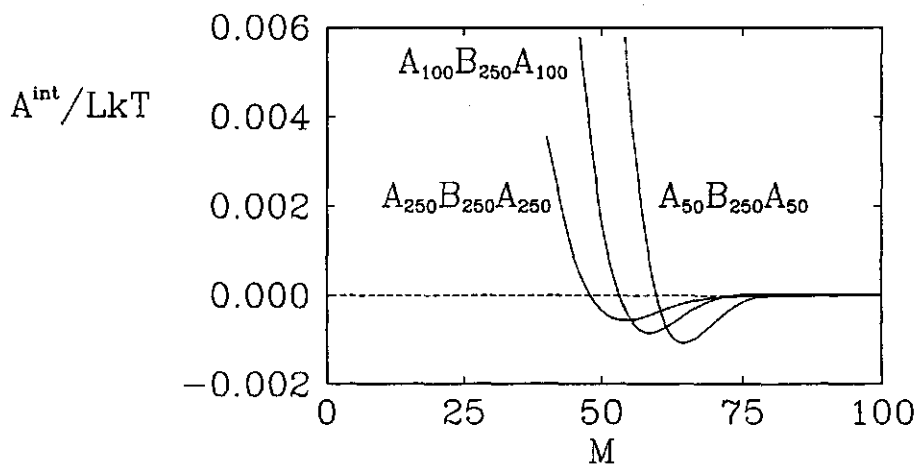

Figure 3.9. *Interaction curves of an ABA-triblock copolymer having a non-adsorbing B-block of 250 B-segments (χ_{BS} = 0) and varying length of the adsorbing A-block (χ_{AS} = -10). The total amounts of polymer correspond to an equilibrium adsorption at large surface separation when $\phi^b = 10^{-4}$. χ_{AO} = 0.5, $\chi_{AB} = \chi_{BO} = 0$.*

3.4 DISCUSSION

We have shown how the free energy of interaction can be calculated from our self-consistent field theory[16] in case of full and restricted equilibrium. The case of restricted equilibrium is physically the most relevant, since in practice the time scale in which surfaces are brought closer is much shorter than that of the transfer of chains. Therefore we will discuss our results for diblock copolymers at restricted equilibrium in comparison with experimental results.

Force-distance profiles for two cylindrical mica sheets covered with polymer can be measured directly with the so-called surface force apparatus (developed by Israelachvili[22]). Several authors[5,9-14] have

reported results on the interaction between adsorbed diblock copolymer layers obtained with such an apparatus. The force F/R, where R is radius of the mica cylinders, is measured typically upto 10 mN/m. Using the Derjaguin approximation[25] the the measured force F/R between the two crossed cylinders can be related to the free energy of interaction for two planar surfaces, as calculated with our theory:

$$\frac{A^{int}}{L} = \frac{Fa_s}{2\pi R} \qquad (3.22)$$

where a_s is the cross-sectional area of a segment. If we assume a segment to have a cross-sectional area of 0.06 nm^2, then the upper experimental limit of 10 mN/m would correspond to a free energy of interaction of 0.024 kT per surface site.

In agreement with the experimental results of Patel et al.[9-11] and Ansarifar and Luckham[13,14] we did not find a clear power law of the type $F \sim D^x$, where D is the distance between the plates for the range upto $A^{int}/LkT = 0.024$. However, if such a power law would apply, our theoretical results as shown in figures (3.7b) and (3.8d) predict an exponent x between -4 and -6. These values do agree very well with the experimental results of Patel et al. and Ansarifar and Luckham, who found exponents of approximately -4. This is considerably stronger than $F(D) \sim D^{-2}$ as estimated theoretically from scaling principles for terminally attached chains. From the results of our theory it follows that an exponent of -2 would be found at much lower separations than reached in the experiments.

The effect of the chain length of the non-adsorbing block of a diblock copolymer has been studied by Patel et al.[9-11], who measured force-distance curves of poly-2-pyridine/polystyrene (PV2P/PS) in a good solvent, toluene (32°C), at various lengths of the non-adsorbing PS-block. At constant length of the adsorbing PV2P-block they have merged their force curves approximately into one master curve by plotting the measured force versus $D/2L_0$, where D is the distance between the two mica sheets and L_0 is a theoretical layer thickness

obtained from scaling laws for terminally anchored chains. In agreement with our results for the hydrodynamic layer thickness, it varies linearly with the length of the non-adsorbing block. However, in contrast to our results for interaction curves at different lengths of the adsorbing block Patel et al. do not obtain one master curve for log A^{int} as a function of $D/2L_0$. This may be due to an improper scaling of the theoretical layer thickness L_0 with the adsorbed amount.

For diblock copolymers in poor solvents we find attraction at large plate separations as a result of osmotic forces, in agreement with experimental results[9-11,12]. The magnitude of the attraction is upto 10 times weaker than for corresponding homopolymers[18], which agrees very well with the observations of Patel et al.[9-11] but not with the measurements of Marra et al.[12]. These latter authors found for PEO/PS diblock copolymers with different block lengths the same order of magnitude of attraction as for a PS homopolymer.

3.5 Conclusions

The free energy of interaction can be calculated in a straightforward way from our previously presented self-consistent field theory for the adsorption of block copolymers from a multicomponent mixture. We have extended the concepts of full- and restricted equilibrium, as introduced by Scheutjens and Fleer for a binary mixture, towards a multicomponent mixture.

At full equilibrium, when the molecules can freely diffuse out or into the gap between the two surfaces, we found for diblock copolymers, as a rule, a repulsive interaction. Attractive interaction is onlyfound when the surface affinities of both blocks are not much different.

If the diblock copolymers cannot diffuse out of the gap when the surfaces are brought closer, i.e., in the case of restricted equilibrium, the interaction is always repulsive in good solvents. For poorer solvents for the non-adsorbing block, there is attraction at

large separations. The repulsion is due to the absence of bridging of the copolymers. The attraction in poor solvents is due to osmotic forces (phase separation conditions). Attraction is observed as soon as χ is just above 0.5 since strongly adsorbed diblock copolymers have essentiaslly no translational entropy so that they behave as infinitely long chains. At short distances the interaction is always repulsive because the segments are incompressible.

The interaction curves depend strongly on the chain composition for both full- and restricted equilibrium. There is a direct relation between the repulsion and the adsorbed amount. For good solvents, the separation where the onset of interaction is found increases with increasing adsorbed amount and with increasing length of the non-adsorbing block. In most cases this separation corresponds to twice the hydrodynamic layer thickness. In the case of restricted equilibrium and a good solvent we have been able to scale the interaction curves of a diblock copolymer with the layer thickness, so that they merge approximately into one master curve.

For ABA-triblock copolymers with adsorbing A-segments and non-adsorbing B-segments in a good solvent, we find attraction at large separations because of bridging.

Comparison with experimental data shows, for most cases, excellent agreement.

REFERENCES

(1) D.H. Napper, "Polymeric Stabilization of Colloidal Dispersions", Academic Press, London (1983).

(2) M. Cohen-Stuart, T. Cosgrove, and B. Vincent, Adv. Colloid Interface Sci. 24, 143 (1986).

(3) B. Vincent, Adv. Colloid Interface Sci. 4, 197 (1974)

(4) T.F. Tadros, in "The Effect of Polymers on Dispersion Properties", T.F. Tadros Ed., Academic Press, London (1982), 1.

(5) H.J. Taunton, C. Toprakcioglu, and J. Klein, Macromolecules 21, 3333 (1988).

(6) A. Hopkins, and G.J. Howard, J.Polymer Sci. part A-2 9, 841 (1971).

(7) J.A. Baker, and J.C. Berg, Langmuir 4, 1055 (1988).

(8) J.V. Dawkins, and G. Taylor, Faraday Trans. I 76, 1263 (1980).

(9) S.S. Patel, PhD thesis, University of Minnesota (1988).

(10) G. Hadziioannou, S. Patel, S. Granick, and M. Tirrell, J.Amer.Chem.Soc. 108, 2869 (1986)

(11) S. Patel, M. Tirrell, and G. Hadziioannou, Colloid Surfaces 31, 157 (1988).

(12) J. Marra, and M.L. Hair, Colloids Surfaces 34, 215 (1989).

(13) M.A. Ansarifar, and P.F. Luckham, Polymer 29, 329 (1988)

(14) M.A. Ansarifar, and P.F. Luckham, Polymer Communications 29, 177 (1988)

(15) J.F. Tassin, R.L. Siemens, W.T. Tang, G. Hadziioannou, J.D. Swalen, and A. Smith, J.Phys.Chem. submitted (1988).

(16) O.A. Evers, PhD Thesis, Wageningen (1989), Chapter 1; Macromolecules, submitted

(17) J.M.H.M. Scheutjens, and G.J. Fleer, J.Phys.Chem. 83, 1619 (1979); ibid. 84, 178 (1980)

(18) J.M.H.M. Scheutjens, and G.J. Fleer, Macromolecules 18, 1882 (1985)

(19) O.A. Evers, PhD Thesis, Wageningen (1989), Chapter 2; Trans.Faraday Soc. I, submitted.

(20) B van Lent, PhD Thesis, Wageingen (1989), Chapter 4; J. Colloid Interface Sci., submitted

(21) J.M.H.M. Scheutjens, G.J. Fleer, and M.A. Cohen Stuart, Colloids and Surfaces 21, 285 (1986)

(22) J.N. Israelachvili, and G.E. Adams, Nature (London) 262, 774 (1976); Trans.Faraday Soc. I 74, 975 (1978)

(23) K. Lodge, Adv. Colloid Interface Sci. 19, 27 (1983)

(24) J Klein, J.Colloid Interface Sci. 111, 305 (1986)

(25) J.N. Israelachvili, "Intermolecular and surface forces", Academic Press, London (1985)

Summary

The aim of this study was to develop a statistical thermodynamic theory for the adsorption of linear flexible block copolymers from a multicomponent solution. This has been accomplished by a more general derivation of the self-consistent field theory of Scheutjens and Fleer for adsorption of homopolymer from a binary mixture, introducing local segment potentials for any type of segment.

In chapter 1 the statistical thermodynamic analysis for a multicomponent mixture (including block copolymers) near a surface is given in detail. Near the surface, a density gradient for every type of molecule is found due to spatial restrictions and mutual interactions between segments and between segments and the surface. Every individual segment is subjected to a local (segment) potential, which depends on the distance from the surface and on its chemical nature. We use a lattice model to evaluate the contact energies and the conformation count. The segment potential is derived from the maximum term in the canonical partition function. Like in the original derivation of Scheutjens and Fleer we maximize the canonical partition function with respect to the number of molecules in each particular conformation. However, to perform the necessary partial differentiations under the appropriate boundary conditions we apply the method of Lagrange multipliers. From the segment potentials we can calculate for every particular conformation its statistical weight as a multiple product of Boltzmann factors (one for each segment) and its contribution to the overall segment density profile. In Appendix III of chapter 1 a set of equations is formulated from which the segment potentials can be found in a self-consistent manner by standard numerical techniques.

A number of results on the segment distribution of di- and triblock copolymers is given. Diblock coplymers are found to adsorb with the adsorbing block rather flat on the surface and the less or non-adsorbing block in one dangling tail protruding far into the solution. A comparison with terminally anchored chains shows overall agreement but also typical differences.

In chapter 2 the physical background of the theory is briefly reviewed. Results on the adsorbed amount and the hydrodynamic layer thickness of adsorbed di- and triblock copolymers are given. We find a strong dependence of these parameters on the chain composition. When the total length and bulk solution volume fraction of a diblock copolymer are kept constant, a maximum is found in the adsorbed amount as a function of the fraction of adsorbing segments. The fraction of adsorbing segments corresponding to this maximum could be named "the optimal fraction"; it is found to decrease with increasing chain length, increasing bulk solution volume fraction, increasing surface affinity of the more strongly adsorbing block, and decreasing surface affinity of the weakly adsorbing block. From these results we have been able to relate in a simple way the adsorbed amount of an AB-diblock copolymer (where A adsorbs more strongly than B) to the adsorbed amount of an A-homopolymer of equal length. A linear relation is obtained between the adsorbed amount of AB-diblock copolymer (as compared with an A-homopolymer) and the block length ratio r_B/r_A, where r_A and r_B are the lengths of the A-block and the B-block, respectively. Usually, diblock copolymers form thick adsorbed layers, with a hydrodynamic layer thickness that depends strongly on the adsorbed amount. This thickness is of the order of 10 to 30 % of the length of the B-block. For BAB-triblock copolymers with adsorbing A-segments and non-adsorbing B-segments we find lower adsorbed amounts as compared to an AB-block copolymer with the same total number of A- and B-segments

The interaction between adsorbed layers of block copolymers is examined in chapter 3. The calculation of the free energy of interaction is straightforward. We elaborate the concept of full equilibrium and that of restricted equilibrium for a multicomponent

mixture. Full equilibrium refers to the case that all molecules in the mixture are free to diffuse out or into the gap between the surfaces. Hence, in full equilibrium all molecules have a constant chemical potential when the surfaces are brought closer. If one or more of the components are unable to leave the gap when the surfaces come closer we have a restricted equilibrium and the chemical potentials of those molecules will not be constant. Usually, the interaction between adsorbed layer of adsorbed diblock copolymers at full equilibrium is found to be repulsive, in contrast to the case of homopolymers where the interaction is always attractive. At full equilibrium, when the surfaces are brought closer, homopolymers desorb and form bridges resulting in attraction between the surfaces. Since diblock copolymers hardly form any bridges when the surface affinities of both blocks differ enough, no attraction is found at full equilibrium. For the same reason we find always repulsion in a good solvent when the amount of diblock copolymer is kept constant (restricted equilibrium). The onset of the repulsion increases with increasing adsorbed amount and with increasing length of the non-adsorbing block. The interaction curves at various lengths of the adsorbing- and non-adsorbing block could be scaled onto approximately one master curve. When the solvent quality for the non-adsorbing block becomes poor ($\chi > 0.5$), there is an attraction at large separation as a result of osmotic forces (phase separation), even at restricted equilibrium. In fact, adsorbed diblock copolymers behave like infinitely long homopolymer chains in solution, which phase separate when χ is above 0.5. For ABA-triblock copolymers with adsorbing A-segments and non-adsorbing B-segments, we find attraction at not too small separations in a good solvent for the B-blocks, because now bridging is again possible: adsorbing segments are found at both extremities of the chains.

This model has provided a detailed insight in the properties of adsorbed block copolymer layers and should be a useful tool for the development and optimization of experiments and products in which copolymer adsorption plays a role.

Samenvatting

Statistische Thermodynamica van Adsorptie van Blok Copolymeren

Het doel van het in dit proefschrift beschreven onderzoek was het ontwikkelen van een statistisch thermodynamische theorie voor de beschrijving van het adsorptiegedrag van lineaire flexibele blokcopolymeren. Dit is bereikt door de zelfconsistent veld-theorie van Scheutjens en Fleer voor adsorptie van homopolymeren aan een vast/vloeistof-grensvlak op een meer algemene wijze af te leiden.

Flexibele lineaire polymeermolekulen zijn lange ketens die bestaan uit een aaneenschakeling van vele honderden tot duizenden kleine eenheden, monomeren of segmenten genoemd. Het is duidelijk dat deze lineaire polymeren een wel heel bijzondere opbouw hebben. Bijvoorbeeld, een gestrekte polymeerketen bestaande uit 5000 monomeereenheden heeft een lengte van ongeveer 1 micrometer en een doorsnede van circa 0,2 nanometer. Deze verhouding komt overeen met die van een kabel met een diameter van 1 centimeter en een lengte van maar liefst 50 meter! Wanneer van buiten af geen krachten op een polymeermolekuul worden uitgeoefend en de segmenten nauwelijks wisselwerking met elkaar hebben, dan zal de ruimtelijke vorm van het polymeermolekuul in oplossing onder invloed van thermische bewegingen gemiddeld een min of meer bolvorminge kluwen zijn. Polymeren worden homopolymeren genoemd wanneer alle segmenten gelijk zijn. Een polymeermolekuul dat uit meer dan één type segment is opgebouwd wordt een copolymeer genoemd. Afhankelijk van de aaneenschakeling van de verschillende monomereenheden zijn er verschillende soorten copolymeren te onderscheiden. Zoals de titel van dit proefschrift al doet vermoeden, beperkt het beschreven onderzoek zich tot

blokcopolymeren. In blokcopolymeren zijn de monomeereenheden gegroepeerd in blokken; elk blok bevat alleen segmenten van hetzelfde type. Bijvoorbeeld, een PVP-PS diblokcopolymeer bestaat uit twee blokken: één deel van de keten is opgebouwd uit vinylpyridine (VP) en het andere deel uit monomeren styreen (S).

Wanneer molekulen zich ophopen aan een grensvlak dan spreekt men van adsorptie. Polymeren adsorberen (hechten) in het algemeen goed aan oppervlakken. Dit vindt zijn oorzaak in het grote aantal segmenten waarmee elk polymeermolekuul in contact met het oppervlak kan komen. Door aan een oppervlak polymeren te hechten kunnen de eigenschappen van dit oppervlak verbeterd worden. Een voor de hand liggend voorbeeld in dit verband is het beitsen van hout. Maar ook adsorptie van polymeren aan oppervlakken welke niet voor het blote oog zichtbaar zijn, is van groot belang voor ons dagelijks leven. We kunnen hierbij denken aan kolloïden. Kolloïdale systemen bevatten microscopisch kleine deeltjes, kolloïden, die een doorsnede van ongeveer 0,01 tot 1 micrometer hebben. Door aan deze deeltjes polymeren te hechten, ontstaat een "harige" geadsorbeerde laag die voorkomt dat deze kolloïdale deeltjes samenklonteren. Kolloïdale systemen die we niet graag op de bodem van het glas dan wel de pot samengeklonterd zien, zijn bijvoorbeeld voedingsmiddelen, verf, cosmetica en inkt. Blokcopolymeren zijn buitengewoon goede "stabilisatoren" van kolloïdale oplossingen. Doordat vaak slechts één blok van het copolymeermolekuul aan het oppervlak adsorbeert, onstaat aan het oppervlak een dikke harige beschermende laag van het minst adsorberende blok. In dit onderzoek is bestudeerd hoe de geadsorbeerde hoeveelheid blokcopolymeer en de stabiliteit van kolloïdale systemen afhangen van het oplosmiddel, het type oppervlak en de samenstelling van het blokcopolymeer.

Adsorptie van homopolymeren en de invloed hiervan op de stabiliteit van kolloïdale systemen is met succes beschreven door de theorie van Scheutjens en Fleer. Het is juist daarom dat deze theorie als uitgangspunt is genomen voor de beschrijving van adsorptie van blokcopolymeren uit een polymeeroplossing. In hoofdstuk 1 wordt de volledige statistisch thermodynamische afleiding van de theorie

gegeven. In de nabijheid van een oppervlak zal voor elk soort polymeer een dichtheidsgradient worden gevonden als gevolg van ruimtelijke begrenzingen en de wisselwerking tussen segmenten en oppervlak als ook tussen segmenten onderling. Ieder individueel segment "voelt" een lokale potentiaal, welke afhangt van de afstand tot het oppervlak en van het soort segment. In de theorie wordt een roostermodel gebruikt om de wisselwerkingen en de mogelijke verdeling van de molekulen over de ruimte (conformaties) te berekenen. In navolging van Scheutjens en Fleer wordt de kanonieke toestandssom gevonden als funktie van het aantal molekulen in elke conformatie. De lokale segmentpotentiaal wordt afgeleid van de grootste term in de kanonieke toestandssom met behulp van Lagrange-multiplicatoren. Met de segmentpotentialen is het statistisch gewicht van een gegeven conformatie te berekenen. Dit gewicht is een meervoudig produkt van Boltzmann-faktoren (één voor elk segment). Het aantal molekulen in een gegeven conformatie is evenredig met het statistisch gewicht van deze conformatie. Verschillende resultaten voor de verdeling van segmenten van geadsorbeerde di- en triblokcopolymeren worden gegeven. Diblokcopolymeren blijken te adsorberen met het adsorberende blok "plat" op het oppervlak. Het minder goed of niet adsorberende blok vormt een staart die ver in de oplossing steekt. Geadsorbeerde diblokcopolymeren vertonen in het algemeen grote overeenkomst met eindstandig verankerde ketens, maar er zijn enkele typische verschillen.

In het tweede hoofdstuk wordt de theorie kort samengevat en resultaten gegeven voor de geadsorbeerde hoeveelheid en de hydrodynamische laagdikte van geadsorbeerde di- en triblokcopolymeren. Vooral de invloed die de monomeersamenstelling van het blokcopolymeer heeft op deze parameters wordt in detail onderzocht. Wanneer de totale lengte en de bulkconcentratie van een diblokcopolymeer constant worden gehouden, vinden we een maximum in de geadsorbeerde hoeveelheid als funktie van de fraktie adsorberende segmenten. De fraktie corresponderende met het adsorptiemaximum wordt "optimale fraktie" genoemd; zij neemt af met toenemende ketenlengte, toenemende bulkconcentratie en bij

een groter wordend verschil in affiniteit van de twee polymeerblokken voor het oppervlak. Het bleek mogelijk uit deze resultaten een eenvoudige lineaire relatie op te stellen tussen de geadsorbeerde hoeveelheid van een AB-diblokcopolymeer (in verhouding tot die van een A-homopolymeer) en de bloklengte verhouding r_B/r_A. Hierin is r_A het aantal segmenten van het adsorberende A-blok en r_B dat van het niet adsorberende B-blok. Meestal vormen diblokcopolymeren dikke geadsorbeerde lagen. De hydrodynamische laagdikte is sterk afhankelijk van de geadsorbeerde hoeveelheid en bedraagt 10 tot 30 % van de lengte van het B-blok. Voor BAB-triblokcopolymeren, waarin het A-blok goed adsorbeert en de twee B-blokken niet, worden in vergelijking tot AB-diblokcopolymeren lagere geadsorbeerde hoeveelheden gevonden.

De interaktie tussen geadsorbeerde lagen van blokcopolymeren is geanalyseerd in het derde hoofstuk. Het concept van volledig evenwicht en beperkt evenwicht, zoals oorspronkelijk door Scheutjens en Fleer ingevoerd, is verder uitgewerkt voor een multicomponent-mengsel. Wanneer alle molekulen de ruimte tussen twee oppervlakken vrij kunnen verlaten of binnengaan, spreken we van volledig evenwicht. Dan hebben alle molekulen dus een constante chemische potentiaal. Als één of meer soorten molekulen niet tussen de oppervlakken vandaan kunnen wanneer de oppervlakken naar elkaar toegebracht worden, dan spreken we van beperkt evenwicht. Een reeks resultaten voor zowel volledig als beperkt evenwicht wordt gegeven. De interaktie tussen geadsorbeerde lagen van diblokcopolymeren is vrijwel altijd repulsief, zelfs in volledig evenwicht. Bij homopolymeren is deze interaktie in volledig evenwicht altijd attraktief. De oorzaak van dit verschil is gelegen in het feit dat diblokcopolymeren bijna geen polymeerbruggen kunnen vormen tussen de twee platen. De plaatafstand waar de repulsie begint neemt toe met toenemende geadsorbeerde hoeveelheid polymeer en met de lengte van het minst adsorberende blok. De interaktiekurven onder verschillende omstandigheden kunnen door een geschikte schaling vrijwel door een gemeenschappelijke kurve worden weergegeven. Wanneer het oplosmiddel slecht is voor het minst adsorberende blok,

wordt zelfs in beperkt evenwicht op niet te kleine plaatafstand aantrekking gevonden als gevolg van osmotische effecten (fasescheiding). ABA-blokcopolymeren waarvan de A-blokken goed adsorberen, kunnen wel bruggen vormen omdat beide uiteinden van de keten op een ander oppervlak kunnen adsorberen. Ook in een goed oplosmiddel wordt dan aantrekking gevonden.

Tenslotte kunnen we stellen dat het in dit proefschrift beschreven model een gedetailleerd inzicht kan verschaffen in de eigenschappen van geadsorbeerde blokcopolymeerlagen en een geschikt instrument vormt voor het ontwikkelen en optimaliseren van experimenten en produkten waarin copolymeeradsorptie een belangrijke rol speelt.

Curriculum Vitae

Olaf Arend Evers werd op 25 december 1959 geboren te Utrecht. In 1978 behaalde hij het diploma Atheneum B aan het Wagenings Lyceum te Wageningen. Aansluitend werd gestart met de studie Moleculaire Wetenschappen aan de Landbouwuniversiteit te Wageningen. Het ingenieursexamen werd op 25 januari 1985 behaald. De doctoraalstudie omvatte de vakken Kolloïdchemie (verzwaard hoofdvak) en Natuurkunde (hoofdvak). De praktijktijd van zes maanden werd vervuld bij het Zintl Instituut van de Technische Hogeschool Darmstadt in de Bondsrepubliek Duitsland.

Per 15 april 1985 trad hij voor een periode van drie jaar in dienst van de Landbouwuniversiteit bij de vakgroep Fysische en Kolloïdchemie. In deze periode werd het onderzoek voor dit proefschrift verricht.

Sinds 1 oktober 1989 is hij werkzaam bij BASF AG te Ludwigshafen am Rhein in de Bondsrepubliek Duitsland.

Nawoord

Gelukkig is een proefschrift, ook al staat er maar één naam op de voorpagina, meestal niet het resultaat van enkele jaren eenzame arbeid. Zowel bij het onderzoek als bij het schrijven van dit proefschrift zijn een aantal mensen direkt of indirekt betrokken geweest.

Aan Jan Scheutjens heb ik meer dan alleen een zeer goede leermeester gehad. Hij liet mij alle vrijheid voor eigen initiatief. Wanneer problemen opdoemden, stond hij altijd klaar om als steun en stimulator te dienen. Van zijn grenzeloze vindingrijkheid en kritisch inzicht heb ik veel geleerd en geprofiteerd.

Altijd was het mogelijk om bij Gerard Fleer aan te kloppen om van zijn scherp analytisch (uitdrukkings)vermogen en kritisch oog gebruik te maken. Zijn direkte bijdrage aan dit proefschrift is essentieel geweest. Zijn niet aflatende inzet voor de gehele polymeergroep is zeker ook aan mijn onderzoek ten goede gekomen.

Binnen de polymeergroep was het goed onderzoek doen en dat niet in de laatste plaats dankzij enthousiaste collega's en studenten. Zo denk ik met plezier terug aan de diskussies met Peter Barneveld over computers en bestuderingssystemen, maar ook aan de samenwerking met Marcel Böhmer aan het polyelektrolietonderzoek.

Tot slot wil ik iedereen bij de Vakgroep Fysische en Kolloïdchemie danken voor de hulp, de prettige sfeer en de onderhoudende koffiepauzen.